AIR FORCE INSTITUTE OF TECHNOLOGY

AIR UNIVERSITY
UNITED STATES AIR FORCE

SCHOOL OF ENGINEERING

WRIGHT–PATTERSON AIR FORCE BASE, OHIO

Unclassified
Security Classification

DOCUMENT CONTROL DATA - R & D

(Security classification of title, body of abstract and indexing annotation must be entered when the overall report is classified)

1. ORIGINATING ACTIVITY (Corporate author)
Air Force Institute of Technology (AFIT - EN)
Wright-Patterson Air Force Base, Ohio 45433

2a. REPORT SECURITY CLASSIFICATION
Unclassified

2b. GROUP

3. REPORT TITLE
INTRODUCTION TO THE ELECTROMAGNETIC PULSE

4. DESCRIPTIVE NOTES (Type of report and inclusive dates)
AFIT Thesis

5. AUTHOR(S) (First name, middle initial, last name)
Otho V. Kinsley
Major USAF

6. REPORT DATE	7a. TOTAL NO. OF PAGES	7b. NO. OF REFS
March 1971	200	189

8a. CONTRACT OR GRANT NO.	9a. ORIGINATOR'S REPORT NUMBER(S)
b. PROJECT NO. N/A	GNE/PH/71-4
c.	9b. OTHER REPORT NO(S) (Any other numbers that may be assigned this report)
d.	

10. DISTRIBUTION STATEMENT
This document has been approved for public release and sale: its distribution is unlimited

11. SUPPLEMENTARY NOTES	12. SPONSORING MILITARY ACTIVITY
	AFIT Wright-Patterson AFB, Ohio

13. ABSTRACT

This thesis constitutes an introductory survey of the electromagnetic pulse (EMP) caused by a nuclear weapon burst. The survey is separated into (1) driving mechanism, (2) the electric field of the symmetric nuclear burst, (3) the electromagnetic field from bursts whose environment is asymmetric due to density variations or the geomagnetic field's presence, (4) pulse transmission, and (5) pulse interaction. This survey was collected from the unclassified literature and is presented here in a consistent notation and language. The presentation is intended to emphasize concepts and understanding and is not intended as a design handbook. To this end the author has attempted some mathematical simplification of certain phenomena. These simplified models are identified when employed and the results obtained are compared to those found in the literature which result from test data or from more exact mathematical models.

DD FORM 1 NOV 65 1473

Unclassified
Security Classification

14 KEY WORDS	LINK A		LINK B		LINK C	
	ROLE	WT	ROLE	WT	ROLE	WT
Electromagnetic Pulse - - Introductory Survey						

INTRODUCTION TO

THE ELECTROMAGNETIC PULSE

THESIS

GNE/PH/71-4

Otho V. Kinsley
Major USAF

GNE/PH/71-4

INTRODUCTION TO
THE ELECTROMAGNETIC PULSE

THESIS

Presented to the Faculty of the School of Engineering
of the Air Force Institute of Technology
Air University
in Partial Fulfillment of the
Requirements for the Degree of
Master of Science

by

Otho V. Kinsley, B.S.
Major USAF

Graduate Nuclear Engineering

March 1971

Preface

This report is intended to acquaint engineers in their first year of graduate school with the fundamentals of the electromagnetic pulse. The mathematics is for the most part orderly starting from Maxwell's equations and the vector potential. In some developments, however, procedures from advanced techniques are applied without a derivation of their validity. The cited references describe these techniques.

When I began this thesis there was concern over keeping it unclassified. I have diligently examined AFR 205-42, (U) Classification of Nuclear Electron Magnetic Pulse (NEMP) Information, dated 12 February 1971. It states, "Basic physics of the theoretical mechanisms by which NEMP is believed to be generated (is unclassified) when classified nuclear device design is not revealed." Real and specific weapon or target system characteristics or properties appear nowhere in this document. It is emphasized that the phenomena described here are based upon hypothetical, unclassified, nuclear burst parameters, e.g., the chosen weapon alpha ($\alpha = 1$) is unclassified because "Purely hypothetical values of α from 0.5 to 2 per shake and gamma pulse durations of a few shakes for an unspecified weapon may be used for purposes of illustration." ((U) Joint AEC-DOD Nuclear Weapons Classification Guide CG-W-3, December 1968, page 45). In my own and in my advisor's opinion this thesis is clearly unclassified.

I would like to thank Dr. Charles J. Bridgman for his guidance and enthusiastic interest and Dr. Gordon K. Soper for his enlightening comments on electromagnetic theory.

Otho V. Kinsley

Contents

List of Figures

List of Tables

Abstract

This thesis constitutes an introductory survey of the electromagnetic pulse (EMP) caused by a nuclear weapon burst. The survey is separated into (1) driving mechanism, (2) the electric field of the symmetric nuclear burst, (3) the electromagnetic field from bursts whose environment is asymmetric due to density variations or the geomagnetic field's presence, (4) pulse transmission, and (5) pulse interaction. This survey was collected from the unclassified literature and is presented here in a consistent notation and language. The presentation is intended to emphasize concepts and understanding and is not intended as a design handbook. To this end the author has attempted some mathematical simplification of certain phenomena. These simplified models are identified when employed and the results obtained are compared to those found in the literature which result from test data or from more exact mathematical models.

THE ELECTROMAGNETIC PULSE

I. Introduction

The primary effects of a nuclear explosion: blast, heat, and radiation, are accompanied by other effects caused by these primary effects interacting with the environment. One such secondary effect is the seismic disturbance in the earth, intense at short ranges and detectable even at very long ranges. Another, the subject of this thesis, is the interaction of the radiation with the environment to cause the motion of charged particles which in turn create far reaching electric and magnetic fields. These electric and magnetic fields can be intense near the weapon and can be radiated to distances far beyond the range of the other effects, even beyond the radiation which was their source. Because this radiated signal can be detected far from the burst point, it is important in policing the nuclear test ban treaty as well as an effect to be considered in atomic defense.

Definitions

The electromagnetic pulse (EMP) from a nuclear weapon may be an electric field or a combination electric and magnetic field which is radiated as an electro-magnetic wave. In the latter case the EMP radiates a broadband signal, i.e., one containing many frequencies, of short duration. Television and radar signals are broadband and high powered but they do not compare to the EMP in amplitude

of the pulse, power output, or in bandwidth of their signal.

The EMP is not the Argus effect, transient radiation effect on electronics (TREE's), nor the blackout effect. Those effects are, respectively, the input of electrons into earth orbit where they cause increased aurora and skyshine; the direct effect of the bomb's radiation on electronic components, e.g., transistor degradation due to the gamma flux; and the absorbtion of radio waves in the ionosphere because of the high, bomb-induced electron density.[1]

The effects of an electromagnetic pulse are due to induced currents or voltages from the interaction of the EMP with a physical system. These effects range from increased noise in a circuit to physical destruction by ohmic heating, usually the former.

Comparisons

Although the basic physics and the magnitudes of lightning generated electromagnetic signals are completely different from EMP, there are enough similarities in their effects to draw some parallels. The static from a lightning stroke can be transmitted around the earth by the earth's magnetic field. Because of the dispersion by the medium through which the signal travels, the received signal sounds like a whistle, hence the name whistlers. Dispersion affects EMP wave shapes similarly. A lightning stroke

takes place in a strong electric field which can induce voltages in conductors not directly affected by the primary stroke. The noise heard on an AM radio after a lightning stroke is due to induced voltages. Many of the techniques useful in protection against lightning strokes are also useful in protecting against EMP effects.

Radar at short ranges can also exhibit many effects similar to EMP. Photoflash bulbs have been fired by the induced currents from a radar signal. In another case the memory of a computer was altered by currents induced by a radar pulse.[2]

Finally we have the radio station as an EMP simulator. Apocryphal stories about the early days of radio reported that fillings in teeth had received radio signals. In such a case, the filling functioned as an unintentional antenna, one of the hazards in protecting against the EMP. A reverse of the previous example is the amateur radio operator's dread, radio frequency interference (RFI), which is the spurious transmission of signals beyond the interior of the radio cabinets. Many of the techniques to prevent leakage of signals also prevents the entry of similar signals.

History

Although an electromagnetic pulse became a seriously studied problem only some time after the first nuclear explosion, similar events have been studied for some time. One of the most widely reported examples of an induced

electric field was Benjamin Franklin's experiment with a kite. Many scientists and engineers have since studied the effects of lightning.

Some authors[3] assert that the EMP was predicted by Enrico Fermi before the Trinity explosion on 16 July 1945. An EMP was expected as evidenced by this quote from Day of Trinity:

> "In the control center Sam Allison was seized by a sudden fear that the explosion would create a lighting effect and pump electrocuting volts into the microphone he gripped. At minus one second he dropped the microphone...."[4]

The same source gives us some indication of the intensity of the first nuclear EMP:

> "Scientists checking on their instruments learned all too quickly how devastating the blast had been. Only a few instruments had survived....The electromagnetic storm paralysed and bent scores of expensive gauges and measurement recorders."[5]

EMP Source Mechanisms

There are three main mechanisms for generating an electromagnetic pulse; current flow, electron-magnetic field interactions, and magnetic field exclusion. These mechanisms are described qualitatively below. Because these mechanisms operate differently in different environments there are many variations possible, but these will be ignored, and each mechanism will be described in a simple form.

The first source mechanism, current flow, is caused by energetic photons propelling electrons through inelastic

scattering processes. Between the scattered electron and its parent ion there is an electric field. If there are asymetries present, unbalanced currents generate both electric and magnetic fields which together radiate a signal. Several sources of this asymetry are:

a. Earth, air interface (surface burst)

b. Case asymetries (case signal)

c. Exponential atmosphere (medium altitude burst)

d. Space, atmosphere interface (high altitude burst)

For all these asymetries gamma rays are more important than are X-rays except for a height of burst above $\sim$ 100 kilometers.

The second major mechanism, electron-magnetic field interaction, operates in the presence of the earth's magnetic field or the field generated by currents due to the explosion. In a dense medium the interaction of electrons with a magnetic field is a secondary effect but does occur. In the thin atmosphere of near space the interaction of electrons with the earth's magnetic field is very important. There are two regions of interaction: around 20-30 kilometers where gammas and neutrons are absorbed and around 100-110 kilometers where X-rays are absorbed. In these regions the earth's magnetic field causes the electrons to move in circular paths, and these accelerated electrons radiate. The radiated signal is energetic and has a low characteristic frequency which is important because low frequencies propagate for long ranges.

The third mechanism is the exclusion of the magnetic field by the expanding ionized sphere. The compression and relaxation of the magnetic field lines radiate a signal, but it is minor compared to the other sources.

In passing we note that the regions of interest and mechanisms can all be considered axially symmetric if local air density and topographic variations are ignored. Because the deviations from axial symmetry cause only second order effects, axial symmetry will be assumed in order to simplify the mathematical description of the problem. We will discuss this point more fully later.

Transmission of the EMP

The radiated EMP is like any other radiated signal in that its propagation can be divided into a near field, an intermediate region, and the far field. The near field may contain a non-radiated component and components which are attenuated rapidly. In the far field only a dipole component is significant. The intermediate region is a combination of the two.

The electromagnetic pulse can be thought of as the summation of a series of trigonometric functions of different frequencies, i.e., a Fourier series. Because a signal's velocity of propagation is usually a function of frequency the shape of the EMP will change with distance.

The signal may be attenuated by the medium. For example, in earth, representative figures show that a

signal will be decreased by 1/e in about 100 feet. In air the attenuation is selective, being more rapid for higher frequencies. In the ionosphere the attenuation is dependent upon the electron density which may have been affected by the nuclear burst. Because an analytical solution for the electric or magnetic fields is virtually impossible, many studies involve numerical solutions to the field differential equations for different situations.

Reception of the EMP

The final area of interest is the reception of the EMP by systems which might be damaged by it. The EMP can enter a susceptible system by induced currents or by conduction currents from magnetic and electric fields respectively. The effects are proportional to such things as area, resistivity, and a coupling coefficient. Some examples in Chapter VII will illustrate reception.

Overview

The next chapter reviews Maxwell's equations because they play a vital role in understanding electromagnetic field relations. The reader who is well grounded in electromagnetic theory may skip this chapter. The succeeding chapters cover the source of the currents, the symmetric burst, asymmetric bursts, transmissio of signals and reception of signals. The asymmetric burst is discussed under three major subdivisions: asymmetric current flow, magnetic field-electron interaction, and magnetic field exclusion.

Each chapter is introduced and summarized. The equations are numbered serially. The appendix details the mathematics behind several processes. A fold-out, page 191, is added to allow Maxwell's equations, conversion factors, and some basic data to be available at all times.

II. Maxwell's Equations

Maxwell's equations describe the behavior of electromagnetic phenomenon in almost all their details (any exceptions appear as a result of quantum effects and do not affect the understanding of EMP). The four Maxwell equations will be introduced through mathematical manipulation and physical arguments. After being introduced they will be used as if they were the basis of electromagnetic phenomenon without regard to their development.

Actually Maxwell originated only one of the four equations, but with it he unified the work of the persons whose names are associated with the other three: Gauss, Ampere, and Faraday. We will consider these in order.

Gauss' Law

Before considering Gauss' law, it is necessary to state the work of C. A. Coulomb. Coulomb formalized the experimental relation between two electric charges as a force proportional to the magnitude of each charge and inversely proportional to their separation distance squared.[7] Coulomb's law is

$$\bar{F} = \frac{\bar{r}\, q_1 q_2}{4\pi \epsilon_0 r^3} \quad \text{(newtons)} \qquad (1)$$

where q_1 , q_2 are the charges in coulombs; $\bar{r}$ is the line between q_1 and q_2 of length r in meters, and ϵ_0 is the

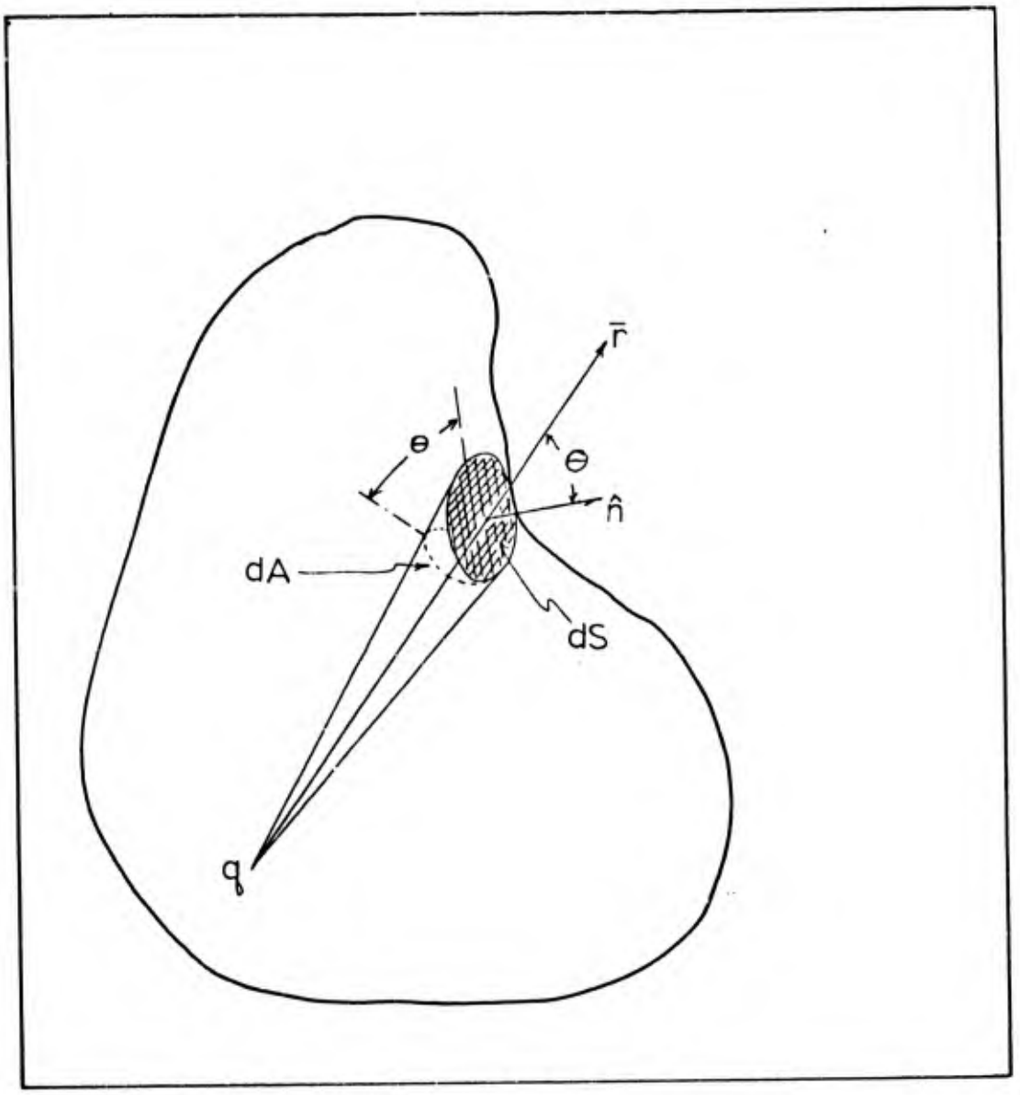

Fig. 1. Gauss' Law.

permittivity of free space (here a proportionality constant) in units of farads per meter. In order to consider the effects due to an isolated charge we introduce the electric field vector, $\bar{E}$, the force on a unit positive charge:

$$\bar{E} = \lim_{q \to 0^+} \frac{\bar{F}}{q} \quad \frac{\text{newtons}}{\text{coul}} \text{ or } \frac{\text{volts}}{\text{m}} \qquad (2)$$

Now Gauss' law relates the total charge within a volume to the total electric field vector, $\bar{E}$, penetrating the bounding surface. Consider a single charge q which is enclosed inside of an arbitrary volume V as shown in Fig. 1. The total surface area of this volume is designated S . By Coulomb's law, the electric field at any point on the surface is

$$\bar{E} = \frac{q\,\bar{r}}{4\pi\epsilon_0 r^3} \qquad (3)$$

where $\bar{r}$ depends upon the location of the charge q and upon the point of the surface which is under consideration. Unless the volume is a sphere with q at the center, $\bar{r}$ changes from one surface point to another. Now let us consider only the field components <u>normal</u> to the surface

$$\bar{E} \cdot \hat{n} = \frac{q\,\bar{r} \cdot \hat{n}}{4\pi\epsilon_0 r^3} \qquad (4)$$

and sum this equality over the entire surface of the arbitrary volume:

$$\oint_S \bar{E}\cdot\hat{n}\,ds = \oint_S \frac{q\,\bar{r}\cdot\hat{n}\,ds}{4\pi\epsilon_0 r^3} \tag{5}$$

The factor $q/4\pi\epsilon_0$ commutes and $\bar{r}\cdot\hat{n}$ may be replaced by $r\cos\Theta$ where Θ is the angle between $\hat{r}$ and $\hat{n}$,

$$\oint_S \bar{E}\cdot\hat{n}\,ds = \frac{q}{4\pi\epsilon_0}\oint_S \frac{\cos\Theta\,ds}{r^2} \tag{6}$$

But, as can be seen from Fig. 1, $\cos\Theta\,ds = dA$ where dA is perpendicular to $\bar{r}$ and dA/r^2 is a differential increment of solid angle, $d\Omega$. The summation over all solid angle is 4π, so

$$\oint_S \bar{E}\cdot\hat{n}\,ds = \frac{q}{\epsilon_0} \tag{7}$$

By superposition, we can extend this argument to a number of charges, q_i, or to a volume distributed charge, $\rho(\bar{r})$, coulombs/m^3, in which case

$$\oint_S \bar{E}\cdot\hat{n}\,ds = \int_{VOL} \frac{\rho(\bar{r})}{\epsilon_0}\,d_{VOL} \tag{8}$$

which is Gauss' law.

Gauss' law can also be expressed in differential form. A theorem due to Gauss himself states that

$$\oint_S \bar{A}\cdot\hat{n}\,ds = \int_{VOL} \nabla\cdot\bar{A}\,d_{VOL} \tag{9}$$

Thus the left hand side of Eq (8) becomes $\int_{VOL} \nabla \cdot \bar{E}\, d_{VOL}$, and we have

$$\int_{VOL} \left(\nabla \cdot \bar{E} - \frac{\rho(\bar{r})}{\epsilon_o} \right) d_{VOL} = 0 \qquad (10)$$

But since the volume is arbitrary, Eq (10) can be zero only if the integrand is zero, which yields Gauss' law in differential form

$$\nabla \cdot \bar{E} = + \frac{\rho(\bar{r})}{\epsilon_o} \qquad (11)$$

which is also the first of Maxwell's equations.[8]

The electric field vector, $\bar{E}$, and ϵ_o may be combined to yield

$$\nabla \cdot \bar{D} = \rho(\bar{r}) \qquad (12)$$

where $\bar{D}$ is known as the displacement vector. We shall return to the divergence of $\bar{D}$ during the discussion of the physical meaning of Maxwell's equations.

Ampere's Circuital Law

Another of Maxwell's equations first appeared as Ampere's circuital law which states that the magnetic field around a closed loop equals the total current through a surface bounded by the loop. We shall derive an integral statement of this law using the force between current elements and a magnetic field vector $\bar{B}$ which has much the

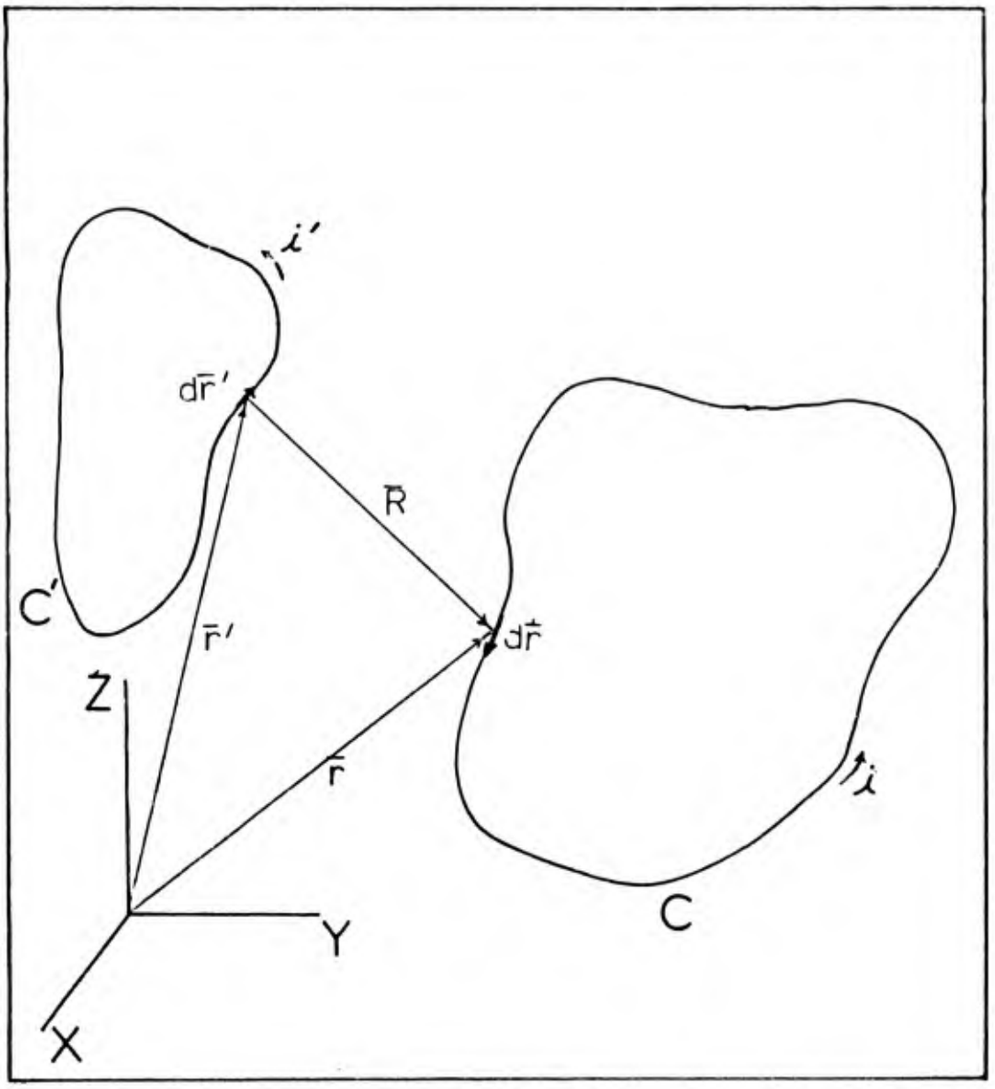

Fig. 2. Ampere's Law.

same fundamental role in a magnetic field as $\bar{E}$ does for the electric field.

Ampere, around 1820, studied the forces between rigid conductors for various values of the current they carried.[9] He arrived at an inverse square relation of the form

$$\bar{F} = \frac{I I'}{4\pi\mu_o^{-1}} \oint_C \oint_{C'} \frac{d\bar{r} \times (d\bar{r}' \times \bar{R})}{R^3} \tag{13}$$

where μ_o = constant of proportionality (magnetic susceptibility $4\pi \times 10^{-7}$ henry/meter).

I, I' = current in circuit (amperes).

$d\bar{r}, d\bar{r}'$ = incremental length of circuit with conventional orientation, i.e., bounded surface is on left of direction of travel.

$\bar{R} = \bar{r} - \bar{r}'$ = vector from $d\bar{r}'$ to $d\bar{r}$ of magnitude R (meters).

and C and C' are any two closed circuits such as shown in Fig. 2. The increment of force that all of circuit C' exerts on an <u>increment</u> of circuit C is

$$d F(\bar{r}) = \frac{I' I \, d\bar{r} \times \oint_{C'} (d\bar{r}' \times \bar{R})}{4\pi\mu_o^{-1}} \frac{}{R^3} \tag{14}$$

Just as in the electrostatic case where $\bar{E} = \bar{F}/q_0$, let us define a magnetic-force-per-element-of-current as a field quantity, $\bar{B}$, which is called magnetic induction (in webers/meter^2),

i.e., $$B(\bar{r}) = \frac{d F_{max}}{I \, dr} \tag{15}$$

or by Eq (14)

$$\bar{B}(r) = \frac{1}{4\pi\mu_0^{-1}} \oint_{C'} \frac{I' d\bar{r}' \times \bar{R}}{R^3} \tag{16}$$

Compare with $\bar{E}(r) = \frac{1}{4\pi\epsilon_0} \frac{q\bar{R}}{R^3}$

where the primed coordinates refer to the source of the field in contrast to the unprimed coordinates which are field points.

By using vector identities and the properties of the del operator, ∇, we shall derive three useful relations: continuity of the $\bar{B}$ vector; a vector potential $\bar{A}$; and Ampere's circuital law. Since $\nabla\left(\frac{1}{R}\right) = \bar{R}/R^3$ the expression for $\bar{B}$ becomes

$$\bar{B} = \frac{1}{4\pi\mu_0^{-1}} \oint_{C'} I' d\bar{r}' \times \nabla\left(\frac{1}{R}\right) \tag{17}$$

By the vector identity $d\bar{r}' \times \nabla\left(\frac{1}{R}\right) = \nabla \times \frac{d\bar{r}'}{R} - \frac{1}{R} \nabla \times d\bar{r}'$

Eq (17) becomes

$$\bar{B} = \frac{1}{4\pi\mu_0^{-1}} \left[\oint_{C'} I' \nabla \times \left(\frac{d\bar{r}'}{R}\right) + \oint_{C'} I' \left(-\frac{1}{R}\right) \nabla \times d\bar{r}' \right] \tag{18}$$

but the last term is zero because the del operator is over the unprimed (or field) coordinates

or $$\bar{B} = \frac{1}{4\pi\mu_0^-}\oint_{C'} \frac{I'\nabla \times d\bar{r}'}{R} \tag{19}$$

Further, the del operator commutes since it still does not affect the field-source terms,

thus $$\bar{B} = \nabla \times \left[\frac{1}{4\pi\mu_0^{-1}}\oint_{C'} \frac{I' d\bar{r}'}{R}\right] \tag{20}$$

By taking the divergence of this expression we see that,

$$\nabla \cdot \bar{B} = \nabla \cdot \nabla \times \left[\frac{1}{4\pi\mu_0^{-1}}\oint_{C'} \frac{I' d\bar{r}'}{R}\right] \tag{21}$$

but because of the vector identity $\nabla \cdot \nabla \times (\ ) = 0$,

$$\nabla \cdot \bar{B} = 0 \tag{22}$$

Equation (22) is a mathematical statement of the continuity of the $\bar{B}$ vector and is another of Maxwell's laws.

The bracketed function in Eq (20) is designated the vector potential, $\bar{A}$. Now $\bar{B} = \nabla \times \bar{A}$ in <u>all</u> cases. From vector analysis

$$\nabla \times (\ ) = -\nabla^2(\ ) + \nabla(\nabla \cdot (\ )) \tag{23}$$

which, for the magnetic induction has a zero final term; therefore

$$\nabla \times \bar{B} = -\nabla^2 \bar{A} \tag{24}$$

Carrying out the indicated Laplacian operation on $\bar{A}$ gives

$$\nabla \times \bar{B} = \frac{\bar{J}}{\mu_o^{-1}} \tag{25}$$

or

$$\nabla \times \bar{H} = \bar{J} \tag{26}$$

where $\bar{J}$ is the source-current density in amperes-meter^{-2}

and

$$\bar{H} = \mu_o^{-1} \bar{B} \tag{27}$$

where $\bar{H}$ the magnetic field in amperes/meter.

Summing the current density through a surface S bounded by a curve C leads to Ampere's circuital law. Integrating Eq (26)

$$\int_S \bar{J} \cdot d\bar{S} = \int_S \nabla \times \bar{H} \cdot d\bar{S} \tag{28}$$

and by Stoke's theorem

$$\int_S \nabla \times \bar{H} \cdot d\bar{S} = \oint \bar{H} \cdot d\bar{\ell} \tag{29}$$

therefore

$$I = \oint \bar{H} \cdot d\bar{\ell} \tag{30}$$

where $I = \int_S \bar{J} \cdot d\bar{S}$ is the total current through the surface. Equation (30) is Ampere's circuital law, the steady state

form of one of the Maxwell equations. The general form will be shown after noting two time dependent relations.

Faraday's Law

Faraday's law, the third of the Maxwell equations, was developed about 1852 by M. Faraday and, independently by J. Henry, but by right of first publication Faraday's name is commonly associated with the effect.[10] These men experimentally found that the voltage induced in a circuit was proportional to the rate of change of magnetic flux

$$V = -\frac{d\psi}{dt} \tag{31}$$

where ψ is the total magnetic flux in webers through the surface of the circuit:

$$\psi = \int_S \bar{B}\cdot d\bar{s} \tag{32}$$

and

$$V = \oint \bar{E}\cdot d\bar{l} \tag{33}$$

where V is in volts. From Eqs (31), (32), and (33) we have the integral form of Faraday's law[11]

$$\oint \bar{E}\cdot d\bar{l} = -\frac{d}{dt}\int_S \bar{B}\cdot d\bar{s} \tag{34}$$

For the differential or point formulation we transform the line integral to a surface integral by Stoke's theorem and have

$$\int_S \nabla \times \bar{E} \cdot d\bar{s} = -\int_S \frac{\partial \bar{B}}{\partial t} \cdot d\bar{s} \tag{35}$$

where $S \neq S(t)$ or

$$\int_S \left[\nabla \times \bar{E} + \frac{\partial \bar{B}}{\partial t} \right] \cdot d\bar{s} = 0 \tag{36}$$

Because the surface S is arbitrary, the integrand must be zero and

$$\nabla \times \bar{E} + \frac{\partial \bar{B}}{\partial t} = 0 \tag{37}$$

which is the differential form of Faraday's law and another of Maxwell's equations.

Conservation of Charge

Before we examine a gedanken experiment which illustrates Maxwell's contribution, let us consider conservation of charge or the continuity equation. In a volume V, the net change of charge is $\partial\rho/\partial t$ which must equal the flow into or out of the surface, given by $\nabla \cdot \bar{J}$ or

$$\frac{\partial \rho}{\partial t} = -\nabla \cdot \bar{J} \tag{38}$$

The minus sign is present to account for the outward normal to the surface.

Maxwell's Contribution

A discrepancy which J. C. Maxwell's contribution removes can best be seen by applying Ampere's circuital law to surfaces I and II in Fig. 3. The current which flows into the capacitor for a time has a magnetic field associated with it. The magnetic field found by considering surface I is $H = I/\ell$; but considering surface II $H = 0$ since there is no current through that surface. In 1861 Maxwell proposed a current, $\frac{\partial \bar{D}}{\partial t}$ (called displacement current), so that Eq (26) becomes

$$\nabla \times \bar{H} = \bar{J} + \frac{\partial \bar{D}}{\partial t}$$

which experiment soon proved to be correct. This displacement current removes the illust ated discrepancy.[13]

Maxwell's Equations

A summary of our results shows the Maxwell equations:

$$\text{I} \qquad \nabla \cdot \bar{D} - \rho(\bar{r}) = 0 \qquad (39)$$

$$\text{II} \qquad \nabla \cdot \bar{B} = 0 \qquad (40)$$

$$\text{III} \qquad \nabla \times \bar{E} + \frac{\partial \bar{B}}{\partial t} = 0 \qquad (41)$$

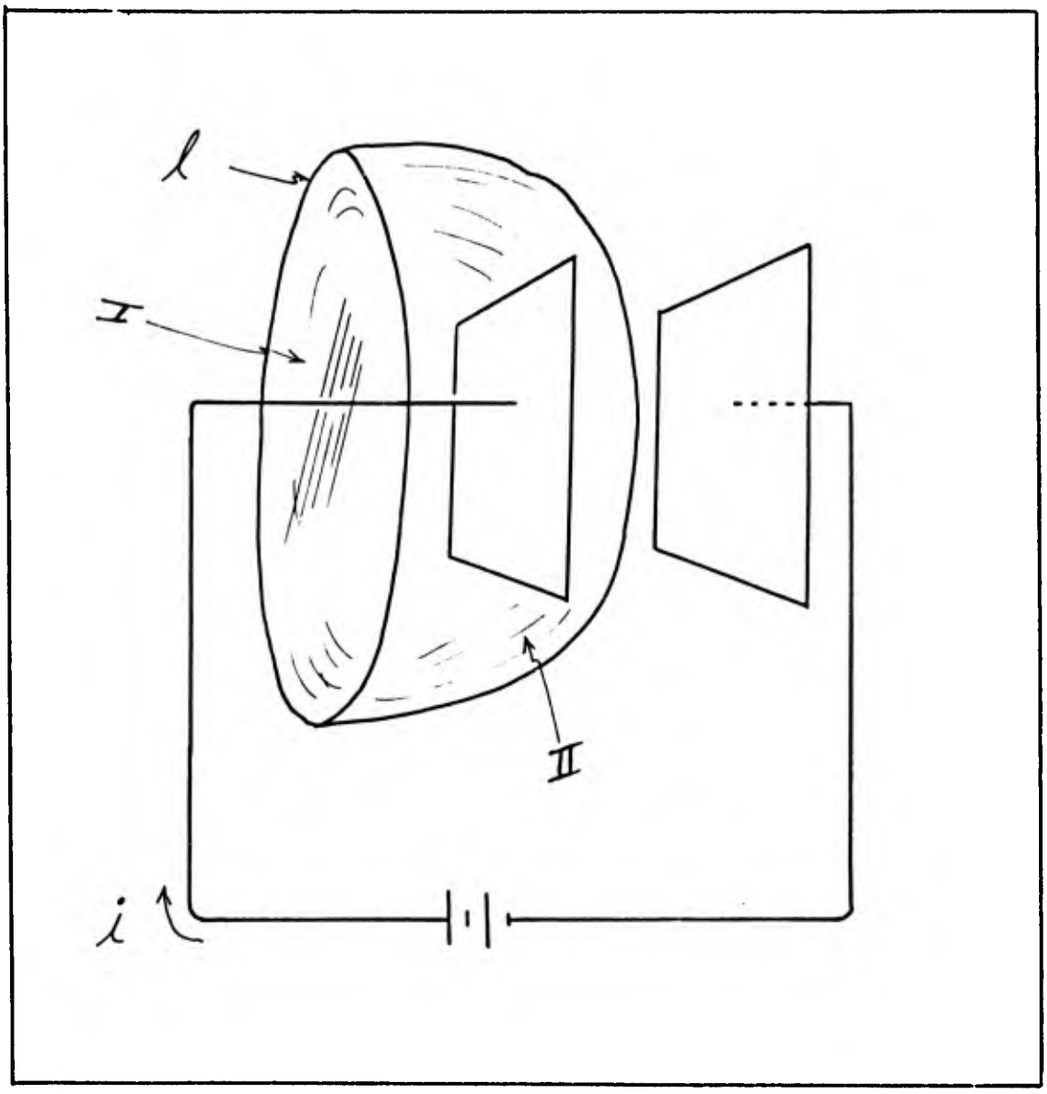

Fig. 3. Maxwell's Contribution. The current loop penetrates two surfaces. Surface I is penetrated by the wire of the circuit. Surface II is not penetrated by the wire but instead passes through the capacitor's plates. Surface I and II have a common boundary.

$$\text{IV} \qquad \nabla \times \bar{H} \quad - \frac{\partial \bar{D}}{\partial t} \quad - \bar{J} \quad = 0 \qquad (42)$$

and two additional equations: $\bar{H} = \mu_o^{-1} \bar{B}$ and $\bar{D} = \epsilon_o \bar{E}$.

Note the similarity between the equations and that $\bar{E}$ and $\bar{D}$ hold places similar to $\bar{B}$ and $\bar{H}$ respectively; also note that ϵ_o and μ_o^{-1} have similar functions. This can aid in transferring mathematical ideas from one type of field to the other.

In Eq II we see that there is no magnetic pole distribution comparable to the charge distribution in Eq I. That is a statement that no isolated N or S magnetic poles exist or every point in space is magnetically "neutral". This has its parallel in Eq III where we see no magnetic current, $\bar{J}_{\text{N-poles}}$ or $\bar{J}_{\text{S-poles}}$ is evident.

Word Picture

A word picture of the physical meaning of Maxwell's equations is possible.

Equation I, $\nabla \cdot \bar{D} - \rho(\bar{r}) = 0$, implies that the $\bar{D}$ vectors start on positive charges and end on negative charges; in the presence of material such that $\bar{D} \neq \epsilon_o \bar{E}$, the ends of the $\bar{E}$ vectors can be thought of as associated with induced charges, and $\bar{D}$ vectors continue to be attached to real charges.[14] (See Fig. 4).

Equation II, $\nabla \cdot \bar{B} = 0$, states that $\bar{B}$ vectors form continuous loops. The distinction between $\bar{B}$ and $\bar{H}$ is

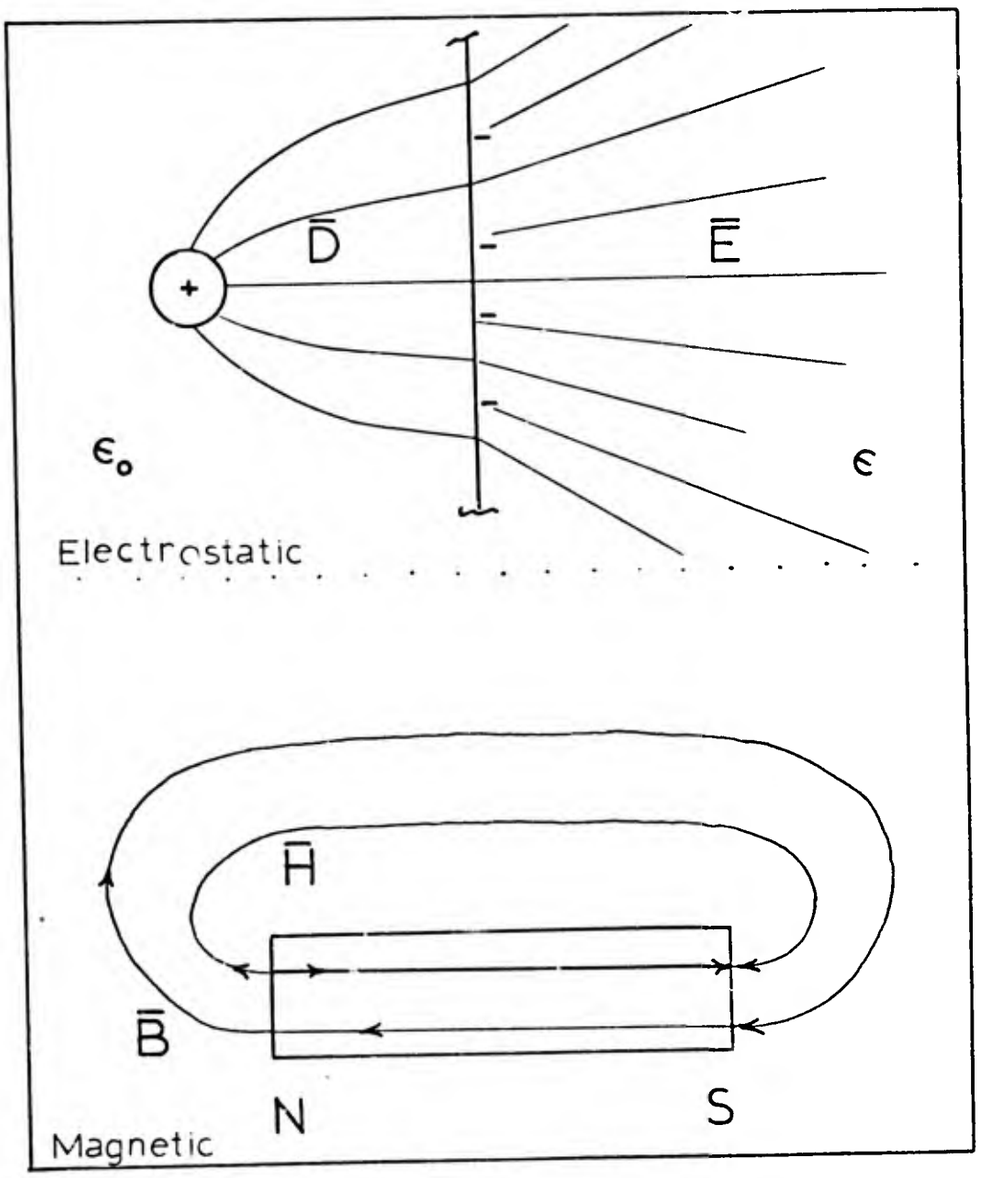

Fig. 4. Illustration of Continuity of Field Lines.

similar to that between $\bar{E}$ and $\bar{D}$ but with $\bar{H}$ being created by induced or amperian currents and $\bar{B}$ due to true currents. $\bar{H}$ vectors start and stop on isolated poles which can be imagined for their mathematical convenience.

Equation III, $\oint \bar{E} \cdot d\bar{\ell} = -\frac{\partial}{\partial t} \int_S \bar{B} \cdot d\bar{s}$ (integral form), shows that a changing magnetic field creates an electric field.

Equation IV, $\oint \bar{H} \cdot d\bar{\ell} = \frac{\partial}{\partial t} \int_S \bar{D} \cdot d\bar{s} + \int_S \bar{J} \cdot d\bar{s}$ (integral form), shows that a changing electric field creates a magnetic field and so does a steady current.

Boundary Conditions

In general the boundary conditions on the field vectors are that the normal component of $\bar{B}$ is continuous, the tangential component of $\bar{E}$ is continuous, the normal component of $\bar{D}$ changes by the value of any boundary surface charge density (σ_s) and the tangential component of $\bar{H}$ changes by the value of the surface current density ($\bar{J}_s$).[15] In equations we have

$$B_n - B_n' = 0 \tag{43}$$

$$E_t - E_t' = 0 \tag{44}$$

$$D_n - D_n' = \sigma_s \tag{45}$$

$$H_t - H_t' = J_s \quad \text{(perfect conductor)} \tag{46}$$

Two additional relations are helpful in dealing with electromagnetic problems: the Lorentz force and Ohm's law.

Lorentz Force Equation

The Lorentz force equation is easily derived from the theory of special relativity. (The equation's second term is a relativistic correction to the force $q\bar{E}$).[16] Here we shall only present the equation and suggest that it is true; it is

$$\bar{F} = q\bar{E} + q\,\bar{v} \times \bar{B} \tag{47}$$

where $\bar{v}$ is the velocity of the charge q relative to the field $\bar{B}$. In the absence of an electric field $\bar{E}$, the equation is (for a differential of charge dq):

$$d\bar{F} = dq\,\bar{v} \times \bar{B} \tag{48a}$$

$$= dq\,\frac{d\bar{r}}{dt} \times \bar{B} \tag{48b}$$

$$= \frac{dq}{dt}\,d\bar{r} \times \bar{B} \tag{48c}$$

$$= i\,d\bar{r} \times \bar{B} \tag{48d}$$

which is the vector form of the defining equation for $\bar{B}$. Thus we have indicated the validity of the Lorentz equation.

Ohm's Law

Finally we have Ohm's law, $V = IR$ or as we shall use it

$$\bar{J} = \sigma \bar{E} \tag{49}$$

Conclusion

Maxwell's equations and the constitutive equations presented here are slightly restricted in that some linear relations (specifically $\bar{D} = \epsilon_o \bar{E}$ and $\bar{H} = \mu_o^{-1} \bar{B}$) were used whereas reality is usually non-linear. These restrictions should not affect the material as presented in this thesis.

In general, the vector and scalar potentials are easier to deal with than are the $\bar{E}$ and $\bar{B}$ vector relations; the point forms of Maxwell's equations are more useful than the integral forms; and adroit use of physical insight, well chosen boundaries, and appropriate simplifications are needed to solve Maxwell's equations.

III. Current Source

Overview

The electric and magnetic fields of the EMP are generated by currents near a nuclear burst. These currents are the motion of electrons or ions outside a sphere which contains a nearly full ionized plasma in which there is no net current flow (This isothermal burst sphere is the fireball of early times up until hydrodynamic separation*). The initial motion is that of electrons moved by energetic photons by Compton scattering hence the name Compton current.

After a photon-electron interaction, momentum must be conserved and since the photons move radially outward, so too will most of the electrons. This movement of electrons is a current, the asymmetries of which dictate the electromagnetic field to expect. For example, an external magnetic field (such as the earth's geomagnetic field) causes the electron to turn generating currents which subsequently radiate an EMP. Figure 5 summarizes the process.

The behavior of the currents generated depends largely upon the behavior of the photon sources. In this chapter we will consider photon sources (gamma sources, X-ray sources and neutrons as a source); the photon attenuation; and finally the relation of photon flux to current.

---

*Glasstone, Samuel. The Effects of Nuclear Weapons, AFP 136-1-3. Washington: Department of Defense, April 1962. (Page 71)

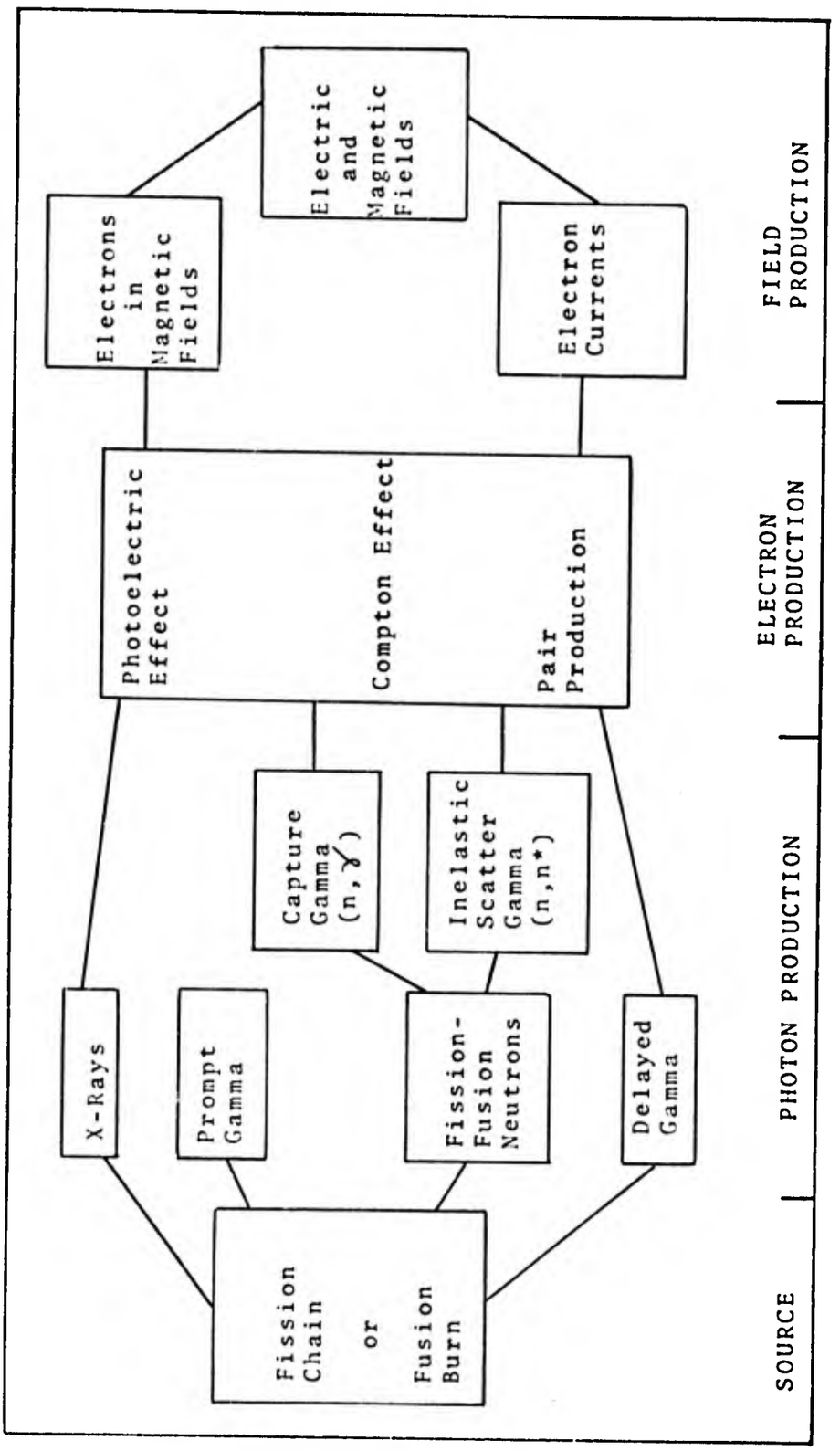

Fig. 5. Block Diagram of Steps in Generating an EMP.[17]

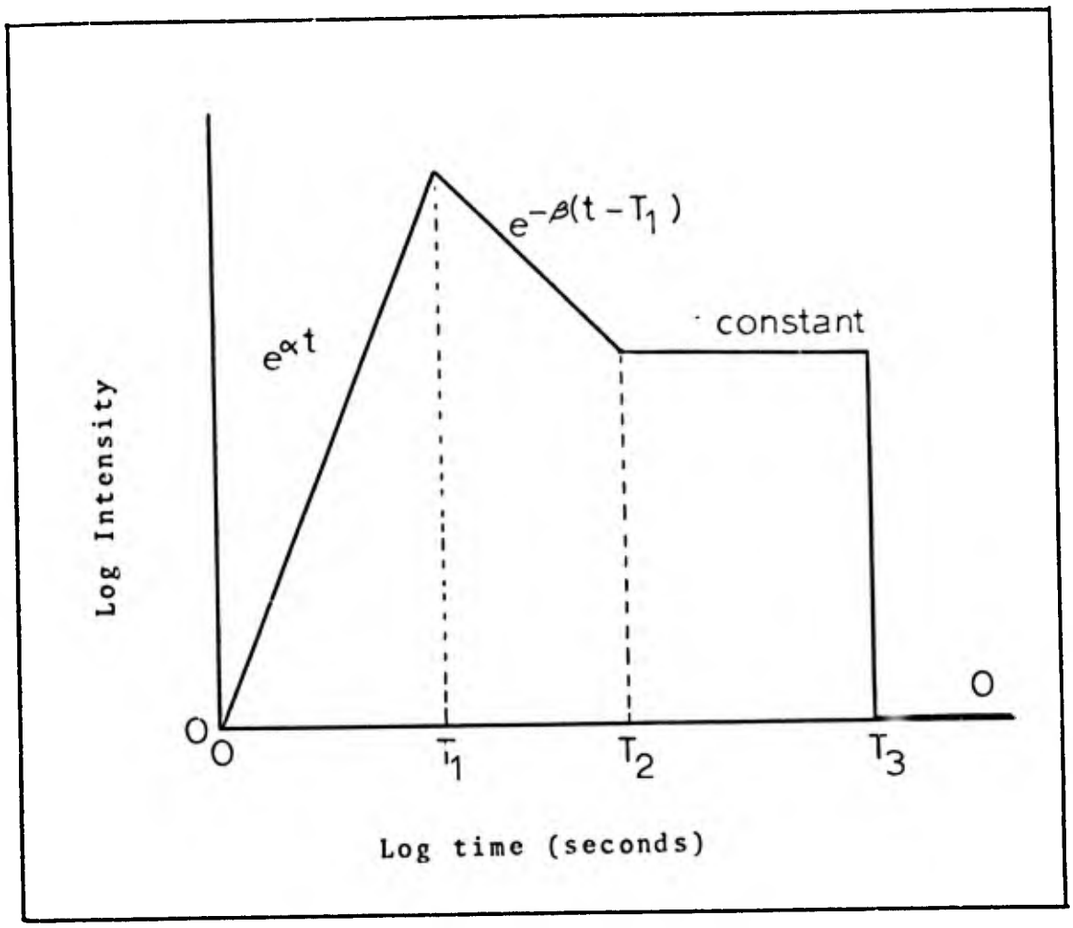

Fig. 6. Time Dependence of Bomb X-Ray or Gamma Output.[18]

Photon Production

Figure 5 shows that several photon sources are present. We will discuss the time and magnitude behavior of gamma rays, X-rays, and neutrons in the following sections. Simplified models of the sources will also be discussed.

Gamma Rays. The gamma source can be modeled by a point source whose intensity grows exponentially to a peak, then decays exponentially at a slower rate for a time, then is constant, and finally drops to zero. This is illustrated in Fig.6. For some uses the central source is modeled by a sphere of finite radius. In this thesis we will assume the gamma source to be

$$\frac{dN}{dt} = \frac{Y \epsilon f(t)}{E} \tag{50}$$

where Y is the yield of the explosion (in MeV), E is the average photon energy (MeV), ϵ is the fraction of the yield released as gammas, $f(t)$ is the time variation of the source, and N is the number of gamma rays.[19] This time variation is normalized so that

$$\int_{-\infty}^{\infty} f(t)\,dt = 1 \tag{51}$$

The assumed time variation is (on the basis of Fig. 6)

$$f(t) = 0 \qquad , t \in (-\infty, 0) \tag{52}$$

$$f(t) = 0 \qquad , t \in (T_3, \infty) \tag{53}$$

$$f(t) = A e^{\alpha t} \qquad , t \in [0, T_1] \tag{54}$$

$$f(t) = B e^{-\beta(t-T_1)} \qquad , t \in (T_1, T_2] \tag{55}$$

$$f(t) = C \qquad , t \in (T_2, T_3] \tag{56}$$

where we chose $T_1 \sim 3/\alpha$; $T_2 \sim 30\, T_1 = 90/\alpha$; $T_3 \sim 300\, T_1 = 900/\alpha$ and $10\beta = \alpha$. Through the boundary conditions that $f(T_i^-) = f(T_i^+)$ we have

$$B = A e^{\alpha T_1} \tag{57}$$

$$C = B e^{-\beta(T_2 - T_1)} \tag{58a}$$

$$= A e^{\alpha T_1} e^{-\beta(T_2 - T_1)} \tag{58b}$$

By normalization we have $A \cong \alpha/225$

For Example 1 let us find the gamma source function of a one megaton explosion which emits 0.3 percent of its yield as 1.5 MeV gamma rays. We have

$$\frac{dN}{dt} = 10^3 (kt) \cdot \frac{2.61 \times 10^{25}}{1.5 (MeV)} (MeV/kt)(0.003) \cdot \frac{10^8}{225} e^{\alpha t} \tag{59a}$$

or

$$\frac{dN}{dt} = 231 \times 10^{31} e^{\alpha t} \quad \frac{\text{gammas}}{\text{second}} \qquad t \in [0, T_1] \qquad (59b)$$

where we have chosen a hypothetical alpha of 10^{+8} second^{-1}.

The spectrum used in the preceding example was a monoenergetic photon source. Using the Maienschein prompt gamma spectrum, R. E. LeLevier found that at sea level the main contribution to the Compton current was due to 1.5 MeV gammas out to 500 meters and due to 2.5 MeV gammas at 1000 meters (Fig. 7).[20] Therefore we shall use 1.5 MeV as the mean photon energy throughout this thesis.

This mean energy is due to a combination of prompt fission gammas and inelastic scatter gammas. The spectrum of fission gamma rays has a mean energy of $\sim$ 1 MeV, a 1 MeV gamma implies an average forward-scatter energy of 0.4 MeV for the Compton electrons. Because fission and fusion neutrons have energies which exceed the threshold energy for inelastic scatter with case materials, a second, distinct spectrum of gammas is produced which has a mean energy of $\sim$4-5 MeV. The average electron forward energy from 4 MeV gammas would be $\sim$ 2.5 MeV. The ion pair production due to a 1.5 MeV photon is $\sim 2 \times 10^4$ ion pairs per photon (see Eq (99a)) which compares well with 3×10^4 cited by Karzas and Latter.[21]

The gamma spectrum grows harder farther from the source because the higher absorption at low energies removes the low energy photons. The spectrum grows harder with time

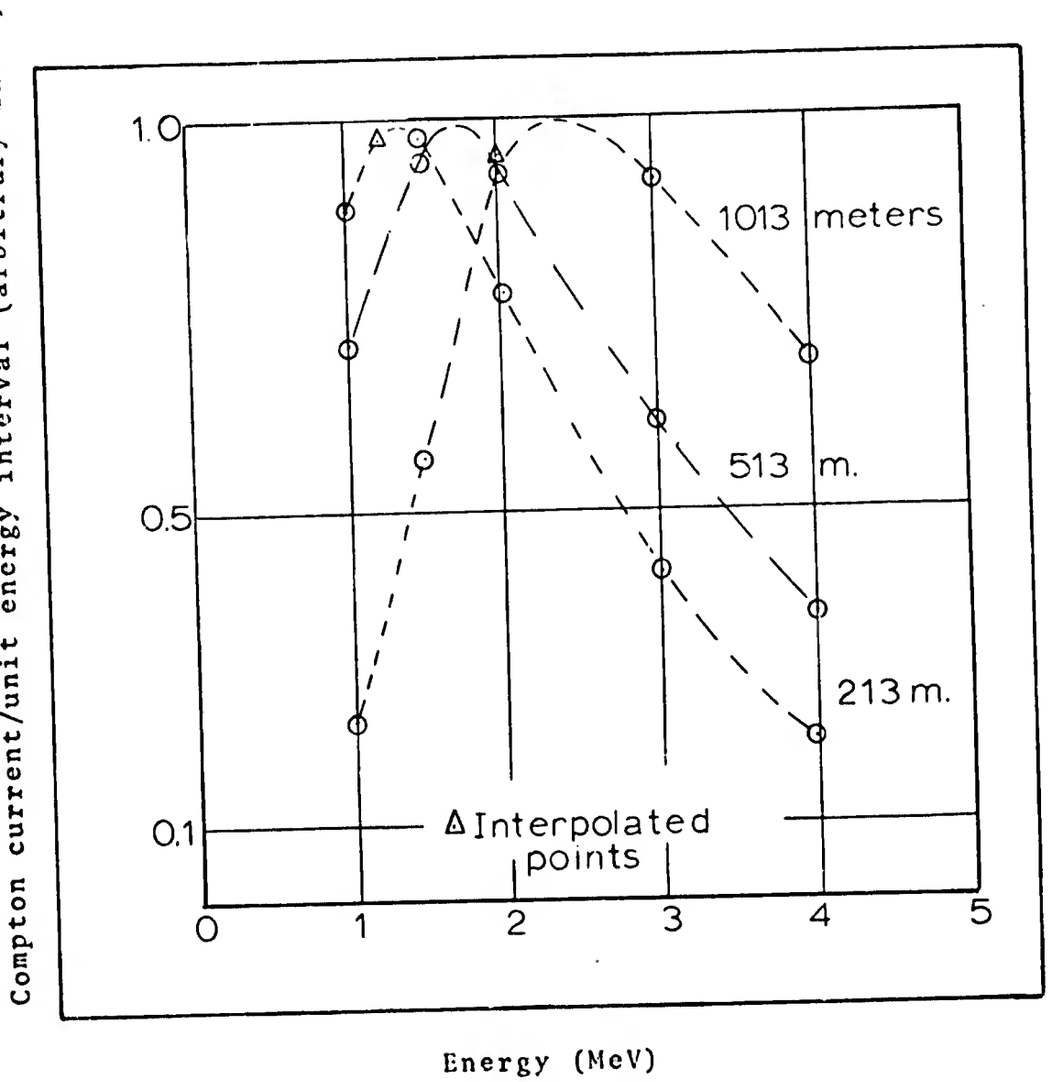

Fig. 7. Compton current per unit energy interval for the Maienschein spectrum.[20]

since the average energy of the nitrogen capture gammas is ~ 5 MeV,[22] much higher than the assumed initial average of 1.5 MeV.

X-Rays. The extremely energetic particles and contained heat energy within the interior of the fireball quickly equilibriate and are then the equivalent of a blackbody. Karzas and Latter[23] state that the X-ray output can be modeled by a 1000 eV (1 KeV) blackbody; the mean energy of a 1 KeV blackbody is 3.8 KeV. About 80 percent of the yield of fission weapons is emitted as X-rays. We shall assume a 1 KeV X-ray spectrum and assume that the X-rays follow the same time and space variations as gamma rays, Eq (50).

Neutrons. Prompt fission gammas are the major source of early gammas, but at later times neutron inelastic scattering in the air, and neutron inelastic scattering and capture in the ground produce most of the gammas. Still later, the isomeric decay of fission fragments, neutron capture in the air, and, finally, gammas following beta decay of fission products dominate the photon source.[24] In space the processes depending on the presence of air must be neglected. Neutrons interact in several other ways, e.g., (n,d); (n,p); and elastic scattering which can produce an energetic ion. These may require study in a detailed calculation of the EMP.[25] All of the interactions listed would produce intense ionization and affect the conductivity of the region in which they occur.

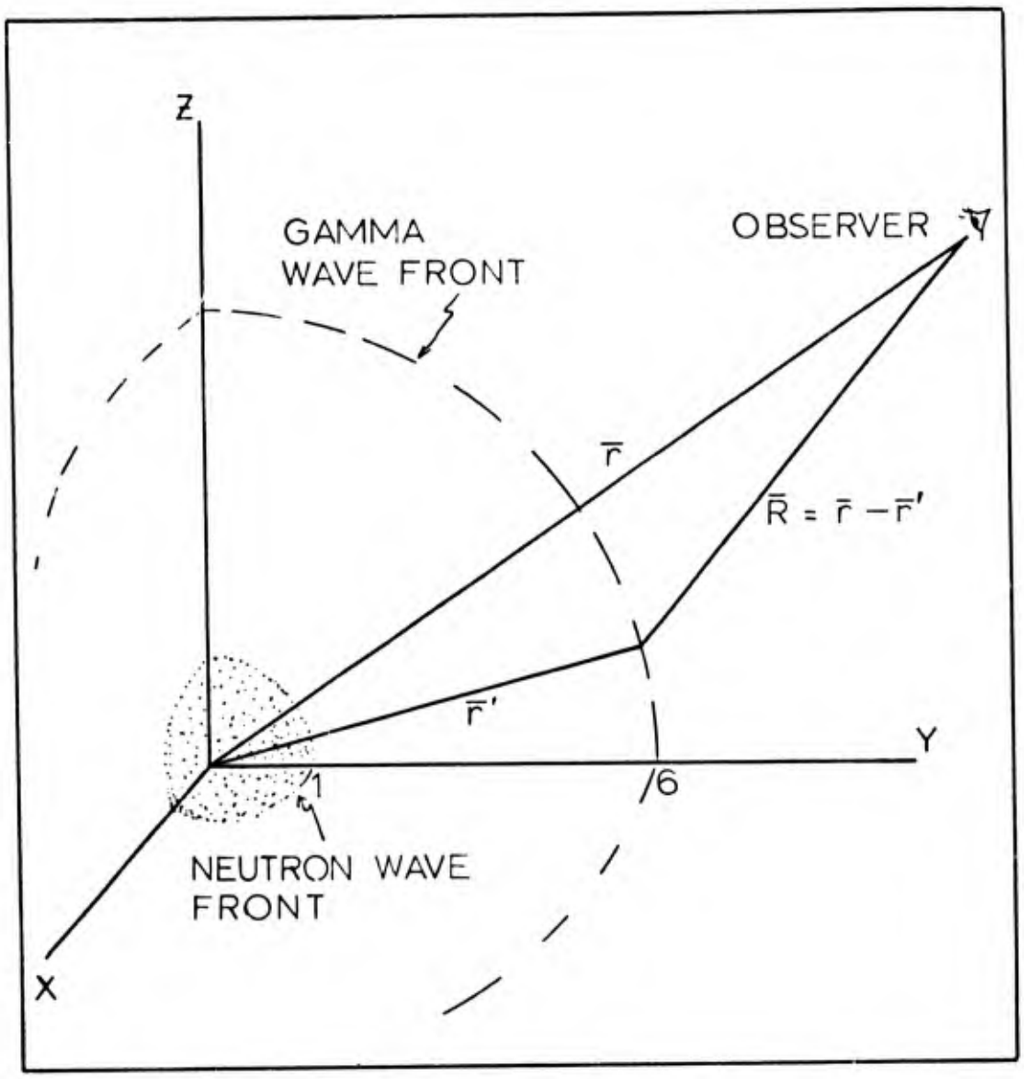

Fig. 8. Stationary Neutron Source Model. The observer at P can approximate the gamma source as a point until the neutron wave front is comparable in size with $\bar{r}$.

A typical inelastic scatter reaction is the nitrogen reaction

$$N^{14}(n,n\gamma)N^{14}$$

which may occur when the incident neutron energy exceeds the threshold energy. The cross section for this reaction is about 0.5 barns if the neutron energy is $\gtrsim$ 7 MeV and 4-5 MeV photons are emitted.[26]

The gammas produced by neutrons account for the late time behavior of the source. This neutron source can be modeled or approximated by the "rattle" or stationary source model which assumes that all neutron induced gammas originate from the burst point itself. (See Fig. 8.) In this model, neutrons rattle about near the burst point being absorbed according to their velocity v and inelastic scatter cross section $\sum(n,n^*)$. This results in a gamma ray production rate of

$$\frac{dN}{dt} = N(t)_{o_n} v \sum(n,n^*) \tag{60}$$

where $N(t)_{o_n}$, is the number of neutrons present at time t and is

$$N(t)_{o_n} = N_o e^{-\sum vt} \tag{61a}$$

$$= N_o e^{-\beta t} \tag{61b}$$

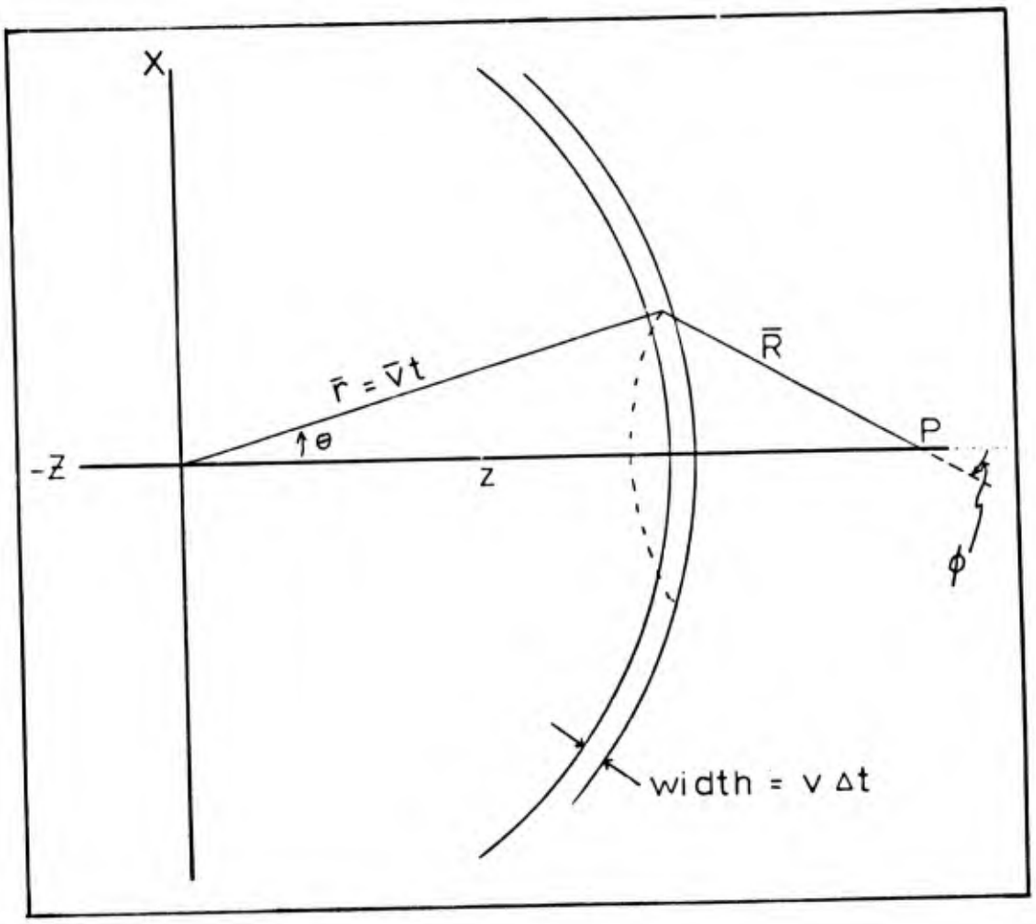

Fig. 9. Spherical Shell Model for Monoenergetic Neutron Pulse. Current and ionization rates at P can be calculated by the use of spherical harmonics. The neutron shell is modeled by a square pulse.[28]

or the gamma production rate is proportional to $e^{-\beta t}$.[27]

This approximation is good while the radius of the expanding shell of neutrons is small compared to the distance to an external observer. A 14 MeV neutron has a velocity of 1.52×10^7 meters-sec^{-1} or $\sim 1/6$ the velocity of light so we see that the gamma flux does precede the neutrons for early times.

A model valid at later times is the shell model which assumes that the neutrons are in a shell whose radius increases at the velocity of the neutrons. Shaeffer and Hale describe the shell model which is illustrated in Fig. 9. The current and ionization rates will peak when the neutron shell arrives at the observer point due to the decreased effect of the $1/r^2$ attentuation of the gammas emitted from the shell.[29] Shaeffer uses this model for a spherical shell of monoenergetic neutrons; Hale[30] compares this model with more accurate calculations.

Photon Attenuation

The virgin or unreacted flux from a point source is given by

$$\phi(\bar{r},t) = \frac{dN(t)}{dt} g(\bar{r}) \tag{62}$$

or

$$\phi(\bar{r},t) = \frac{dN(t)\, e^{-\int_0^r \mu_a(r)dr}}{dt \;\; 4\pi r^3} \bar{r} \tag{63}$$

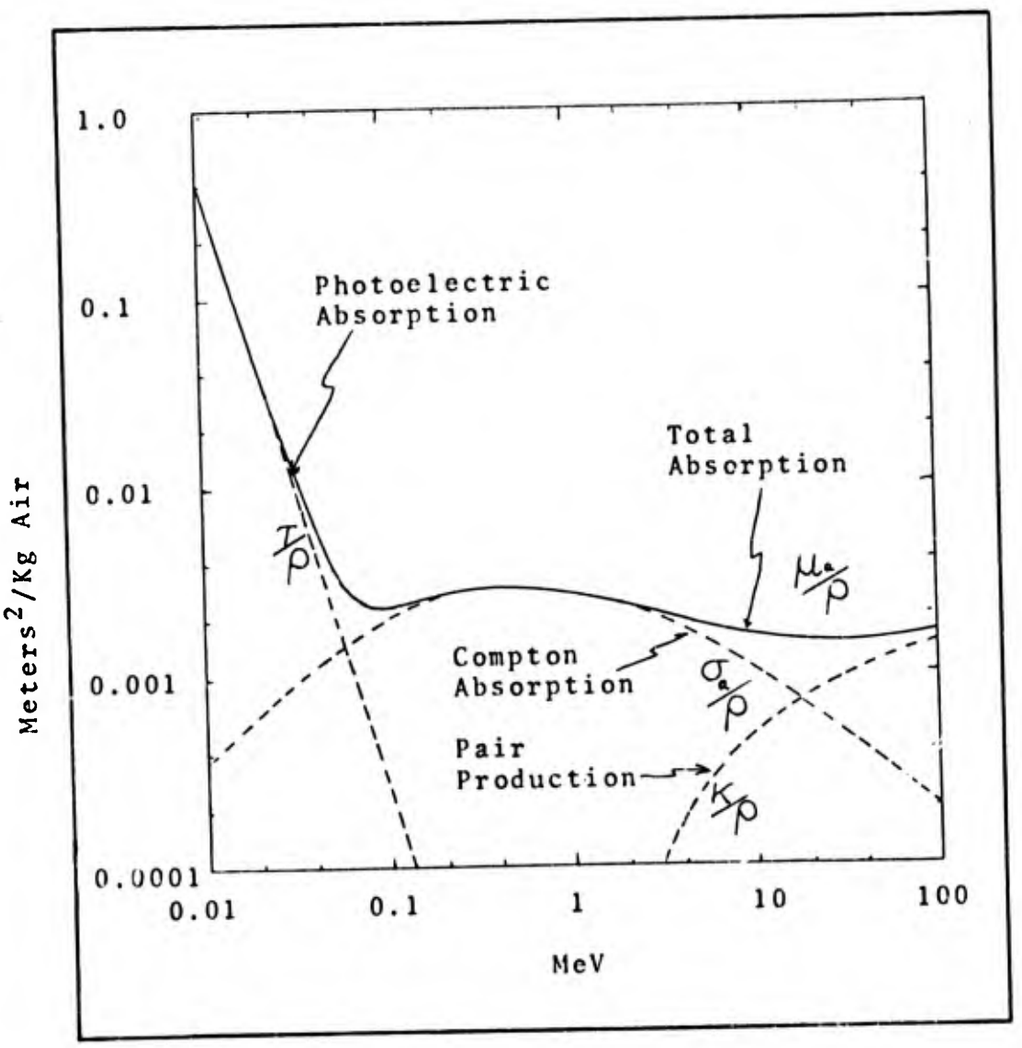

Fig. 10. Mass Attenuation Coefficients for Photons in Air. The curve marked "total absorption" is $(\mu_a/\rho) = (\sigma_a/\rho) + (\tau/\rho) + (\kappa/\rho)$ where σ_a , τ and κ are the corresponding linear coefficients for Compton absorption, photoelectric absorption, and pair production; ρ is the air density. For example at 1.5 MeV the Compton absorption is 2.4×10^{-3} meter^2/kg of air; at 0° C and 760 mm Hg pressure, the density of air is $\rho = 1.293$ kg/m^3.[31]

where $\bar{r}$ is radial position (meters) and $\mu_a(r)$ is a cross section for photon removal (meter^{-1}).[32] The assumptions that allow this function to be used for all purposes include time independent cross sections, no scattered photons; and no time retardation.

These assumptions are valid for a rapidly increasing source rate; one much larger than the rate of change of electron density due to scattered photons. If the source rate is rapidly decreasing the Compton current and energy deposition rate are mainly determined by the scattered photons, i.e., the photons associated with the build-up factor. If the time variation of the source is slow relative to the time-spreading induced by the multiple scattering then both virgin and scattered photon reactions must be considered.[33]

The cross section for photon removal, μ_a, is the sum of the cross sections for three processes: photoelectric effect, Compton effect, and pair production. Each is dominant in a different energy region as shown by the graph of their cross section, Fig. 10. X-rays are mainly attenuated by the photoelectric effect and gamma rays are most heavily attenuated by the Compton process (for the energies we are concerned with). The forward scatter of photoelectrons is less pronounced than the forward scatter of Compton electrons because the Compton effect does not involve the nucleus and the high gamma momentum is partially transferred to the electron.

At high energies ($>$ 1.02 MeV) pair production dominates. The two particles produced have a radial component to their travel; however they do not contribute to an electric field since they are neutral overall, i.e., an electron and a positron cancel in charge. We shall not consider pair production further.

Photoelectric Effect. The photoelectric effect is due to the force upon an electron due to the electric field, $\bar{E}$, of the incident photon. Because $\bar{E}$ is normal to the incident photon's direction of travel the predominant scatter at low energies is normal to the photon momentum vector. Because all the energy (less the binding energy) of the photon is absorbed by the electron, the electron's momentum is greater than the photon's. To conserve momentum the atom recoils.[34]

Because a bound electron is in an energy well, the incident photon's energy must exceed the well's energy deficiency in order to free the electron. This implies that the cross section for photoelectric effect will take sudden jumps as the photon energy increases enough to free more tightly bound electrons from an atom's inner shells. The increase in cross section is due to the increase in the number of available interaction particles. Of all the major air constituents, oxygen has the largest absorption edge at 0.532 KeV, well below the average energy (3.8 KeV) emitted by a 1.0 KeV blackbody.[35]

Overall, however, the photoelectric cross section decreases as photon energy increases. The decrease can be thought of as due to the decrease in the time available for the $\bar{E}$ vector to accelerate the electron (the frequency increases as the photon's energy increases so the $\bar{E}$ vector direction changes more rapidly).

The angular distribution of the photoelectron becomes more forward biased as the photon energy increases, but the biasing is not really strong until the photon energy is in the 10's of KeV. An expression relating the electron forward momentum and incident photon momentum is

$$R = \left(1+\frac{2m_oc^2}{h\nu}\right)^{1/2}\langle\cos\theta\rangle = \frac{\text{Average Photoelectron Forward Momentum}}{\text{Photon Momentum}} \qquad (64)$$

where R is $\sim$ 1.5 - 1.6 for photons with energies from 0.5 MeV to zero?[36] Karzas and Latter[37] assign the value $4/5\ v/c$ to the mean cosine of the scatter angle, η, for the photoelectric effect. For photoelectrons with 1 to a few KeV energy they state that $\eta \simeq$ 0.05 to 0.1.

Compton Effect

In our discussion of the Compton effect we shall ignore scattered photons and concern ourselves only with the electron dislodged by a virgin photon traveling radially outward from a central source. The scattered photons are ignored because their energy is about half the incident photon's energy and because their direction is somewhat

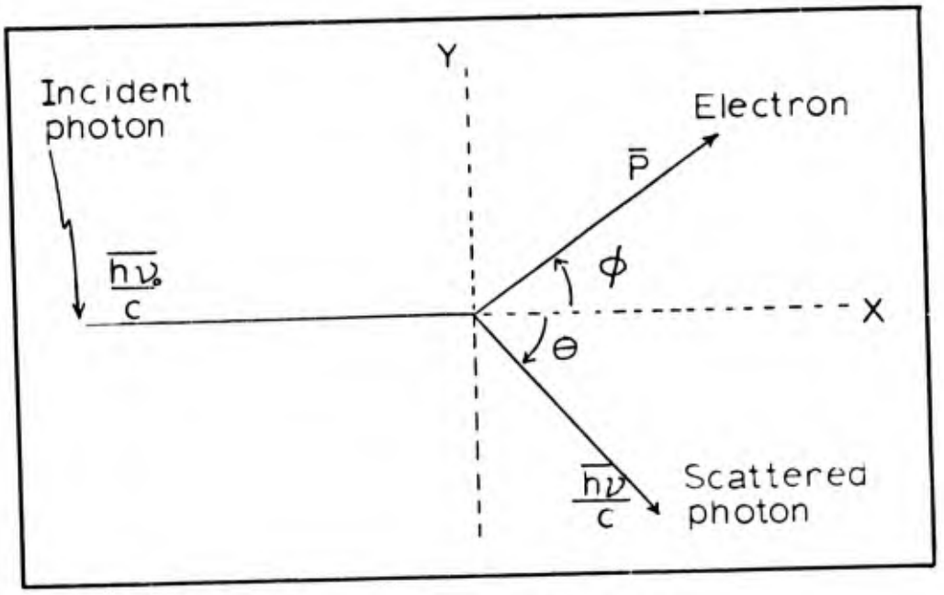

Fig. 11. Compton Scattering.

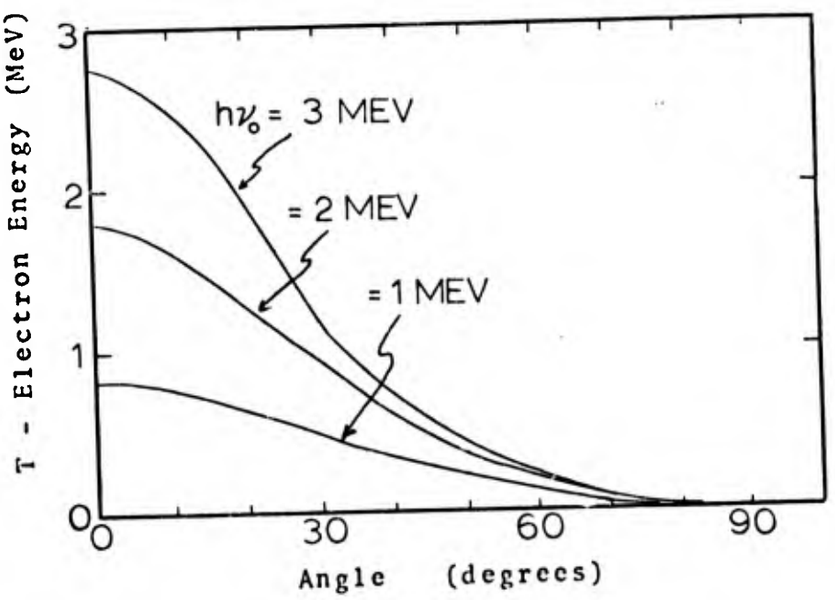

Fig. 12. Compton Electron Energy as a Function of Scatter Angle, Eq (68), for Several Incident Gamma Energies.

random. Because the electrons scattered by these secondary photons would be directed even more randomly, their main contribution to EMP would be to increase the ionization. Since $\bar{E} = \bar{J}/\sigma$ and the conductivity σ is a function of the ionization we see that $\bar{E}$ would decrease if σ increases. Using a buildup factor would result in too large an estimate because a buildup factor has no direction associated with it whereas the direction is needed to calculate the current produced. We propose to look at the maximum threat therefore secondary photons will be ignored.

In Fig. 11, $h\nu_o$ is an incident gamma ray and $h\nu$ is the scattered photon. The electron which was initially at rest at O is given a momentum $\bar{P}$. Because this is a two body problem it can be worked in a plane. Conservation laws and the relativistic expression for kinetic energy allow us to find an expression for the electron kinetic energy as a function of scattering angle and photon energy:

$$\frac{\overline{h\nu_o}}{c} = \frac{\overline{h\nu}}{c} + \bar{P} \qquad \text{(Conservation of Momentum)} \qquad (65)$$

$$h\nu_o = h\nu + T \qquad \text{(Conservation of Energy)} \qquad (66)$$

$$Pc = \sqrt{T(T + 2m_o c^2)} \qquad \text{(Relativistic Energy)} \qquad (67)$$

where

$\bar{P}$ Electron momentum

c Velocity of light

h Planck's constant

$h\nu_o$ Incident Gamma Energy

$h\nu$ Scattered Photon Energy

T Electron Kinetic Energy

m_o Electron rest mass

Solving Eq (65), (66) and (67) for T and, after Evans, letting $\alpha = h\nu_o/m_oc^2$, we have

$$T = \frac{2h\nu_o \alpha \cos^2\phi}{(1+\alpha)^2 - \alpha^2\cos^2\phi} \tag{68}$$

which is plotted in Fig. 12 for several incident photon energies.

The cross section for an electron to be scattered into a cone with walls at ϕ and $\phi + d\phi$ is plotted in Fig. 13. Note the strong forward scatter. If this cross section is altered by an energy fraction, $T/h\nu_o$, the plot is even more forward biased, Fig. 14.[38]

The average energy of the forward scattered electrons was computed using

$$\langle T \rangle = \frac{\int_0^{\pi/2} T(\phi)\,\mu(\phi)\,d\phi}{\int_0^{\pi/2} \mu(\phi)\,d\phi} \tag{69}$$

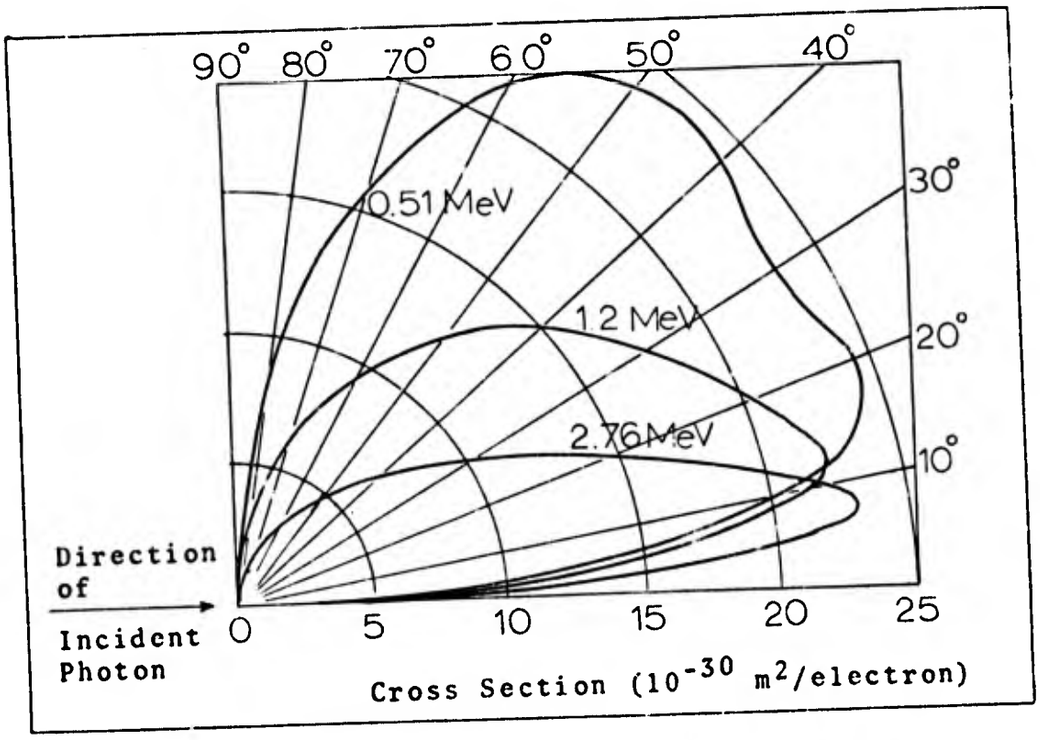

Fig. 13. Number-vs.-angle Distribution of Compton Electrons for Several Incident Gamma Energies.[40]

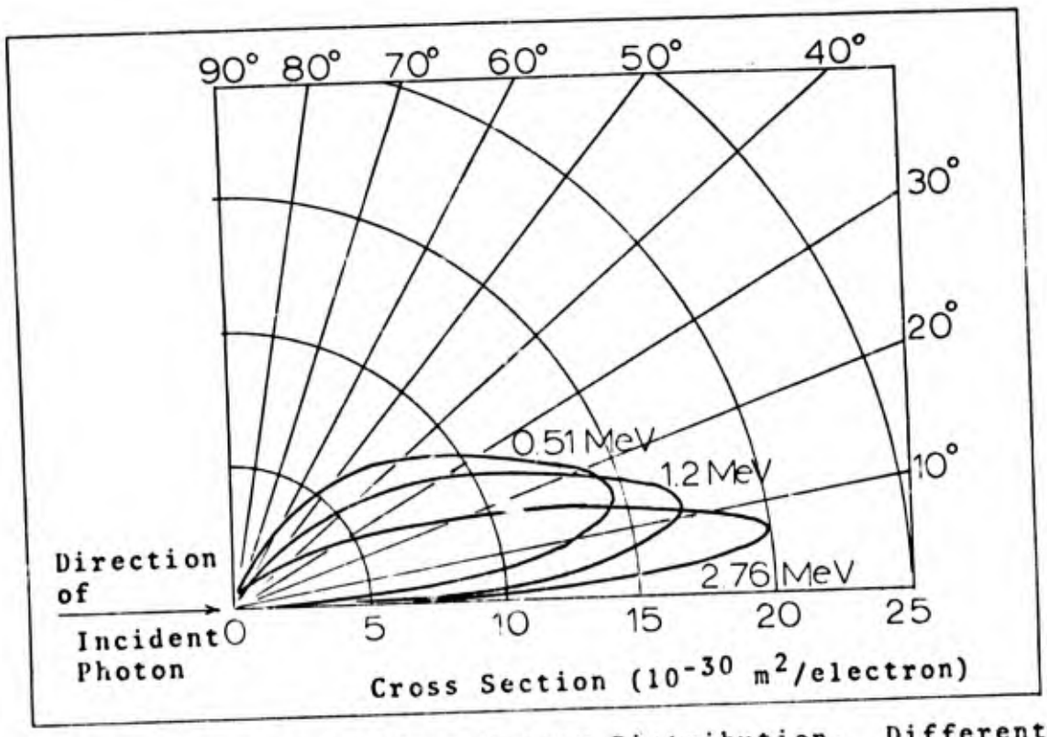

Fig. 14. Compton Effect Energy Distribution. Differential Cross Section per unit Angle for Electron Energy Scattered in the Direction ϕ.[41]

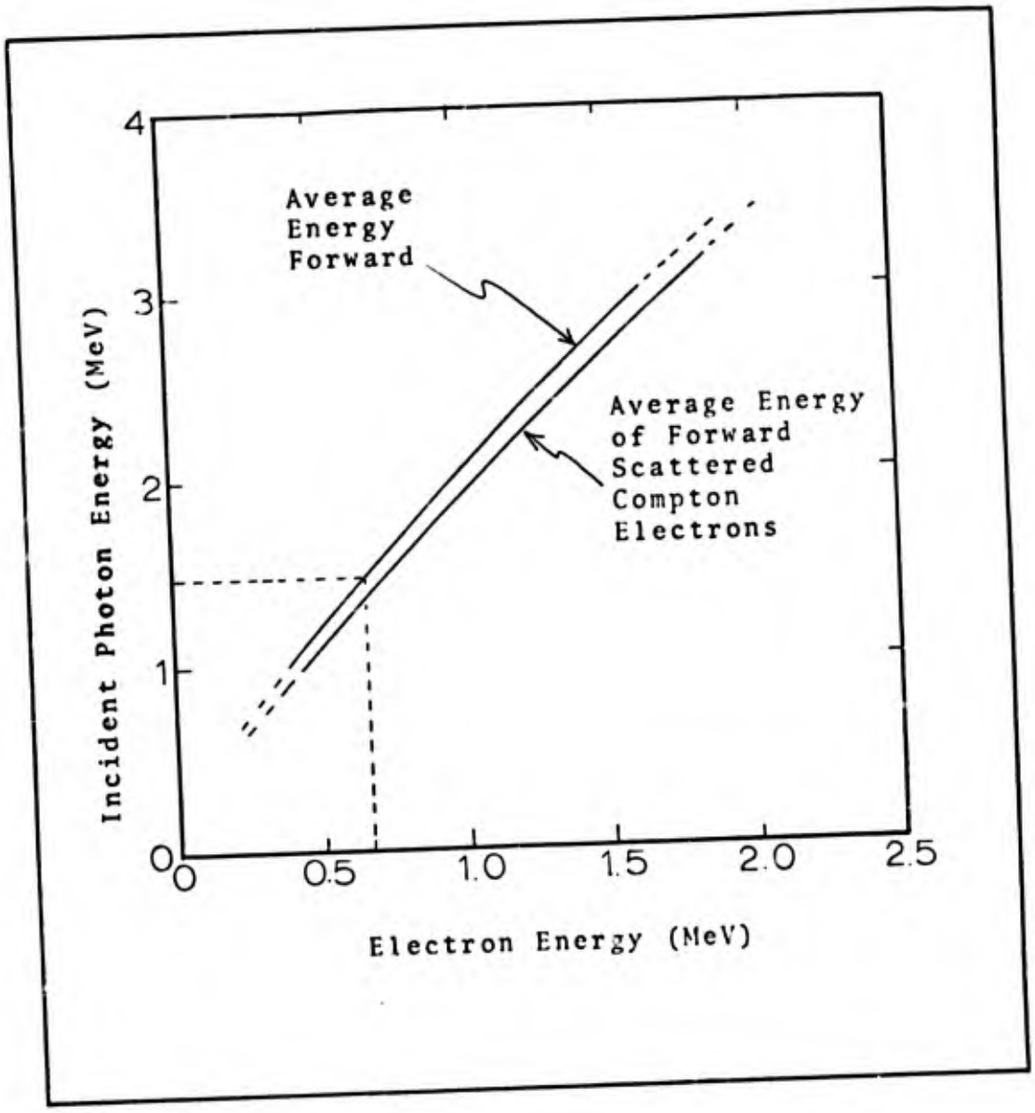

Fig. 15. Average Electron Energy and Forward Energy as a Function of Incident Photon Energy.

where

$\langle T \rangle$ The average electron energy

$T(\phi)$ The scattered electron energy as a function of electron scatter angle

$\mu(\phi)$ The cross section for scatter into an angle $\phi \rightarrow \phi ; d\phi$

The average energy flow parallel to the direction of the incident gamma was found by

$$\langle T_{FWD} \rangle = \frac{\int_0^{\pi/2} T(\phi)\cos\phi \ \mu(\phi)\, d\phi}{\int_0^{\pi/2} \mu(\phi)\, d\phi} \qquad (70)$$

where $T(\phi)\cos\phi$ is the component of the electron energy in the forward direction, T_{FWD} . The results of these two calculations are shown in Fig. 15. The forward energy of the electron created by the "standard" 1.5 MeV gamma is 0.7 MeV.

The Compton Current

Cross Sections. Because the relations developed in this section for use throughout this thesis involve the use of cross sections and mean-free-paths, a few paragraphs will be devoted to discussing them. Many EMP models concern air and its variation with height, e.g., the earth's surface may be represented by air a thousand times as dense as air at STP.[42]

An effective microscopic cross section $_a\mu$ (barns/particle), can be assigned to air because it has a fairly consistent composition below 100 kilometers. The macroscopic cross section,* μ (meter^{-1}), is

$$\mu = N(h)\,{}_a\mu \tag{71}$$

where $N(h)$ is the number of particles per unit volume $(=\rho(h)N_A/GAW(h))$ in particles/m^3 and h is height. The ratio of two cross sections does not vary with altitude:

$$\frac{\mu_i}{\mu_j} = \frac{N(h)\,{}_a\mu_i}{N(h)\,{}_a\mu_j} = \frac{{}_a\mu_i}{{}_a\mu_j} \tag{72}$$

Because of the reciprocal of total cross section is photon mean-free-path λ_i the ratio of mean-free-paths is constant also:

$$\frac{\mu_i}{\mu_j} = \frac{1/\lambda_i}{1/\lambda_j} = \frac{\lambda_j}{\lambda_i} \tag{73}$$

The macroscopic cross section at a particular height can be related to the cross section at a base height through the relative density, ρ/ρ_o :

---

*The cross section, μ_γ , in meters^{-1} is related to the cross sections of Fig. 10 through the density, i.e.,

$$\mu_\gamma(m^{-1}) = \mu_\gamma(m^2\text{-}kg^{-1})\ \rho(kg\text{-}m^{-3})$$

$$\mu_i = \frac{\rho N_A \rho_o}{GAW \rho_o} a\mu \tag{74a}$$

$$= \frac{\rho}{\rho_o} \mu_{l_o} \tag{74b}$$

The mean-free-paths are related by

$$\lambda = \lambda_o / (\rho/\rho_o) \tag{75}$$

In the discussion of the Compton process the total cross section and the Compton cross section were equated to simplify the discussion. In fact the photon flux attenuation is proportional to the total cross section, μ , but the Compton electron production is proportional to the Compton cross section, σ . The difference is small for 1.5 MeV photons.

Another anomaly occurs in the treatment of electron cross section and range. Because an electron can scatter through a large angle while stopping, its mean free path is usually much greater than its mean range (termed mean-free-range (MFR_e)). For example, the electron distribution within a material one mean free path thick which is bombarded from one side by an electron beam is greatest about half way through the material. For this illustration the MFR_e is about half the mean free path, λ_e.[43]

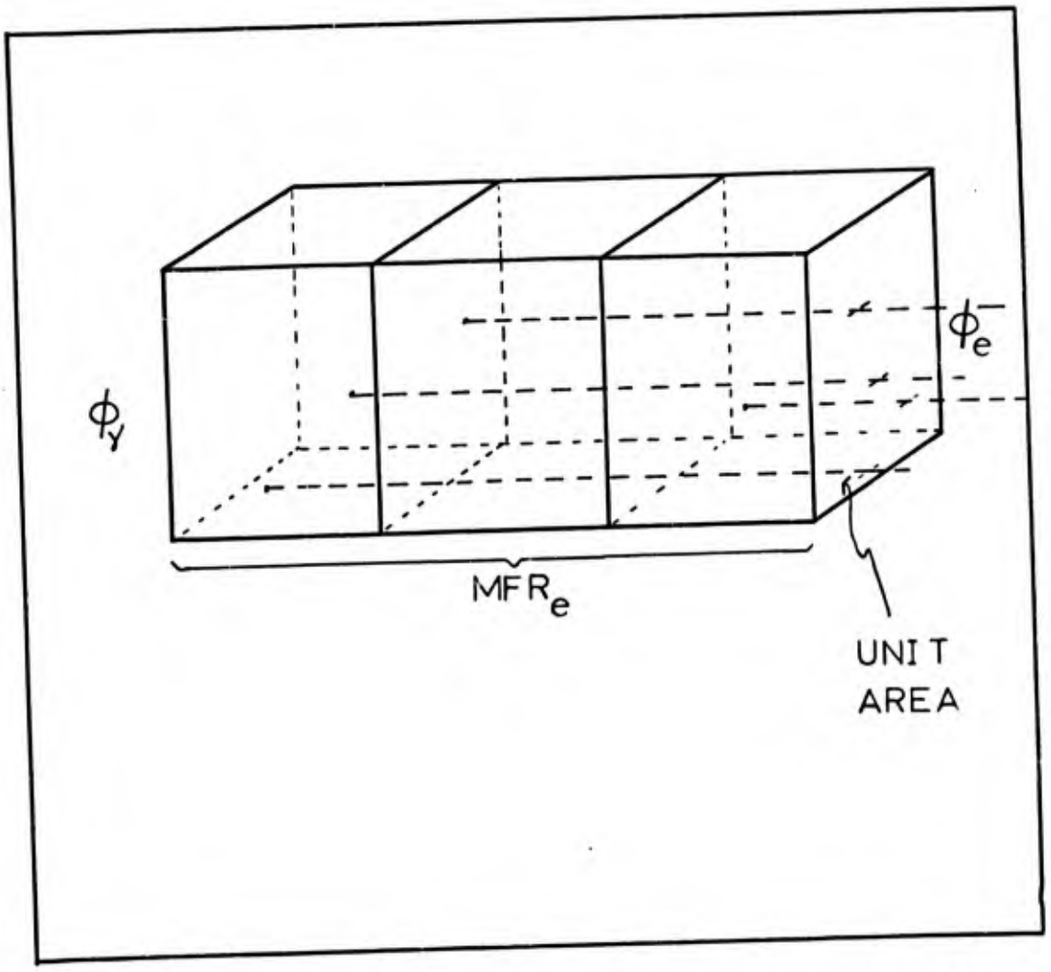

Fig. 16. Electron Flux Production. Electrons produced within one MFR_e of the right face by a constant gamma flux from the left will penetrate the right face. Since the right face has unit area this electron movement is just the electron flux.

The Compton Current. The net forward scatter of electrons is a flow of current which is called the Compton current, $\bar{J}_C$. The rate of generation of free electrons obeys the general reaction rate formula, flux times macroscopic cross section:

$$\text{Electron Production Rate} = \phi_\gamma(r,t)\,\sigma \tag{76}$$

where ϕ_γ is the instantaneous photon flux at the point and σ is the Compton cross section.

A pictoral description of the production of a Compton current supposes a plane wave of photons incident from the left onto a series of rectangular boxes of unit cross section and stacked deep enough so that any electrons formed in the volume will escape out the right end, i.e., the stack is one electron mean-free-range deep (Fig. 16). Assuming that the photon flux does not change over this distance we have

$$\phi_e = \phi_\gamma MFR_e\,\sigma \tag{77}$$

i.e., electron flux is photon-flux times path-length times cross-section-per-unit-path-length. Now current density is electron flux times electron charge

$$\bar{J} = \phi_e e^- \hat{a}_r \tag{78a}$$

or

$$= \phi_\gamma MFR_e \mu\, e^- \hat{a}_r \tag{78b}$$

$$\bar{J}_c = \phi_\gamma \frac{MFR_e}{\lambda_\gamma} e^- \hat{a}_r \qquad (78c)$$

where we have replaced the Compton cross section σ by the total cross section μ ($= 1/\lambda_\gamma$) which assumes that Compton scattering is the only reaction taking place.

If we define an electron cross section $\Sigma_e = 1/MFR_e$ we can re-write Eq (77) as $\phi_e \Sigma_e = \mu_\gamma \phi_\gamma$. Transposing and multiplying by e produces an expression which is the rate of change of the charge density:

$$\frac{\partial \rho}{\partial t} = e(\phi_e \Sigma_e - \mu_\gamma \phi_\gamma) = 0 \qquad (79)$$

This is proportional to the divergence of $\bar{J}_c$ so our development is equivalent to specifying $\nabla \cdot \bar{J}_c = 0$ from Eq (38).

Example 2. This example illustrates the magnitude of the Compton current. The sample nuclear burst has, from Eq (59), a maximum gamma flux rate of

$$\frac{dN}{dt} = 2.3 \times 10^{31} e^{\alpha t} \quad , \; t = T_1 \qquad (80a)$$

$$= 4.6 \times 10^{32} \quad \frac{1.5 \text{ MeV gammas}}{\text{second}} \qquad (80b)$$

Let us find the Compton current at a point one kilometer horizontally from a burst at a height of ten kilometers. The data concerning 10 km altitude is found in Table 3, page 96

and is $\mu_\gamma = 1.11\ km^{-1}$, $\lambda_\gamma = 900$ m and $MFR_e = 9$ m. The flux at the point is

$$\phi_\gamma = \frac{dN}{dt} g(r) \tag{62}$$

$$= 4.6\times10^{32} \frac{e^{-\mu_\gamma R}}{4\pi R^2} \tag{81a}$$

$$= 1.2\times10^{25} \frac{1.5\ MeV\ gammas}{m^2 - sec} \tag{81b}$$

From Eq (78) the electron flux is

$$\phi_e = \phi_\gamma \frac{MFR_e}{\lambda_\gamma} \tag{78c}$$

$$= 1.2\times10^{25} \frac{9}{900} \tag{82a}$$

$$= 1.2\times10^{23} \quad \frac{electrons}{m^2\text{-}sec} \tag{82b}$$

The Compton current is

$$\bar{J}_C = \phi_e e^- \tag{78a}$$

$$= (1.2\times10^{23})(1.6\times10^{-19}) \tag{83c}$$

$$\bar{J} \equiv 2 \times 10^4 \quad \frac{\text{amps}}{\text{m}^2} \qquad (83b)$$

Across a surface about the size of the lead in a wooden pencil (#11 wire) the current would be $\sim$0.01 amperes.

Summary

The actual behavior of a nuclear burst radiation source has been modeled by a monoenergetic (1.5 MeV) point source of gamma rays. Careful analysis would have to consider multiple scattering, actual spectrums, etc. The time behavior of the source model is mainly an exponential rise and slower exponential decay. If X-rays are of concern they are assumed to behave like the gamma source but with the energies of 3.8 KeV, the average energy of a 1 KeV blackbody. Neutron time behavior contributes later parts of the gamma source model; should a simple extension of neutron behavior be necessary the shell model might be used.

The gammas and X-rays are treated like a virgin flux (Eq (63)) from a point source. Of all the photon removal processes the Compton effect is the most important means of propelling electrons forward. The electron's average forward energy is about half the incident photon energy--graphed in Fig. 15.

Equation (78c) relates the Compton current to the photon flux. This equation will be used in the next chapter where we consider the symmetric burst in air.

IV. Electromagnetic Pulse from a Symmetric Burst

Introduction

The symmetric burst is most closely approximated by subsurface bursts and low altitude bursts that do not interact with the earth's surface. The field produced is an electric field inside the expanding sphere of energetic photons from the burst. There will be no magnetic field inside or outside of the expanding sphere and no electric field outside that sphere.

In this chapter an approximate model is used to illustrate the use of Maxwell's equations to find the fields inside and outside a sphere of current. The model concludes with some discussion of its validity.

Following this we will discuss the Compton current and conduction currents. Since the conduction current depends on the ionization of the air and the mobility of the charge carriers, some discussion of these is included. This electric field, which cannot grow indefinitely, is studied to find its maximum or saturated value and the radius from the burst that the saturated value can reach. Finally we conclude the chapter with an example to indicate the magnitude of the effect.

Spherically Symmetric Model

By studying a mathematically simple model for a spherically symmetric nuclear explosion we can see how Maxwell's

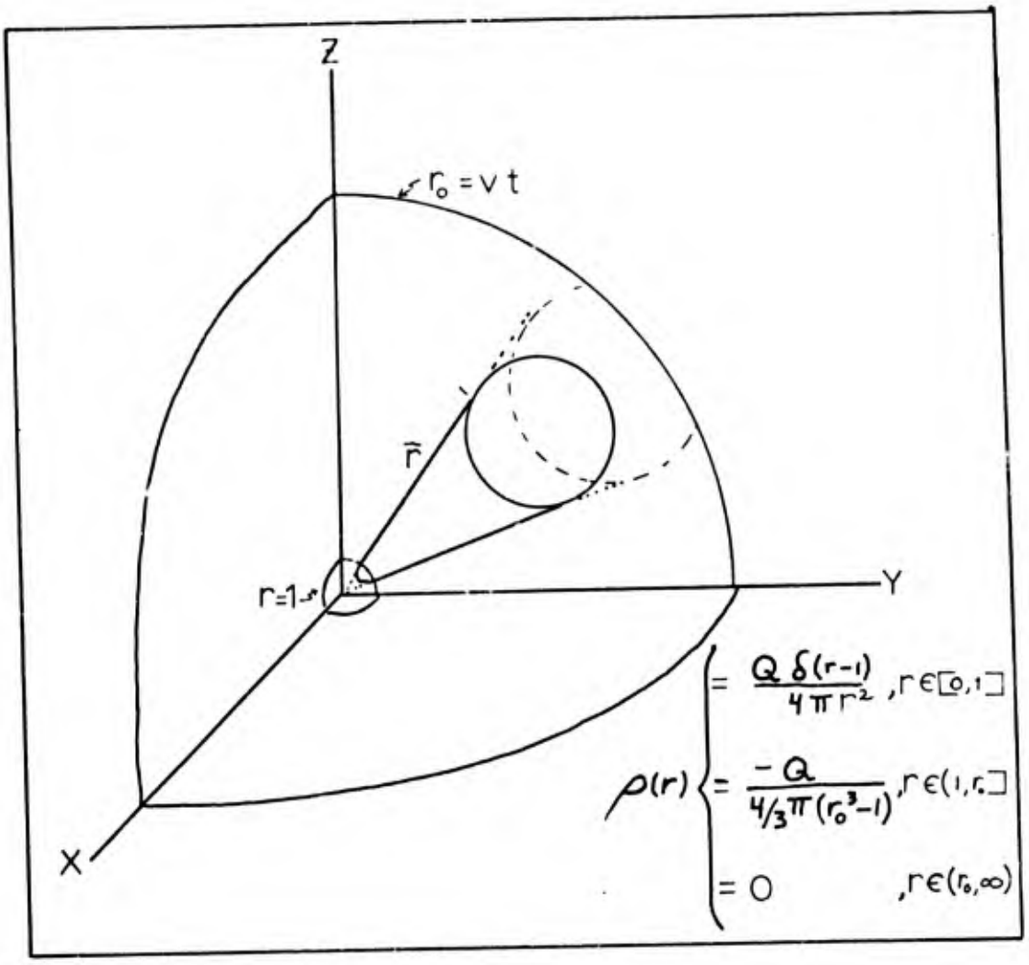

Fig. 17. Model of Spherically Symmetric Nuclear Burst. Characteristics include overall neutrality, positive charge evenly distributed over one meter sphere, and negative charges evenly distributed in shell with expanding outer radius.

equations may be used. The model has some special properties: A constant number of positive ions remain on a sphere of one meter radius and an equal number of electrons are propelled radially outward in such a way that the outer boundary of the electron distribution moves with velocity V and the electrons are evenly distributed between $r = 1$ and $r = r_o = Vt$. Salient features of the model are pictured in Fig. 17. The charge density of the positive ions is given a volume charge density by the use of the Dirac delta function, the use of which is explained in Refs 44, 45, or 46. The volume charge density of the electrons is the total charge divided by the volume between $r = 1$ and $r = r_o$, the moving outer boundary.

Electric Field by Gauss' Law. First let u examine the electric field through the use of Gauss' law in integral form:

$$\text{I.} \qquad \oint_S \bar{E} \cdot d\bar{S} = \int_V \frac{\rho(\bar{r})}{\epsilon_o} dV \qquad (8)$$

The surface bounding the region of interest consists of a spherical outer cap at fixed radius $r(>1)$, an inner spherical cap with radius less than one meter, and a conical surface joining the two caps to complete the picture.

First we will evaluate the left hand side (LHS) of Eq (8). Over the inner cap $\bar{E}$ is zero since any closed surface entirely within the one meter radius encloses no

charge and fields produced by charges outside r = 1 would cancel by symmetry.

Next we consider the conical surface. We know that the outward normal to the cone (which is the direction of $d\bar{S}$) is normal to the radius vector forming the cone. By symmetry conditions any component of $\bar{E}$ must be parallel to $\hat{a}_r$, the radial unit vector. Therefore

$$\int_{CONE} \bar{E}\cdot d\bar{S} = \int_{CONE} E\,\hat{a}_r\cdot d\bar{S} = 0 \qquad (84)$$

which states that no $\bar{E}$ field penetrates the conical surface.

All that remains is the outer cap of surface area $S = r^2\omega$ where ω is an element of solid angle and, by differentiation, $dS = r^2 d\omega$. The LHS of Eq (8) becomes

$$(LHS) = \int \bar{E}\cdot d\bar{S} = \int_0^{\omega} E r^2 d\omega = E r^2 \omega \qquad (85)$$

Now we turn our attention to the right hand side (RHS) of Gauss' integral equation, Eq (8). The RHS can be evaluated by considering three volumes: $r \in [0,1]$; $r \in (1, r)$; and $r > r_o$ (if $r > 6$). These three integrals are

$$(RHS) = \frac{1}{\epsilon_o}\int_0^{\omega}\int_0^{1} \frac{Q}{4\pi}\frac{\delta(r-1)}{r^2} r^2\, d\omega\, dr \;+$$

$$\frac{1}{\epsilon_o}\int_0^{\omega}\int_1^{r} \frac{-Q}{4\pi(r_o^3-1)} r^2 dr\, d\omega \;+\; \frac{1}{\epsilon_o}\int_V [0]\, dV \qquad (86)$$

where $dv = ds\,dr = r^2 d\omega dr$ is the cone's volume element. The result of the integration is

$$(RHS) = \frac{1}{\epsilon_o}\left[\frac{Q\omega}{4\pi} - \frac{Q\omega r^3}{4/3\pi(r_o^3-1)3}\Big|_1^r + (0)\right] \qquad (87)$$

The electric field is found from Gauss' integral equation formed by equating Eqs (85) and (87):

$$\bar{E} = \frac{1}{\epsilon_o}\left[\frac{Q}{4\pi r^2} - \frac{Q(r^3-1)}{4\pi r^2(r_o^3-1)}\right]\hat{a}_r \qquad (88)$$

We note that if $r > r_o$ we have the integrals of Eq (86) but contributions from the first two cancel at $r = r_o$ and the third integral is identically zero. The conclusion: $\bar{E} = 0$ outside the charge boundary.

Magnetic Field by Integral Form of a Maxwell Equation. Let us now consider the magnetic field due to the expanding sphere of charge by using another of Maxwell's equations:

$$\text{IV} \qquad \oint_C \bar{H}\cdot d\bar{l} = \frac{\partial}{\partial t}\int_S \bar{D}\cdot d\bar{S} + \int_S \bar{J}\cdot d\bar{S} \qquad (89)$$

If we consider $\bar{H}$ as the sum of three components in spherical coordinates,

$$\bar{H} = H_r\hat{a}_r + H_\theta\hat{a}_\theta + H_\phi\hat{a}_\phi \qquad (90)$$

we can find the components normal to the radius vector by considering a spherical cap as shown in Fig. 18. We shall

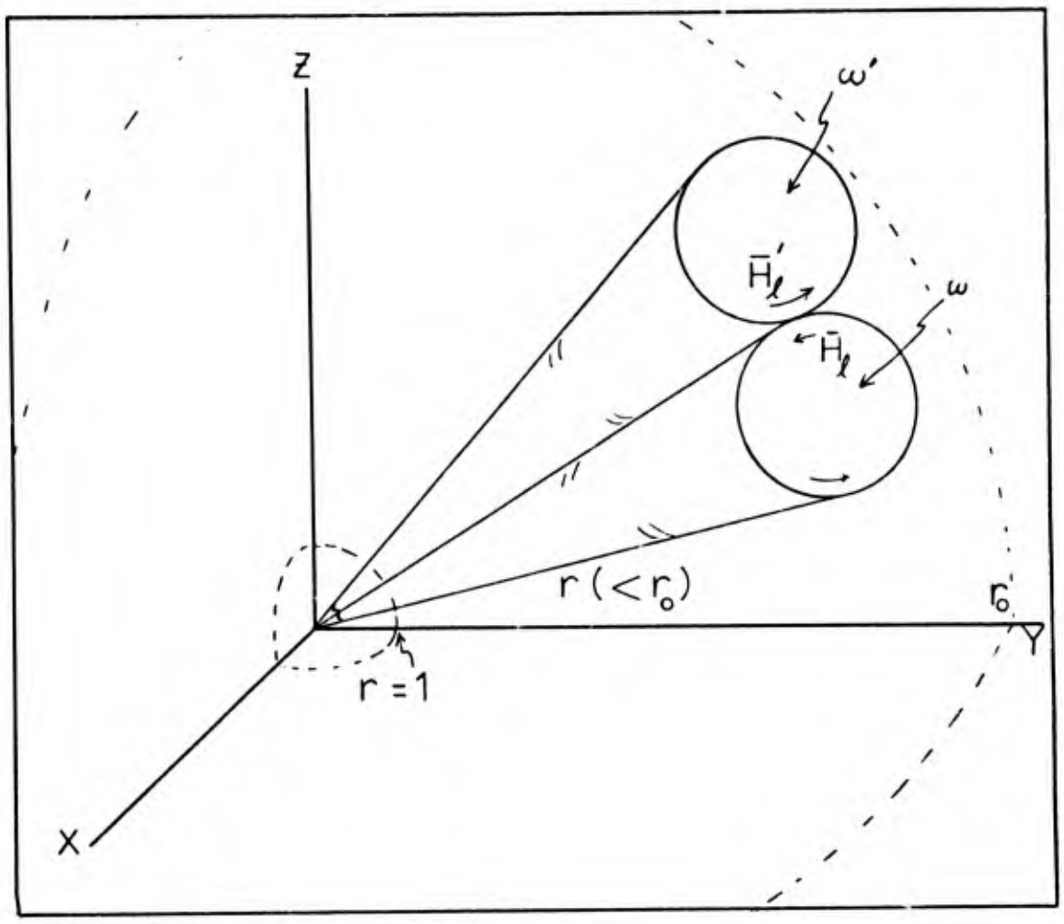

Fig. 18. Illustration of the Cancellation of $\bar{H}$ by Adjacent Incremental Surfaces.

discuss the LHS of Eq (89) to find intuitively that the tangential components of $\bar{H}$ are zero and then we shall evaluate the RHS to arrive at the same conclusion.

We can integrate $\oint \bar{H} \cdot d\ell$ around the circular boundary of ω in Fig. 18. The value of this integral is $H_\ell \, \ell$ where H_ℓ is the component of $\bar{H}$ along $\bar{\ell}$ and ℓ is the path length around the cap. H_ℓ is constant on this path by symmetry. Taking an adjacent cap, ω', we see in Fig. 18 that at its point of tangentcy $\bar{H}_\ell = -\bar{H}'_\ell$ so the sum is zero. Therefore over the entire sphere there is no component of $\bar{H}$ normal to $\hat{a}_r$ and Eq (90) reduces to $\bar{H} = H_r \hat{a}_r$. We shall show later that H_r is zero also.

We now proceed to evaluate the RHS of Eq (89) to show that the components of $\bar{H}$ normal to $\hat{a}_r$ are zero. We carry out the indicated integration without comment.

$$\frac{\partial}{\partial t}\int_S \bar{D}\cdot d\bar{S} = \int_0^\omega \frac{\partial D}{\partial t} r^2 d\omega \tag{91a}$$

$$= \frac{r^2\omega(-Q)(r^3-1)}{4\pi r^2} \frac{\partial \frac{1}{(r_o^3-1)}}{\partial t} \tag{91b}$$

$$\int_S \bar{J}\cdot d\bar{S} = \int_V \nabla\cdot\bar{J}\, dV = -\int_V \frac{\partial \rho}{\partial t} dV \tag{92a}$$

$$= \int_0^{\omega}\int_1^{r} \frac{-Q}{4/3\pi} \frac{\partial\left(\frac{1}{r_o^3-1}\right)}{\partial t} r^2 dr\, d\omega \qquad (92b)$$

$$= \frac{Q(r^3-1)\omega}{4\pi} \frac{\partial\left(\frac{1}{r_o^3-1}\right)}{\partial t} \qquad (92c)$$

The two parts of the RHS of Eq (89), Eqs (91b) and (92c), are the same but opposite in sign so their sum is zero. Since the area of integration was specified only as ω, the length of the boundary is arbitrary therefore $\bar{H}$ normal to $\hat{a}_r$ must again be zero.

By choosing another surface it might be possible to show that $H_r = 0$ also, but we choose to show that by using Faraday's law.

Magnetic Field by Using Faraday's Law. In order to show that all the components of $\bar{H}$ are indeed zero we use the electric field, previously found, in Faraday's law, $\nabla \times \bar{E} = -\mu_o^{-1} \partial \bar{H}/\partial t$. The electric field, Eq (88), can be written

$$\bar{E} = E_r(r)\hat{a}_r \qquad (93)$$

By carrying out the curl operation on this field

$$\nabla \times \bar{E} = \frac{1}{r \sin\theta} \begin{vmatrix} \hat{a}_r & r\hat{a}_\theta & r\sin\theta\hat{a}_\phi \\ \frac{\partial}{\partial r} & \frac{\partial}{\partial \theta} & \frac{\partial}{\partial \phi} \\ E_r & 0 & 0 \end{vmatrix} \qquad (94)$$

we get $$\nabla \times \bar{E} = 0 \tag{94b}$$

or $$\mu_o^{-1} \frac{\partial \bar{H}}{\partial t} = 0 \tag{95}$$

This last equation integrates to show that $\bar{H}$ is a constant. But at $t = 0, \bar{H} = 0$ therefore $\bar{H} = 0$ for all time whether this point in question is inside or outside $r_o = vt$.

Discussion. The model we have just discussed is inadequate to model the effects found in the vicinity of a nuclear burst. A more realistic model would have to consider that the current density increases very rapidly, almost a step function, and the radius of the region containing a source current is increasing at the speed of light. Also the flux of gamma rays which drives the current is decreasing due to geometric ($1/r^2$) attenuation and photon removal in addition to its late time-dependent decrease. For the time dependence of Chapter III the gamma flux would be "on" for a time equivalent to $\sim$ 2700 meters and the width about the peak is $\sim$ 300 meters.

The 300 meter peak pulse region propagates outward creating a strong electric field that would be limited in magnitude (called saturated) by the increased conductivity of the air, a point to be discussed in the next section. Still later the driving mechanisms would not be able to saturate the field, and later still no part of the driving pulse would be

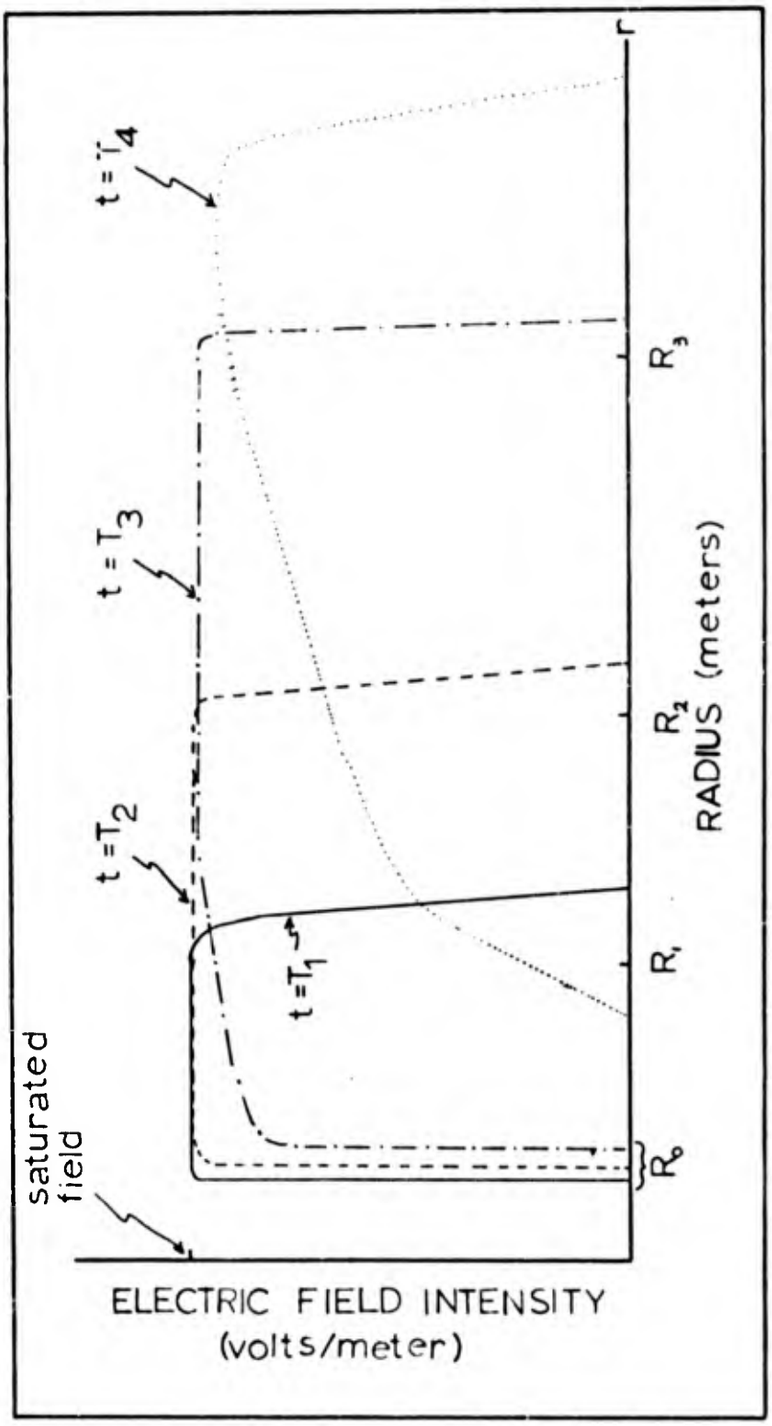

Fig. 19. Electric Field Behavior. At T_1 a saturated field is formed to R_1; at T_2, R_o has moved out and the saturated field extends to R_2 but is becoming unsaturated at R_o; At T_3 the saturated region has a front and rear lip and R_o is still moving outward; and at T_4 there is no saturated region and the entire field starts dissipating.

strong enough to saturate the field so the entire field would decay by electron and ion conduction.

A realistic central region, the isothermal sphere, would contain no electric field (just as in our model). This is true since the isothermal sphere is a highly ionized, electrically neutral region. The radius, R_o in Fig. 19, of the central sphere would grow slowly with time. The current flow and electric field would be "on" to some large value just outside the isothermal system.

The qualitative behavior of the electric field is illustrated in Fig. 19.

Despite the increased complexity of this process there would be no electric field external to the gamma wavefront and no magnetic field anywhere, just as in our simple model.

Conduction Currents

Electromagnetic fields in general and the EMP in particular are generated by flowing currents or charge distributions. In a nuclear burst the separation of a Compton electron and its parent ion creates an electric field which will cause currents in a conducting medium. The total current density, $\bar{J}$, is then the sum of this conduction current (J_E) and the Compton current ($\bar{J}_c$) or $\bar{J} = \bar{J}_E + \bar{J}_c$ (where we ignore all other form of current-polarization, etc.). Using Ohm's law, $\bar{J}_E = \sigma \bar{E}$, we have

$$\bar{J} = \bar{J}_c + \sigma \bar{E} \tag{96}$$

where σ is the conductivity (in mhos/meter).

The conductivity depends upon the number of charge carriers available and their freedom to move. The initial number of charge carriers is governed by the number of ion pairs (an ion and an electron) that the energetic Compton electron produces as it is slowed in a medium. The very mobile free electrons carry most of the current but they rapidly become attached to atoms which are much less mobile than electrons. The conductivity is then the summation of all the carriers times their mobilities:

$$\sigma(\bar{r},t) = \sum_{i=1}^{M} \mu_i(\bar{r},t)\, N_i(\bar{r},t)\, q_i \qquad (97)$$

where μ_i is the mobility (velocity per unit field in meters^2 volt^{-1} second^{-1}); q_i the charge on the i^{th} particle type; and N_i the particle density of the i^{th} species (in particles-meter^{-3}). The mobility can be function of the electric field, but we shall ignore that dependence in this thesis.

In order to see the importance of the conductivity to any analysis of the EMP let us find a differential equation for the electric field in the symmetric burst. In a symmetric burst Maxwell's equation $\nabla \times \bar{H} = \bar{J} + \frac{\partial \bar{D}}{\partial t}$ becomes

$$\bar{J}_c + \sigma \bar{E} + \frac{\partial \epsilon_o \bar{E}}{\partial t} = 0 \qquad (98)$$

since there is no magnetic field. Only the conductivity and the driving current $\bar{J}_c$ control this equation. Its terms are

interrelated since the Compton current ionizes the air which then conducts with a conductivity σ . Fig. 20a illustrates the interrelationship of the processes involved.[48]

Because the parameters N_i in Eq (97) are net particle densities we will study particle production then particle attrition. Later we shall consider the mobilities of the various particles.

Charged Particle Production. The charged particles whose motion is the conduction current are produced as a high energy electron loses its energy through collisions in the medium.

The process, illustrated in Fig. 20b,begins when a photon, shown incident from the left, propells an electron, the primary electron, through the medium.[49] The primary electron with kinetic energy T_e loses most of its energy in collisions with neutral atoms along its path, some of which become ionized. The secondary electrons do not contribute to the electric field because they do not move far but this massively ionized region does form a conduction path along which currents flow to neutralize the electric field between the primary electron and its parent ion.

As the primary electron loses energy its velocity decreases (which is important in magnetic field interactions). The rate of decrease in velocity (or energy) is greatest toward the end of its range and at the end of the range the rate becomes erratic. This erratic energy loss causes the primary electron's range to vary 15 percent for a given initial electron velocity.[50] However, we assume that the

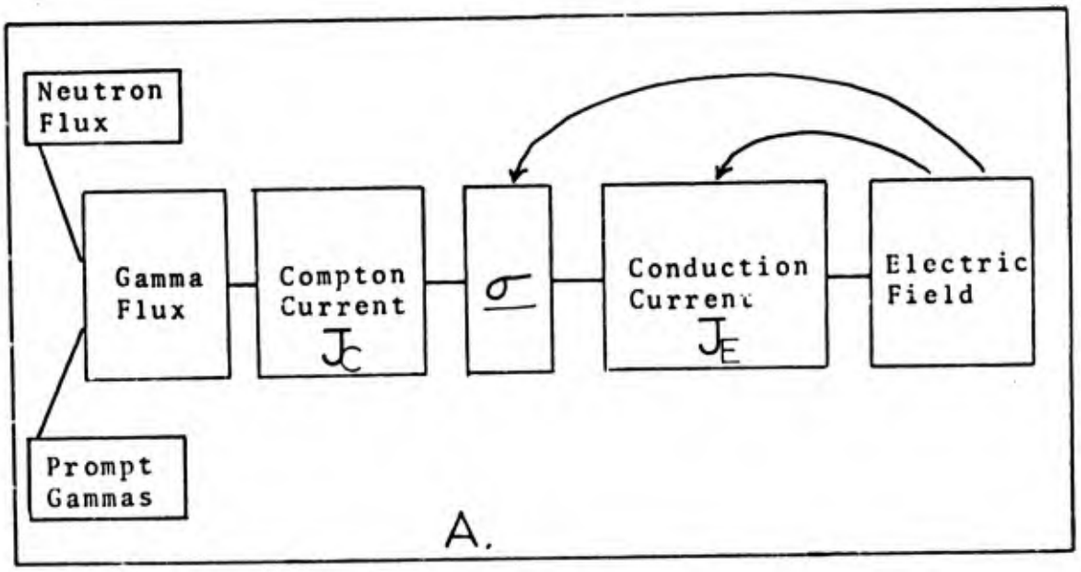

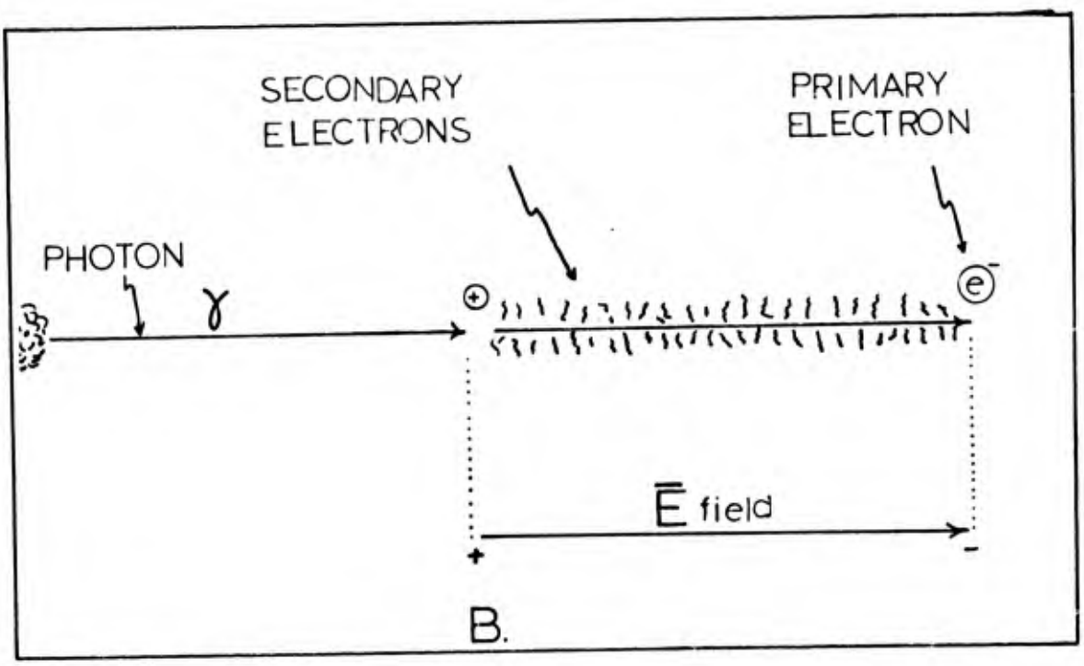

Fig. 20. Interrelationship of Field and Currents and History of Electrons in Air. In A we show the interrelationship of fields and currents. In B we illustrate a photon propelling an electron forward. The subsequent electron motion generates an electric field and an ionized conduction path.

ion pair production rate and primary electron velocity are constant until the electron abruptly stops at the end of its range.

The mechanism of energy loss is the single ionization of an atom along the primary electron's path. This energy loss is quite constant from element to element.[51] We shall take this energy loss to be a 32.5 electron-volts/ion-pair for an $\sim$ 1 MeV electron in air[52]. Therefore the number of ion pairs formed by a primary electron is

$$\text{Number of Ion Pairs} = \frac{T_e(10^6)}{32.5} \tag{99a}$$

$$= 3.08 \times 10^4 \quad \frac{\text{ion pairs}}{\text{1 MeV electron}} \tag{99b}$$

where T_e is the electron energy in MeV. The number of ion pairs created is also the number of electrons and number of positive ions produced. We shall deal with complete expressions for the production and loss of charged particles after considering the loss mechanism.

Air Chemistry. The loss mechanisms are more than the neutralization of the charged particles by the recombination of an electron with an ion. Under air chemistry we will consider the reactions between ions and between electrons and ions. Each reaction has a specific rate constant which may be affected by temperature, environment (e.g., humidity), and mixing that takes place. Although there are many types of reactions,[53] we shall only consider four of them as

Table 1

Hypothetical Parameters for EMP Studies

Burst Data

Yield Y =	1 KT*	1 MT*	Fissions/Kiloton 1.5×10^{23}
Prompt X-Rays	0.7 Y	0.5 Y	X-Ray Temperature 1 KeV
Prompt Gamma	0.01 Y	0.003 Y	
Prompt Neutrons	0.01 Y	--	Average X-Ray Energy 3.8 KeV
Delayed Gamma	0.02 Y	0.03 Y	Average Gamma Energy 1.5 MeV
Delayed Beta	0.02 Y	--	
Debris	0.25 Y	--	

Growth Constant α 10^8 sec^{-1} Decay Constant β 10^7 sec^{-1}

Radiation Data (See also Table 3 for range information)
Average Compton Electron Energy--0.74 MeV
Average Forward Energy of Compton Electron--0.68 MeV
Ion Pairs Formed/0.7 MeV Electron--2.0×10^4

Environment (See Table 3 also for Air Density)
Geomagnetic Field--5×10^{-5} webers/m^2
Earth density may be represented by 1000 air density
Air is 0.7 N_2 and 0.3 O_2; particle density at STP
2.55×10^{25} m^{-3}

---

*Dickinson, H. and P. Tamarkin. "Systems for the Detection and Identification of Nuclear Explosions in the Atmosphere and in Space." IEEE Proceedings, 53:1921-1933 (December 1965). p 1932.

Other data referenced elsewhere in this thesis. No Classified Sources Consulted.

important in relatively dense atmospheres; all calculations will assume standard temperature and pressure, (STP).

The four reactions are

a. The source reaction: A neutral atom receives enough energy to become ionized

$$X + \Delta E \longrightarrow X^+ + e^- \quad (e.g., O_2 + \Delta E \rightarrow O_2^+ + e^-) \tag{100}$$

This process was discussed in the preceding section. The product of the reaction rate for the production of Compton electrons, $R_e = \mu \phi_\gamma$, and the number of ion pairs produced per primary electron, Eq (99a), is the source term for electrons and positive ions:

$$S_e = S_+ = \mu \phi_\gamma(\bar{r}, t) \frac{T_e(10^6)}{32.5} \tag{101}$$

Inserting numbers from Table 1 into this equation gives

$$S_e = S_+ = 6.67 \times 10^{-2} \frac{(0.7 \times 10^6)}{32.5} \phi_\gamma \tag{102a}$$

$$= 1.5 \times 10^3 \phi_\gamma \tag{102b}$$

where ϕ_γ is the gamma flux.

b. The electron attachment reaction,

$$X + e^- + M \longrightarrow X^- + M \quad (e.g., O_2 + e^- + M \rightarrow O_2^- + M) \tag{103}$$

usually procedes in the presence of a third body, M, because the third body is needed to conserve momentum in the reaction between a light electron and the heavy X atom. For air the 0_2 reaction is extremely fast and is the one we shall consider exclusively. As an aside we note that the reaction rate constant or attachment frequency, ν_a', has units meter^6-second^{-1}. Often this is altered by multiplying this figure by the number of M molecules present and by the number of 0_2 molecules present (which is equal to a volume fraction of M. This is allowable because the fraction of 0_2 which becomes ionized is negligible). The attachment frequency is $\nu_a' = 7.4 \times 10^{-43}$ m^6-sec^{-1} which at STP in air is equivalent to $\nu_a = \nu_a' N_{O_2} N_M$ or $\nu_a = \nu_a'(0.2N_M)N_M$ or, finally, $\nu_a = 1.02 \times 10^8 sec^{-1}$ where N_M is the particle density of air at STP, 2.68×10^{25} particles-m^{-3}.[54]

c. The electron-ion recombination reaction

$$X^+ + e^- + M \longrightarrow X + M \quad (e.g., N_2^+ + e^- + M \text{—} N_2 + M) \qquad (104)$$

is shown as a three body reaction because of the momentum consideration. The reaction has about the same reaction rate for N_2 and 0_2 so we will consider the reaction as happening for any particle in air. The reaction rate we will use is $\alpha_r' = 7.5 \times 10^{-38}$ m^6 - sec^{-1} or $\alpha_r = 2.0 \times 10^{-12}$ m^3-sec^{-1} where we have absorbed the third body term into the reaction rate constant.[54]

d. The mutual neutralization reaction

$$X^+ + Y^- \rightarrow X + Y \quad (\text{e.g., } O_2^+ + N_2^- \rightarrow O_2 + N_2) \tag{105}$$

will be assigned the reaction rate $\alpha_i = 2.3 \times 10^{-12} \text{sec}^{-1}$ for all reactions whether X and Y are alike or different.[54]

(Other reactions are important in the upper atmosphere but unimportant in the denser regions. For a complete description of the many reactions see Freyer[55] or Whitten and Poppoff.[56] Usually the change in importance of a reaction is a function of the number of reactants, i.e., air density. This is especially true where a third body is necessary.)

The number of each species of charge carrier is governed by the balance between loss and production. By using the continuity equation

(rate of change) = (sources) - (losses) - (leakage) (106)

we can write a differential equation for the number of each species.[57] We shall assume that the leakage term is zero, i.e., no mixing or transport. With this assumption the continuity equations for the electrons and positive and negative ions are

$$\frac{dN_e}{dt} = S_e - \nu_a N_e - \alpha_r N_+ N_e \tag{107}$$

$$\frac{dN_+}{dt} = S_e - \alpha_r N_+ N_e - \alpha_i N_+ N_- \qquad (108)$$

$$\frac{dN_-}{dt} = \gamma_a N_e - \alpha_i N_+ N_- \qquad (109)$$

where S_e is the source of electrons, N_e is the number of electrons/m^3; N_+ is the number of positive ions/m^3; and N_- is the number of negative ions/m^3.[58] As always, the change rates are the product of the number of each reactant and the reaction rate constant. The fact that charge is conserved gives us the equation

$$N_+ = N_e + N_- \qquad (110)$$

which implies that one of the three linear first order differential equations (107), (108), or (109) is not an independent equation.

The three equations were integrated in Appendix B after making a simplifying assumption which we look at now. Let us alter and insert numbers into Eq (107):

$$\frac{dN_e}{dt} = S_e - N_e(\gamma_a + \alpha_r N_+) \qquad (111a)$$

$$= S_e - N_e(1.02\times10^{8} + 2.0\times10^{-12} N_+) \qquad (111b)$$

For $\alpha_r N_+$ to be comparable to ν_a, the positive ion density must be $\sim 10^{19}$ m^{-3}. We state that because the positive ion density is below this figure we will ignore $\alpha_r N_+$. More justification for this assumption is presented in Appendix B.[59]

The integrated electron density equations for various time intervals in the source function are

$$N_e(t) = \frac{S_e(r)}{\alpha + \nu_a}(e^{\alpha t} - e^{-\nu_a t}) \qquad ,t \in (0, T_1) \qquad (112a)$$

$$N_e(t) \cong \frac{S_e(r)e^{\alpha T_1}}{\nu_a - \beta}\left[e^{-\beta(t-T_1)} - \left(\frac{\beta + \alpha}{\nu_a + \alpha}\right)e^{-\nu_a(t-T_1)}\right] ,t \in (T_1, T_2) \qquad (112b)$$

$$N_e(t) = N_e(T_2)\,e^{-\nu_a(t-T_2)} + \frac{S_e(r)}{\nu_a}(1 - e^{-\nu_a(t-T_2)}) \quad ,t \in (T_2, T_3) \qquad (112c)$$

$$N_e(t) \cong N_e(T_3)\,e^{-\nu_a(t-T_3)} \qquad ,t > T_3 \qquad (112d)$$

where

$S_e(r)$ = Original source strength (electrons/sec-m^3)

α, β = Time constants of source (sec^{-1}).

$(0, T_1)$ = Interval of building source strength.

(T_1, T_2) = Interval of decaying source strength.

(T_2, T_3) = Interval of constant source strength.

$t > T_3$ = Interval of zero source strength.

$N_e(T_i)$ = Electron density at interval's start.

ν_a, α_i, α_r = Reaction rate constants (meters^n/sec).

For times greater than the lower boundary of the particular interval the equations become

$$N_e(t) = \frac{S_e(r)\, e^{\alpha t}}{\alpha + \nu_a} \qquad ,t \in (T', T_1) : T' > 0 \qquad (113a)$$

$$N_e(t) = \frac{S_e(r)\, e^{\alpha T_1}}{\nu_a - \beta}\, e^{-\beta(t - T_1)} \qquad ,t \in (T_1', T_2) : T_1' > T_1 \qquad (113b)$$

$$\left.\begin{aligned} N_e &= \frac{S_e}{\nu_a} \\ N_+ = N_- &= \sqrt{\frac{S_e}{\alpha_i}} \end{aligned}\right\} \qquad ,t \in (T_2', T_3) : T_2' > T_2 \qquad (113c)$$

$$N_e = 0 \qquad ,t \gg T_3 \qquad (113d)$$

Rather than discussing the behavior of these equations we present the curves in Fig. 21 found by integration of Eqs (107) and (108) for early time. The late time behavior is estimated from the form of Eqs (113 c, d). There are several facts to be noted in these curves: (1) The positive ion density has a maximum around 10^{19} ions/m^3 so the earlier

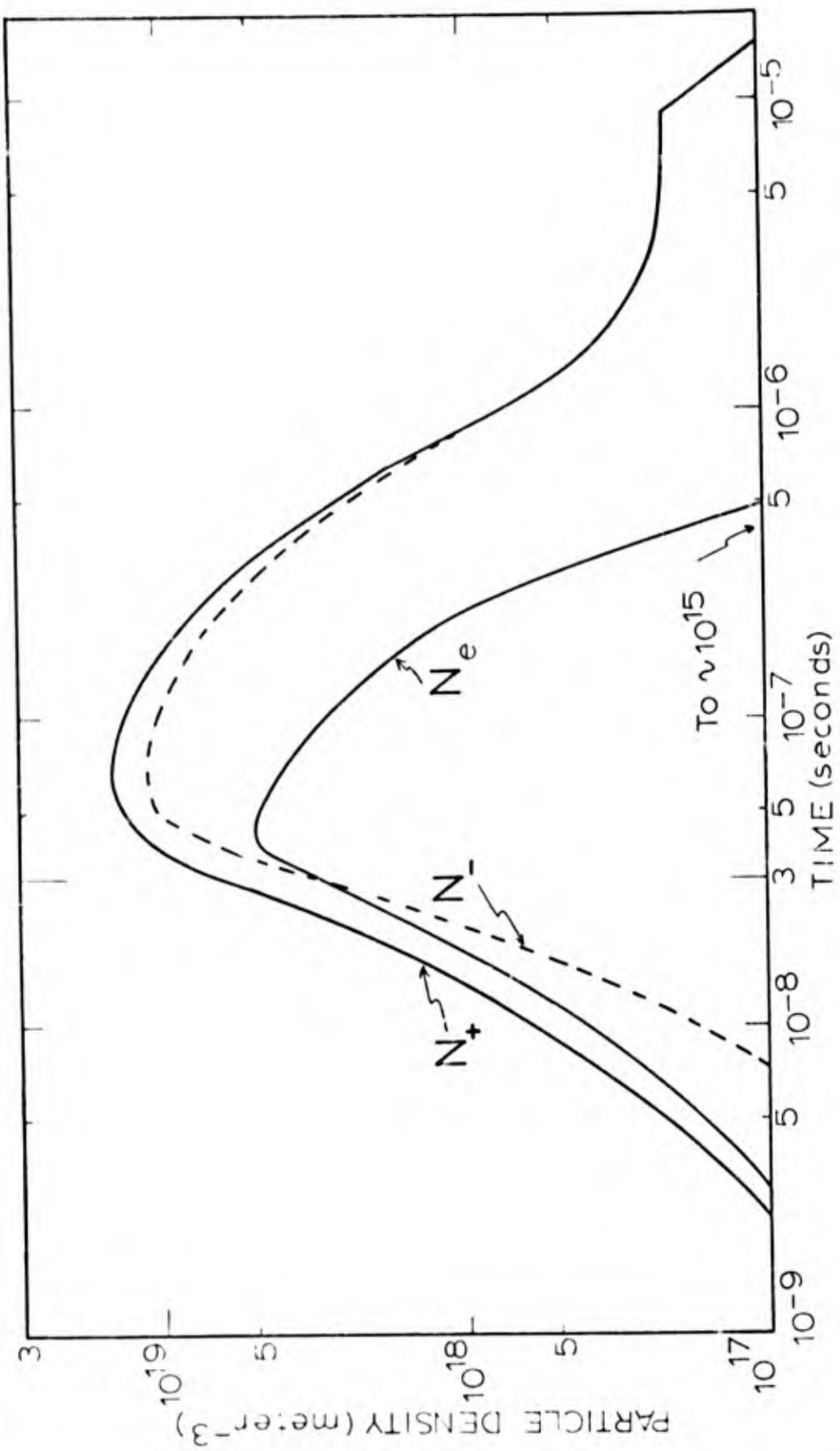

Fig. 21. Charge Particle Densities. Electron, positive ion, and negative ion densities as a function of time with simplified source.

approximation is adequate; (2) The electron and positive ion behavior is similar for $t < 2 \times 10^{-8}$ sec; and (3) The electron density is within a factor of 100 of the ion density until $\sim 10^{-6}$ seconds. This latter point is important as we discuss electron mobility versus ion mobility.

Mobility. The mobilities of the various charged particles are functions of the air density, the applied electric field, and particle characteristics, e.g., mass, ionization, etc. We shall ignore all variations except the difference of mobility between electrons and ions:[60]

Electrons: $\mu_e \sim 1.0$ meter^2-sec^{-1}-volt^{-1} (114)

Ions: $\mu_\pm \sim 10^{-3}$ meter^2-sec^{-1}-volt^{-1} (115)

By writing the conductivity, Eq (97), so the summation is the electron contribution plus all the rest

$$\sigma(t) = \mu_e N_e(t) e + \sum_i{}' \mu_i N_i q_i \tag{116}$$

we can see that

$$\sigma(t) \cong \mu_e N_e(t) e \tag{117}$$

is a good approximation if the electron density is within two orders of magnitude of the ion density.

The balance of this chapter will look at the fields around a symmetric burst. The development follows the AFIT weapons effects lectures.[17]

Electric Field at Early Times

We are now able to compute the electric field around a symmetric nuclear burst. We shall look at the very early field and a later, nearly constant field. Because the initial conductivity and electric field are zero, the early Compton current is much greater than the conduction current:

$$\bar{J}_c \gg \sigma \bar{E} \tag{118}$$

This allows Maxwell's equation $\bar{J}_c + \sigma \bar{E} + \frac{\partial \bar{D}}{\partial t} = 0$ to be simplified to

$$\frac{\bar{J}_c}{\epsilon} = -\frac{\partial \bar{E}}{\partial t} \tag{119}$$

or

$$\frac{\partial \bar{E}}{\partial t} = \bar{\phi}_\gamma \frac{MFR_e e}{\lambda_\gamma \epsilon_o} \tag{120}$$

where

$$\bar{\phi}_\gamma = \phi_{\gamma_o} \frac{e^{-\mu r}}{4\pi r^2} e^{\alpha t} \hat{a}_r \tag{121}$$

The differential equation for the early electric field is then

$$\frac{d\bar{E}}{dt} = \phi_\gamma \frac{e^{-\mu r} MFR_e\, e}{4\pi r^2 \lambda_\gamma \epsilon_o} e^{\alpha t} \hat{a}_r \tag{122}$$

with the boundary conditions $\bar{E} = 0$ at $t = 0$. The solution is

$$\bar{E} = \phi_\gamma \frac{e^{-\mu r}}{4\pi r^2} MFR_e \frac{e}{\epsilon_o} \frac{1}{\alpha} (e^{\alpha t} - 1)\, \hat{a}_r + \cancelto{0}{F(r)} \tag{123}$$

where

λ_γ Gamma mean free path (meters)

MFR_e Electron mean free range (meters)

α Gamma e-fold growth rate (sec^{-1})

e Electron charge (coulombs)

ϵ_o Permittivity ($1/36\pi \times 10^9$ farads/meter)

Saturated Electric Field. Shortly after the previous equation becomes invalid another assumption can be made which leads to a simple equation for the electric field. At some point in time the electric field will be unable to grow because the conduction current will just oppose and cancel the Compton current.[60] At this time the $\bar{E}$ field will not vary in time, i.e., $\partial\bar{E}/\partial t = 0$, and we have what is called the saturated electric field.

From Eq (98) we have

$$-\bar{E} = \frac{\bar{J}_c}{\sigma} \tag{124}$$

The Compton current is given by Eq (68). The conductivity

may be approximated by the electron contribution only since $100\,N_e > N_\pm$ for $t < T_1$, (before recombination or attachment remove the electrons), i.e.,

$$\sigma \cong \mu_e N_e e \tag{117}$$

For N_e we have, by Eq (112a), that the number of electrons is

$$N_e = \frac{S_e(e^{\alpha t} - e^{-\nu_a t})}{\alpha + \nu_a} \tag{112a}$$

so the conductivity becomes

$$\sigma(\bar{r},t) = \frac{T_e(10^6)\mu\ \phi_{\gamma_0}\ e^{-\mu r}(e^{\alpha t} - e^{-\nu_a t})\ \mu_e e}{32.5\quad 4\pi r^2\ (\alpha + \nu_a)} \tag{125}$$

where S_e the electron source term is given by Eq (103). The saturated electric field is then

$$\bar{E} = \left(\epsilon_0 \phi_{\gamma_0} \frac{e^{-\mu r}}{4\pi r^2} \frac{MFR_e}{\lambda_\gamma} \frac{e}{\epsilon} e^{\alpha t}\right) \times$$

$$\left(\frac{T_e(10^6)\, e\, \phi_{\gamma_0}\, e^{-\mu r}(e^{\alpha t} - e^{-\nu_a t})\mu\ \mu_e\ \hat{a}_r}{32.5\quad 4\pi r\quad (\alpha + \nu_a)}\right)^{-1} \tag{126}$$

where we have used Eqs (68) and (119) for $\bar{J}_C$ and σ respectively. By clearing fractions and dividing by $e^{\alpha t}$ we get

$$\bar{E} = \frac{MFR_e\ 32.5\ (\gamma_a + \alpha)}{\left(1 - \frac{e^{-\gamma_a t}}{e^{\alpha t}}\right) T_e(10^6)\ \mu_e}\ \hat{a}_r \qquad (127)$$

Now $e^{-(\gamma_a + \alpha)t} \longrightarrow 0$ as time increases since $\gamma_a \simeq 10^8 P^2$ (where P is pressure in atmospheres) and $\alpha \gtrsim \gamma_a$; therefore the saturated electric field can be written

$$\bar{E}_{sat} = \frac{MFR_e\ 32.5\ (\gamma_a + \alpha)}{T_e(10^6)\ \mu_e}\ \hat{a}_r \qquad (128)$$

which is approximately correct for times up to T_1 , the gamma peak.[61] Notice that $\bar{E}_{sat}$ is not a function of the weapon yield.

Maximum Radius of the Saturated Field. In order to find the maximum radius of the saturated field we could substitute T_1 for t in Eq (123) since the maximum radius occurs when the gamma flux is a maximum. Instead we shall substitute the total gamma flux, γ , found by integrating the flux output from $t = 0$ to $t = T_1$:

$$\gamma = \int_0^{T_1} \phi_\gamma\, dt \qquad (129a)$$

$$= \phi_{\gamma_0} \int_0^{T_1} e^{\alpha t}\, dt \qquad (129b)$$

$$= \frac{\phi_{\gamma_0}}{\alpha}(e^{\alpha T_1}-1) \tag{129c}$$

The equations for the electric field, Eqs (123) and (128), become the following when the field is saturated to its maximum radius:

$$\bar{E} = \phi_{\gamma_0} \frac{e^{-\mu r}}{4\pi r^2} \frac{MFR_e}{\lambda_\gamma} \frac{e}{\epsilon} \left(\frac{e^{\alpha T_1}-1}{\alpha}\right) \tag{130}$$

$$= \frac{MFR_e \; 32.5(\gamma_a+\alpha)}{T_e(10^6) \; \mu_e} \tag{128}$$

Now we can replace $\phi_{\gamma_0}(e^{\alpha T_1}-1)/\alpha$ by γ ; equate the right hand sides; and solve for the terms containing r :[62]

$$r^2 e^{-\mu r} = \frac{\gamma}{4\pi} \frac{e \, T_e(10^6) \, \mu_e}{\lambda_\gamma \epsilon_0 \, 32.5 \, (\gamma_a+\alpha)} \tag{131}$$

This last equation is solvable by iterative procedures.

Example 3. To illustrate the magnitude of the saturated electric field and its maximum radius, we will work an example for a 1 MT burst at an altitude of 10 kilometers.[63] Parameters in Table 1 and in Table 2 will be used.

Table 2

Parameters of a Nuclear Burst at 10 Kilometer Altitude*

Altitude of Burst	: 1.0×10^4 m	P^2 (Atmos. Pres)	: 0.067 $Atmos^2$
Gamma Energy	: 1.5×10^6 eV	ρ (Density)	: 0.427 kg/m^2
Electron Energy	: 0.7×10^6 eV	ν_a (= $10^8 P^2$) Collision rate	: 0.067×10^8 col s^{-1}
Growth Rate (α)	: 10^8 $second^{-1}$	μ_T Macroscopic cross section	: 1.25×10^{-3} m^{-1}
Gamma Production (ϕ_{γ_0})	: 2.3×10^{31} gammas s^{-1}	λ_γ Gamma MFP ($=1/\mu_T$)	: 7.82×10^2 m
Electron Charge	: 1.6×10^{-19} c	μ_e Electron Mobility	: 1.0 m^2 V^{-1} s^{-1}
$MFR_e = 0.01\ \lambda_\gamma$ (by supposition)			

*m-meters, s-seconds, eV-electron volts, V-volts; kg-kilograms, C-coulomb.

Using the numbers provided in Eq (128) we arrive at an E_{sat} = 4 x 104 volts-$meter^{-1}$.
Using Eq (131) we find r_{sat} = 2.4 kilometers.

Summary

The symmetric burst has only an electric field $\bar{E}$ and that only within the gamma pulse wavefront. The magnitude of the field is interrelated with the air's conductivity and the conduction current. The conductivity is the result of the primary electron ionizing the air as it is slowed. The behavior of the conduction path is affected by the rate of removal of charge carriers especially the removal of electrons by attachment to oxygen.

At early times the electron mobility is so much greater than ion mobility that only electrons need be considered. By using certain assumptions the early electric field, saturated electric field, and the maximum radius of the saturated field were found. Values for an example were $\sim 4\times10^{4}$ volts/meter for the saturated field and its maximum radius was $\sim 2.4\times10^{3}$ meters.

V. The Radiated Electromagnetic Pulse

Because a radiated electromagnetic wave requires both $\bar{E}$ and $\bar{H}$ fields, the symmetric nuclear burst could not radiate a signal (there was no magnetic field produced). This is not the case for bursts which are asymmetric or occur in the presence of an external magnetic field. These bursts generate a radiated EMP through three main mechanisms: the asymmetric flow of Compton and conduction currents due to differences in the density of the environment; the asymmetric flow of currents due to the interaction of moving electrons with a magnetic field; and the hydrodynamic exclusion of the earth's magnetic field. As we shall see, a single mechanism is usually dominant at a given height of burst. We shall study each mechanism separately later in the chapter.

Height of Burst

In order to give the reader some insight into which of the mechanisms may dominate as the source of the EMP we shall qualitatively discuss the variation in EMP generation mechanisms with height of burst. We will divide the range of burst heights from surface to far space into five regions. In each region we shall discuss the asymmetries present and categorize the radiated EMP as strong or negligible.

Surface Burst. (See Fig. 22-1A) In the surface burst the main EMP generating mechanism is the asymmetry in the Compton and conduction currents caused by the presence of the earth.

These asymmetric currents radiate much like a dipole antenna. There are other asymmetries present, e.g., variation in the earth's surface and the presence of the geomagnetic field, but their effect is minor compared to the asymmetry due to the earth. If we treat the earth as air with 1000 times the density of air at STP we find that the mean free range of the gammas is 300 meters in air but only 0.3 meters in earth. We conclude that there will be a strong EMP from the surface burst.

Air ($\sim$3-20 km). (See Fig.22-1B) In the relatively dense lower atmosphere ($\sim$3-20 km) X-rays and gamma rays have ranges which are short compared to the scale height of the atmosphere ($\sim$7 km). This means that the range of each will not vary significantly with direction. Also because of the air's density, the Compton electron's range is too short to permit a significant transverse current to be created by the electron's turning under the influence of the geomagnetic field.[64]

For Example 4 let us find the asymmetric attenuation around a nuclear burst in this region at 10 kilometers. We will calculate the e-fold distance for upward and downward travel of gamma rays due only to Compton-effect attenuation. (The e-fold distance is the distance for a value to change by a factor of e or 1/e from an original value, c.f., two-fold decrease.) The macroscopic cross section for 1.5 MeV gammas is 2.5×10^{-3} m^2-kg^{-1} ($= \mu_m$) or 3.1×10^3 m^{-1} at

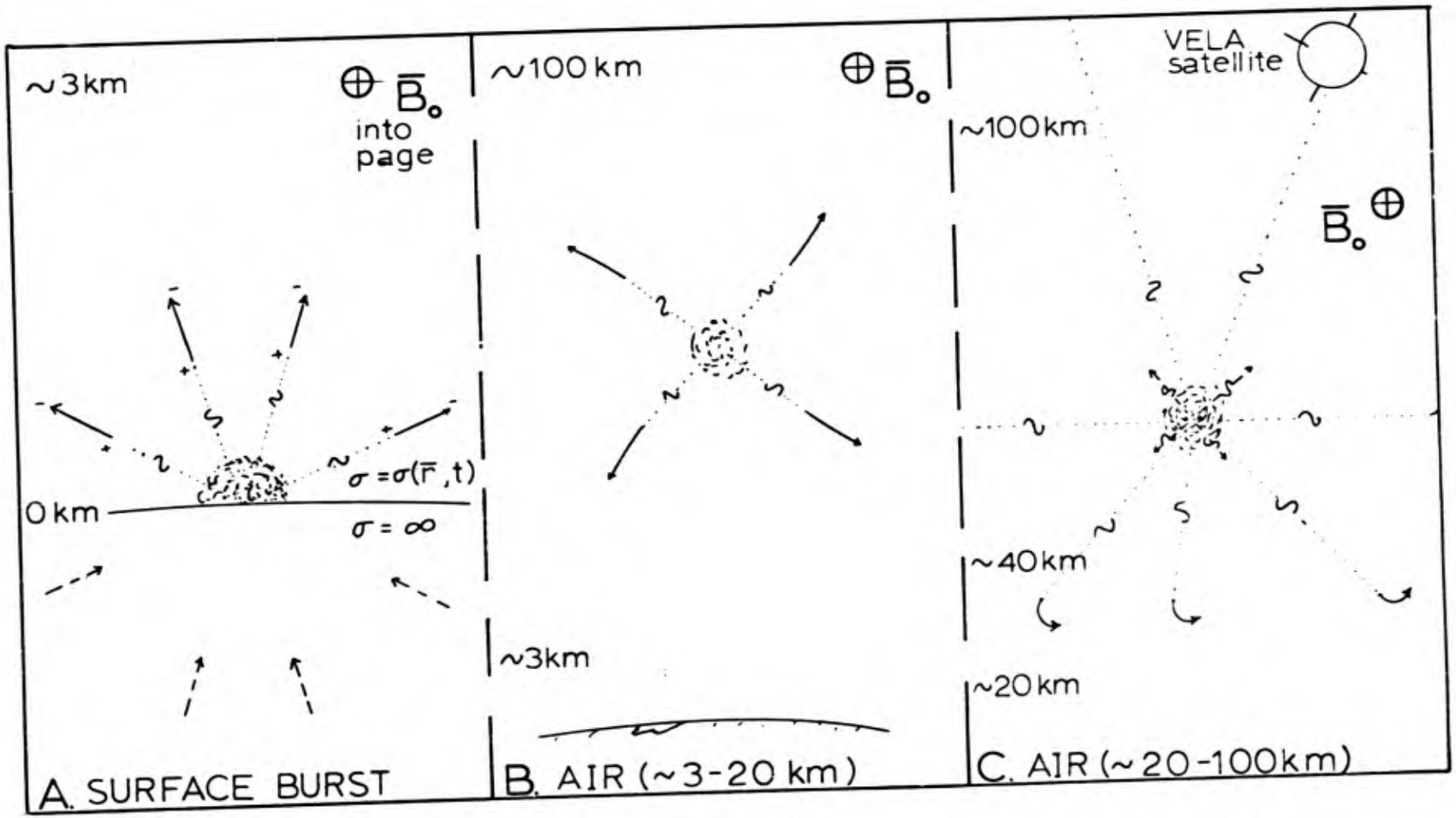

Fig. 22-I. Features of Nuclear Bursts Significant to EMP Production. Gamma rays (..... ∿ .....) are depicted creating currents (——→) in the weapon's surroundings. X-rays (←--- ∿ ---→) behave similarly but are much less energetic. The image currents (←— — — —) below the surface burst flow up and left when the real currents flow up and right, etc.

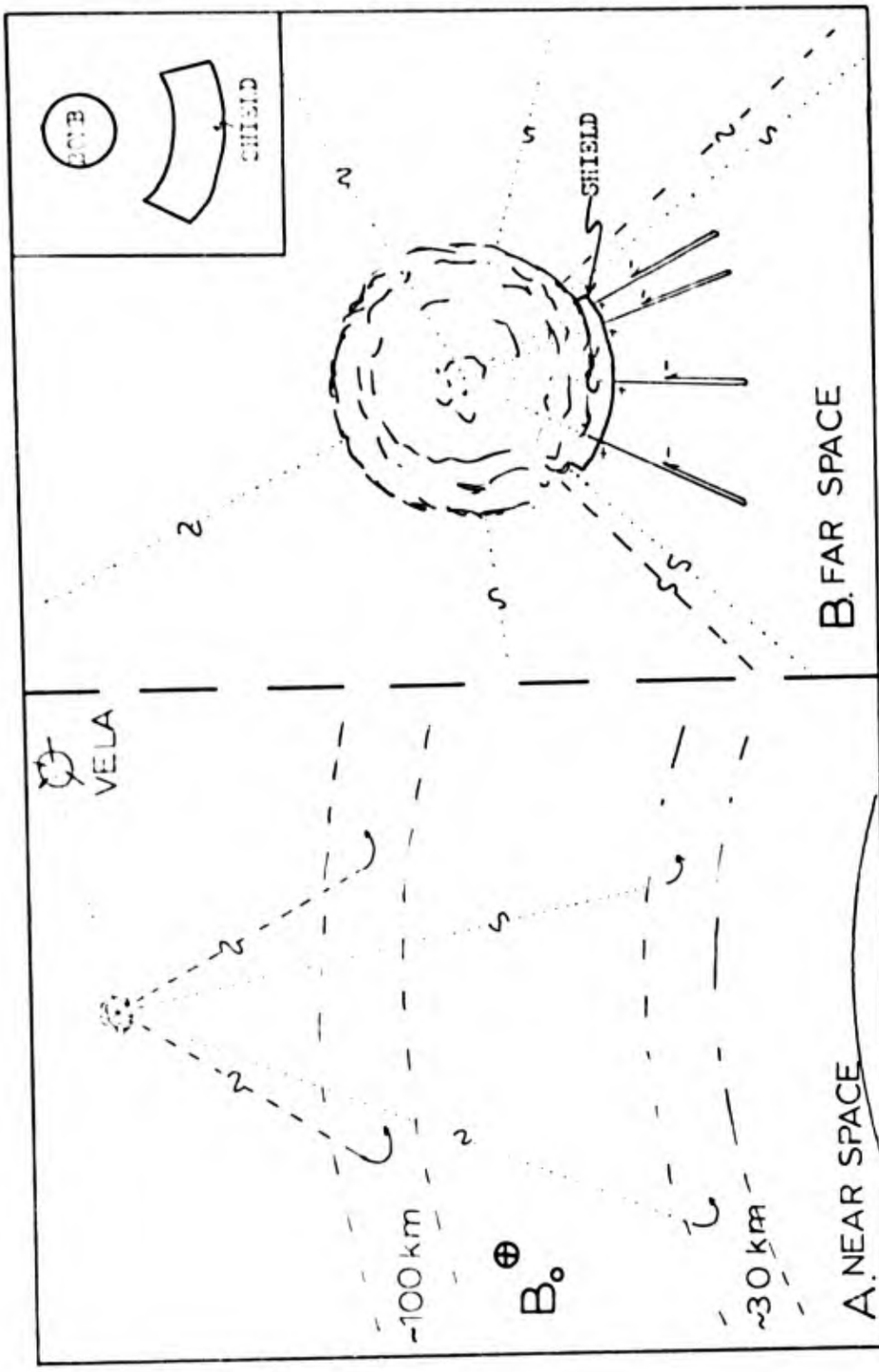

Fig. 22-II. Features of Nuclear Bursts Significant to EMP Production. (cont) The symbology is described on Fig. 22-I. The inset to Fig. 22-IIB shows the relationship of bomb and shield before the explosion.

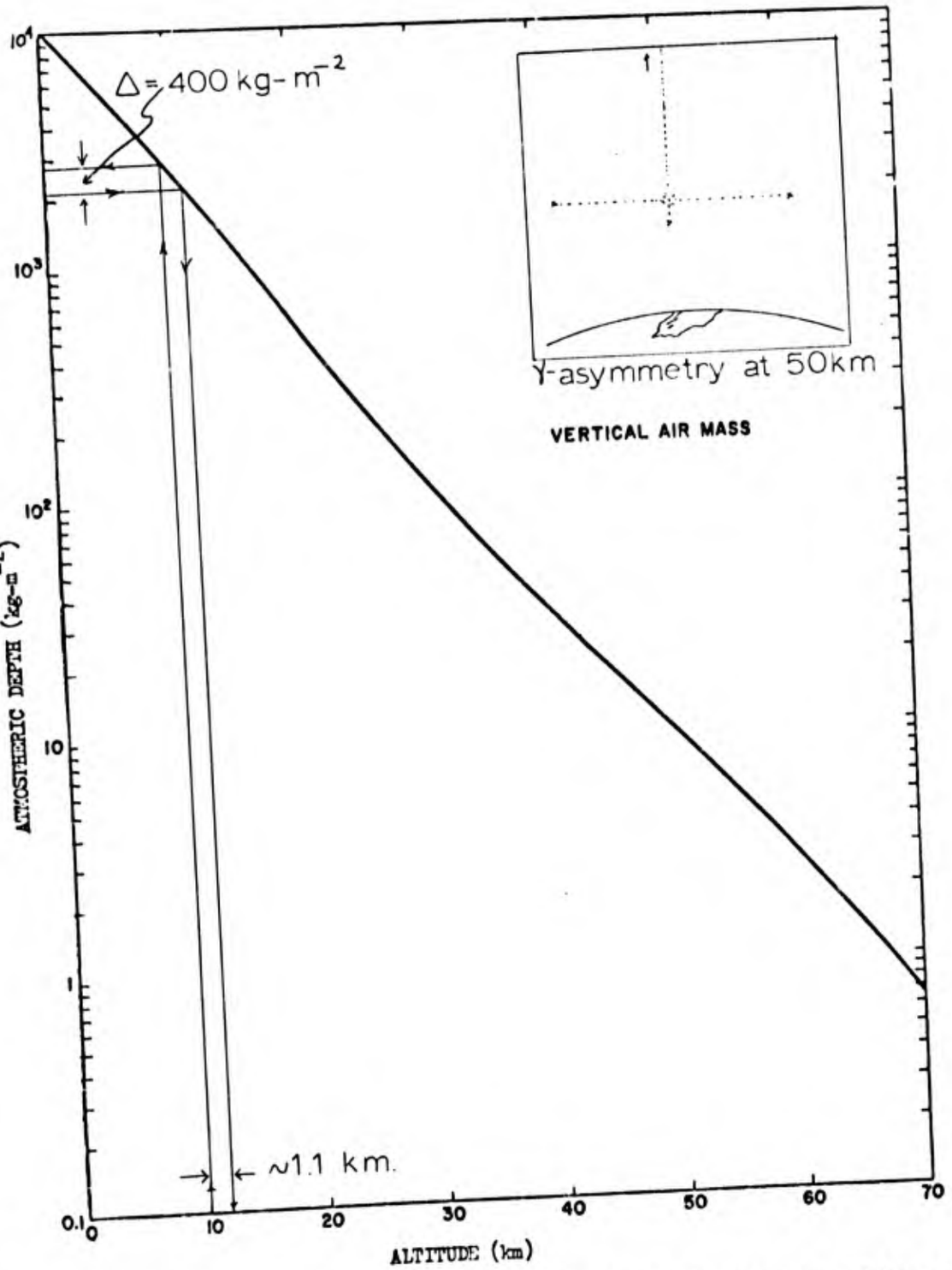

Fig. 23. Vertical Air Mass. The mass of air per unit area in a vertical column extending upward from an altitude (in Km) above sea level.[64] The example is entered at 10 km, proceeds through a change in atmospheric depth of 400 and exits at 11.1 km (See text).

sea level, and the microscopic cross section is 1.2×10^{-28} m^2/particle.[65]

By entering Fig. 23 at 10 kilometers and finding the altitude change required to cause the vertical air mass to change by $1/\mu_m$ (= 400 kg-m^{-2}), we can find the e-fold distances upward and downward. This procedure is indicated for upward attenuation by the arrows on Fig. 23. The e-fold distances, $\sim$ 1.1 km upward and $\sim$ 0.9 km downward (found by using Δ(kg-m^{-2}) into denser air), show in this example that variation in air density causes little asymmetry.

The minor asymmetries, e.g., air density variations, and geomagnetic field, do cause a radiated signal which can be detected over long ranges, but the overall conclusion is that the radiated EMP from a burst in this region is weak.[67]

Air ($\sim$20 - 110 km). (See Fig. 22-1C)The air in the region from $\sim$20 km to $\sim$110 km is thin enough that the gamma rays and neutrons can escape the earth's atmosphere before interacting. A space-borne gamma ray detector above a nuclear explosion within this region could probably detect it.[68] The rest of the gamma rays and neutrons interact in the atmosphere around 20-30 kilometers above the earth. The Compton and conduction currents formed at this 20-30 km height are initially moving outward from the burst but are turned by the geomagnetic field, and these currents, which, because of the turning, are now moving transverse to the radial direction, generate a radiated EMP. There may be a

small contribution to the radiated EMP by the variation of X-ray mean free path with direction but this would be a minor source.

For Example 5 let us calculate the e-fold distance for upward, downward, and horizontal travel of the gamma rays from a burst at 50 km. By using the same procedure used in Example 4 we find the e-fold distance downward is 26 km (50 - 24 = 26). When we try to find an e-fold distance upward we see that there is not enough atmosphere remaining to cause that much attenuation. Horizontally the microscopic cross section times the particle density gives a macroscopic cross section for 50 km of 2.55×10^{-6} m^{-1}. The reciprocal of the macroscopic cross section is the mean free path, $\sim$ 39 km. These three distances are depicted in the inset to Fig. 23.

In summary, the EMP from this region is quite strong due to the transverse currents formed around 20-30 kilometers.

Near Space ($\gtrsim$ 110 km). (See Fig.22-IIA)The downward directed X-rays and gamma rays from a near space nuclear explosion ($\gtrsim$ 110 km) would impinge upon the earth's atmosphere. The X-rays are absorbed strongly around the 100-110 km altitude, and the gammas rays are absorbed strongly around 20-40 km altitude.[69]. Both the photoelectrons and Compton electrons which are produced have mean free ranges that are long enough to allow the electron to be turned by the interaction with the geomagnetic field, For example, a

0.7 MeV electron at 30 km has a mean free range of 204 meters compared to a turning radius of only 10 meters.

Whether the EMP produced by the X-rays absorbed around 110 km or the EMP from the gammas absorbed around 30 km is stronger depends upon the height of the burst: a burst near 110 km would probably generate a stronger signal from X-rays because of the intensity of the X-ray flux: a burst far above 110 km would probably generate a stronger signal by the gamma interaction around 30 km.

In summary, the large transverse currents which result from the interaction of the electrons with the magnetic field in the near space burst produce a strong, far ranging EMP.

Far Space. A nuclear explosion far in space can be expected to produce an EMP due to asymmetries in the case which are represented by a shield in Fig. 22-IIB (this EMP is called the case signal). The case signal is weak, however, largely because the nuclear explosion is energetic enough to completely ionize its immediate vicinity and fully ionized regions are poor radiators.[70] The case signal which does form results from Compton electrons which are propelled outward by the gamma rays being accelerated back to the case by the net positive charge which remains at the burst point. This acceleration produces a signal. Reference 71 contains a complete description of the case signal, including the effects of shielding used in an effort to conceal the explosion.

Table 3

Atmospheric Properties for 0, 10, 50 and 105 Kilometers

Geometric Altitude (Km)	*	0	10	50	105
Scale Height, H (Km)	*	8.34	6.5	8.0	7.1
Density, ρ (Kg/m^3)	*	1.2250	4.1351 (-1)	1.0260 (-3)	2.117 (-7)
Density Ratio to Sea Level, ρ/ρ_o	*	1	3.3756 (-1)	8.3827 (-4)	1.728 (-7)
Number Density of Particles (m^{-3})	*	2.547 (25)	8.598 (24)	2.13552 (22)	4.434 (18)
Gamma Mean Free Path, λ_γ (m)	**	3.0 (2)	9.0 (2)	3.6 (5)	1.7 (9)
X-Ray Mean Free Path, λ_x (m)	**	--	1.5 (-4)	5.0 (-2)	2.5 (2)
14 MeV Neutron MFP, λ_n (m)	***	2.4 (2)	7.2 (2)	2.9 (5)	1.4 (9)
Electron Mean Free Range--0.7 MeV (m)	**	3.0	9.0	3.6 (3)	1.7 (7)
Electron Mean Free Range--3.8 KeV (m)	**	1.4 (-4)	4.0 (-4)	1.6 (-1)	8.1 (2)

* Ref 73
** Calculated using Eqs (132a), (132b), (133a), and (133b).
*** Based on total cross section from Ref 74.

Altitude Correction. Because there may be occasion to work problems involving other altitudes than those given in specific examples, we present altitude correction formulas from Karzas and Latter: The mean free path for gamma rays and X-rays may be corrected by using

$$\lambda_\gamma = \lambda_{\gamma_0} \frac{\rho_0}{\rho} \cong 3\times10^2 \frac{\rho_0}{\rho} \tag{132}$$

$$\lambda_x = \lambda_{x_0} \frac{\rho_0}{\rho} = \frac{10^{-2}}{4} (E_x)^{-3} \frac{\rho_0}{\rho} \tag{132b}$$

and the mean free range of Compton electrons and photoelectrons may be corrected by using

$$MFR_{e_\gamma} = (MFR_{e_\gamma})_0 \frac{\rho_0}{\rho} \cong 3 \frac{\rho_0}{\rho} \tag{133a}$$

$$MFR_{x_e} = (MFR_{x_e})_0 \frac{\rho_0}{\rho} \cong 10^{-5} (E_x)^2 \frac{\rho_0}{\rho} \tag{133b}$$

where E_x is the photoelectron energy in KeV and ρ_0/ρ is the ratio of sea level air density to air density at altitude.[72] Table 3 presents basic data about the atmosphere for the convenience of the reader.

On Investigating the EMP

Before we discuss the three mechanisms which generate the EMP we will look briefly at the methods used for analyzing the actual situations and then enumerate a few of the major assumptions which we use in this thesis.

In the literature, the analysis of the various possible nuclear burst environments seems to start with an assumed model of the burst environment using idealized concepts (e.g., monoenergetic gamma sources from a point, perfect conductors, etc.). Maxwell's equations for this model are written in the appropriate coordinate system and often in the time retarded form.

These equations are usually manipulated somewhat and then simplified by dropping the small or slowly varying terms. Despite all this the equations often must be written in terms of integrals which cannot be solved analytically or left in differential form. Solutions can be obtained by numerical integration on a computer.

On occasion analytic solutions are found but the solutions are often so complex that they disguise the interaction between parameters and the consequences of varying them. Some models lend themselves to an analytic solution but beyond certain limits they predict illogical consequences (the model doesn't apply). The models we will use are more unreal than most of those in the literature but they lead to simpler solutions and do expose the physical principles

behind the EMP. If a differential equation is more illuminating than its solution might be, we do not hesitate to leave it in differential form.

Some of the simplifications which we will use are also used in the more sophisticated studies on the EMP. One assumption is that the burst itself is spherically symmetric, i.e., no case signal. Another is that only one mechanism is operating at any one time, e.g., only air density asymmetries are present. The final simplification which is usually used is the assumption of axial symmetry in the environment, i.e., no variation around some axis, hence the EMP will be independent of the azimuthal parameter ϕ. Because of this symmetry there will be only three electromagnetic field components in spherical coordinates: E_{radial}, $E_{longitudinal}$, and $H_{azimuthal}$ or E_r, E_θ, and H_ϕ (See Fig. 24).

THE SURFACE BURST

The first of the mechanisms for generating an EMP, asymmetries in the Compton and conduction currents due to variations in the density of the environment, is present in all explosions. The asymmetric currents which generate the case signal (See Far Space, page 95) are made asymmetric by variations in the bomb itself. Because the bombs cannot be perfectly symmetric a case signal is always present. The asymmetric currents caused by variations in the air's density

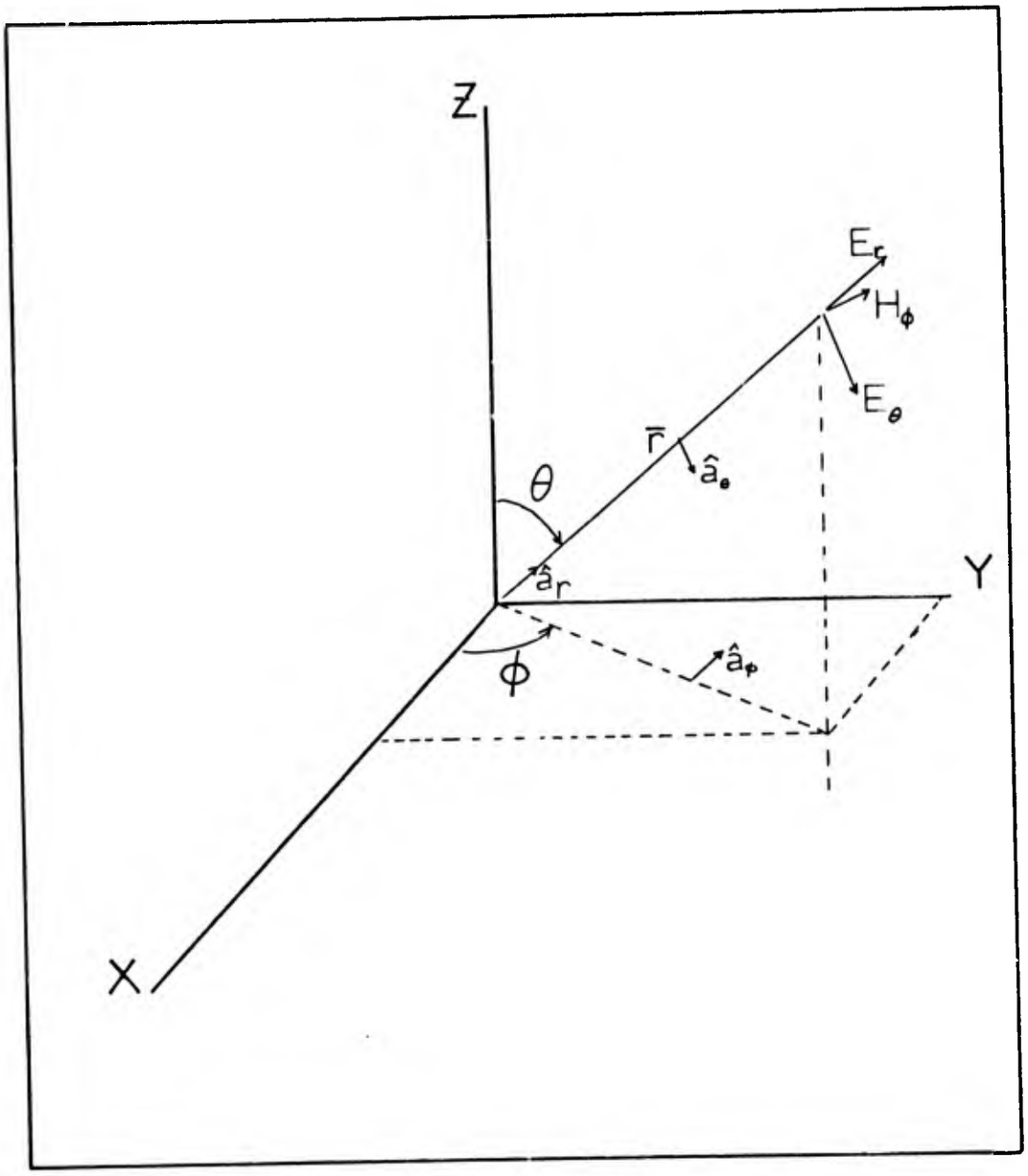

Fig. 24. Electromagnetic Field Components in an Axially Symmetric Environment.

produce only a small EMP in the lower atmosphere and are a secondary EMP source in the upper atmosphere. Because of this minor role we shall ignore variation in air density.

A major asymmetry in density exists at the earth-air interface and is the subject of this section. Here photons and Compton electrons have very short ranges in the ground compared to their range in the air. This causes a high asymmetry in the vertical current flow.

This air-earth asymmetry occurs even for bursts whose fireball does not touch the ground because the gamma's range carries them beyond the fireball. However in this thesis we shall confine our attention to a model based upon a burst on the surface where any photons emitted into the upper hemisphere will travel radially in the air and where any photons emitted into the lower, ground, hemisphere will be absorbed immediately. In this model we take the conductivity of the ground plane to be infinite, i.e., the ground is a perfect conductor, and it is considered flat.

Choosing the surface to be a flat, perfect conductor allows us to use simple image electric currents to discuss the production of electromagnetic fields. These image currents flow, as shown in Fig. 25, antiparallel across the surface or continuously through the surface.[76] The tangential electric field on this surface is therefore zero because the antiparallel flows cancel as they must on a perfect conductor. If the right hand rule for determining the

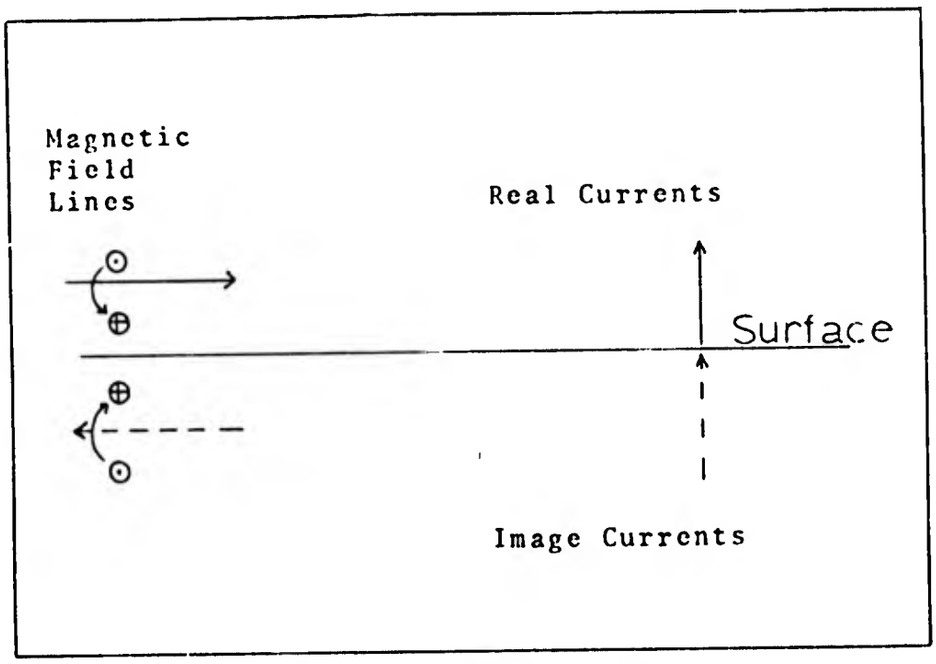

Fig. 25. Image Currents

direction of a magnetic field is applied to the tangential currents above and below the surface, we see that each current produces a magnetic field which is directed into the paper at the surface. Therefore the surface magnetic fields is twice that attributable to the real current. We could say that a mathematical tool identified as a magnetic current has generated the electric fields just above and below this surface.

That the electric and magnetic fields play a mathematically dual role has been stressed throughout this thesis, e.g., writing $\bar{H} = \mu_o^{-1}\bar{B}$ (instead of $\bar{B} = \mu_o\bar{H}$) to emphasize the similarity with $\bar{D} = \epsilon_o\bar{E}$. We shall use this duality to find a magnetic dipole later.

Three Phases of EMP Generation for a Surface Burst

The surface burst can be examined for early, intermediate and late times. The current-production method and simplifying assumptions differ in each phase. We call these phases the gamma pulse phase, the saturated field phase and the ionic conduction phase.

Gamma Pulse Phase. In the very early moments of a nuclear burst an intense, nearly immediate pulse of gamma rays is emitted. These create currents that flow just behind a wavefront that is moving outward at the speed of light. Any electromagnetic signals generated can travel no faster than light so no signal is observed until the passage of the gamma pulse. To successfully analyze a pulse of this nature would require the full use of Maxwell's equations in retarded time. However to picture the events we can assume the Compton electrons form a radial electric field in a shell within the gamma wavefront and above the earth's surface (See Fig. 26a). Even the electrons just above the surface do not have enough time to react to the fields caused by the image currents just below the surface. In this case we will use the electric field given by the early time equation from the symmetric field analysis, Eq (123):

$$\bar{E} = \phi_{\gamma_0} \frac{e^{-\mu r}}{4\pi r^2} \frac{MFR_e}{\lambda_\gamma} \frac{e}{\epsilon_o} \frac{(e^{\alpha t} - 1)}{\alpha} \hat{a}_r \qquad (123)$$

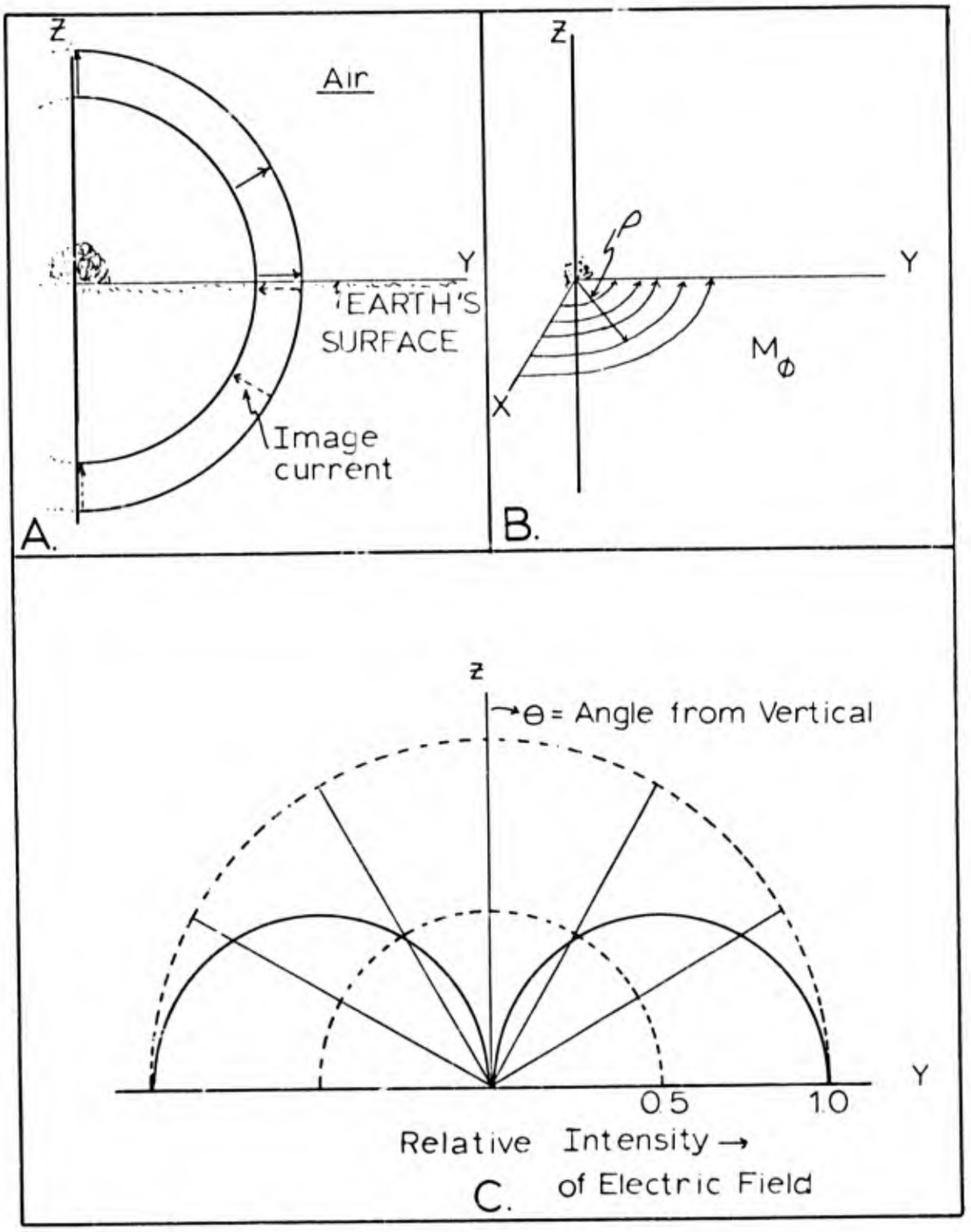

Fig. 26. Surface Burst. In A, the current and image current are moving in opposite directions in a narrow pulse which is moving outward. In B the effective magnetic current filaments are depicted.[79] In C we show the radiation pattern for this magnetic dipole radiator.[80]

Because this pulse is moving at the speed of light we assume that we can approximate its effect by an instantaneous switching-on of the entire source from the burst point to a point at which the source currents are insignificant. We restate the previous approximation about ignoring retarded time by saying that an external observer would see nothing until the production from the entire field reaches him.

In order to see that only the ground plane contributes to the magnetic field, we find the time rate of change of magnetic field, $\partial \bar{B}/\partial t$. We do this by taking the curl of the radial electric field, but $\nabla \times \bar{E}$ is zero everywhere except at the ground plane (This is true because we are taking the curl of a radial vector which is a function of r only, except where the current switches in direction). Since only the ground plane values of the current contribute to the magnetic field, and hence the radiated signals, let us replace the radial electric field by magnetic current loops (Fig. 26b) and find the magnitude of the magnetic dipole moment which is formed and then, by duality again, return to the fields in terms of the $\bar{H}_\phi$ vector.[77]

The magnetic currents are found simply by replacing the electric field $\bar{E}_r$ by $\bar{M}_\phi$; the magnetic surface current density:[78]

$$\bar{M}_\phi = \phi_0 \frac{MFR_e}{\lambda \gamma} \frac{e}{\epsilon_0} \frac{1}{\alpha 4\pi} \left(\frac{e^{-\mu r}}{r^2} \right) f(t) \hat{a}_\phi \qquad (134)$$

where we have replaced $(e^{\alpha t} - 1)$ by $f(t)$. Because this method depends upon variables which vary sinusoidally in time, we shall think of $f(t)$ as <u>one</u> component of the Fourier series representation of the electric field's time dependence.[81] We shall not carry out the Fourier analysis indicated but this should present no conceptual difficulties for, hopefully, the reader is acquainted with Fourier analysis and realizes that it is possible.[82] In any case we re-write Eq (134) to clarify later steps:

$$M_\phi = C\frac{e^{-\mu r}}{r^2} \tag{135}$$

where the C replaces the constants in Eq (134) and the time dependence is implied.

In order to find the total magnetic dipole moment we must integrate the dipole moments of filaments of magnetic current. A filament of magnetic current K is $dK = M_\phi d\rho$ where ρ is now the radius vector in the ground plane.[83] The total magnetic dipole moment of the source is then

$$KS = \int_S S\,dK \tag{136}$$

where S is the surface bounded by the magnetic current, (Fig. 26b)

or

$$KS = \int_0^R \pi \rho^2 M_\phi d\rho \tag{137}$$

hence $$KS = \pi \int \rho^2 C \frac{e^{-\mu\rho}}{\rho^2} d\rho \qquad (138)$$

This expression must be integrated from zero to the outer boundary of the source region and is

$$KS = \frac{-\pi C e^{-\mu\rho}}{\mu} \Bigg|_0^R = \frac{\pi C}{\mu} - \frac{\pi C e^{-\mu R}}{\mu} \qquad (139)$$

($e^{-\mu R} \cong 0$)

but since the value at the outer boundary is negligible we set it equal to zero. This equation is just the electromagnetic dual of a dipole of electric current. The magnetic field of a dipole antenna and its image at the ground plane is

$$\bar{H}_\phi = \frac{\pi C}{\mu} e^{-jkr} \sin\theta \frac{\omega \epsilon_o}{\lambda r} \hat{a}_\phi \qquad (140)$$

which is valid for distances far outside the boundary regions (See Fig. 26c).[84] The variables in this equation are the propagation constant k ; the angle from the observer to the plane's normal θ ; the radian frequency of the particular component ω ; the wavelength of the particular component λ ; the permittivity of free space ϵ_o ; and the radial distance r. Note that the time dependence is still an implied function with a particular frequency.

The electric field is found by the relation $E_\theta = Z_o H_\phi$ which is applicable for fields far from the source (i.e., in the radiated field):[85]

$$E_\theta = Z_o \frac{\pi C}{\mu} e^{-jk.r} \sin\theta \frac{\omega \epsilon_o}{\lambda r} e^{j\omega t} \quad (141)$$

where we have inserted the time variation (in exponential notation).

Finally we take the real instantaneous value of this equation to get the usual form of the electric field equation:

$$E_\theta = \sqrt{2} Z_o \frac{\pi C}{\mu} \frac{\epsilon_o \omega}{\lambda} \frac{\cos(\omega t - kr)}{r} \sin\theta \quad (142)$$

where the $\sqrt{2}$ results from the conversion of root mean square amplitudes to instantaneous amplitude. The field we have found varies sinusoidally and is propagating outward as evidenced by the $\cos(\omega t - kr)$ term. This is the variation found in the expression for the radiation far from a dipole antenna source.

In order to estimate the magnitude of the field we shall replace C and insert sample values into this equation:

$$E_\theta = \sqrt{2} Z_o \frac{\pi}{\mu} \frac{\phi_o}{4\pi} \frac{MFR_e}{\lambda_\gamma} \frac{e}{\epsilon_o \alpha} \frac{\omega \cos(\omega t - kr)\sin\theta}{\lambda r} \quad (143)$$

$$E_\theta = \frac{\sqrt{2} Z_o \phi_o MFR_e}{4\alpha} \frac{2\pi c \cos(\omega t - kr)\sin\theta}{r \lambda^2} \quad (144)$$

where $Z_o = 120\pi$ (Intrinsic impedance of free space)

$MFR_e = 3$ meters

$e = 1.6 \times 10^{-19}$ coulombs

$\alpha = 10^8$ sec^{-1}

$\phi_t = 3.4 \times 10^{25}$ photons

$c = 3 \times 10^8$ meters-sec^{-1}

Inserting these numbers we get the following expression:

$$E_\theta \cong 4\times10^{10} \frac{\cos(\omega t - kr)\sin\theta}{r\lambda^2} \qquad (145)$$

This function is true only for fields far from the source. If we choose 10 km and frequencies of 1 Mhz and 10 Mhz we get peak values of 4.5×10^2 and 4.5×10^4 volts per meter respectively for the two frequencies. This model must break down as the frequency grows higher. One discrepancy is present because we did not actually compute any Fourier coefficients when we conceptually replaced $f(t)$ by its Fourier series.

Saturated Field Phase. In the surface burst, at times approximately equivalent to the time at which the electric field is saturated, the EMP generation mechanism is different from that of the gamma pulse phase. The electric field may be nearly constant during this time because the current density and conductivity have similar dependence on time (See Eqs (126) and (127)). These currents which are electronic in character (rather than ionic) flow to a large

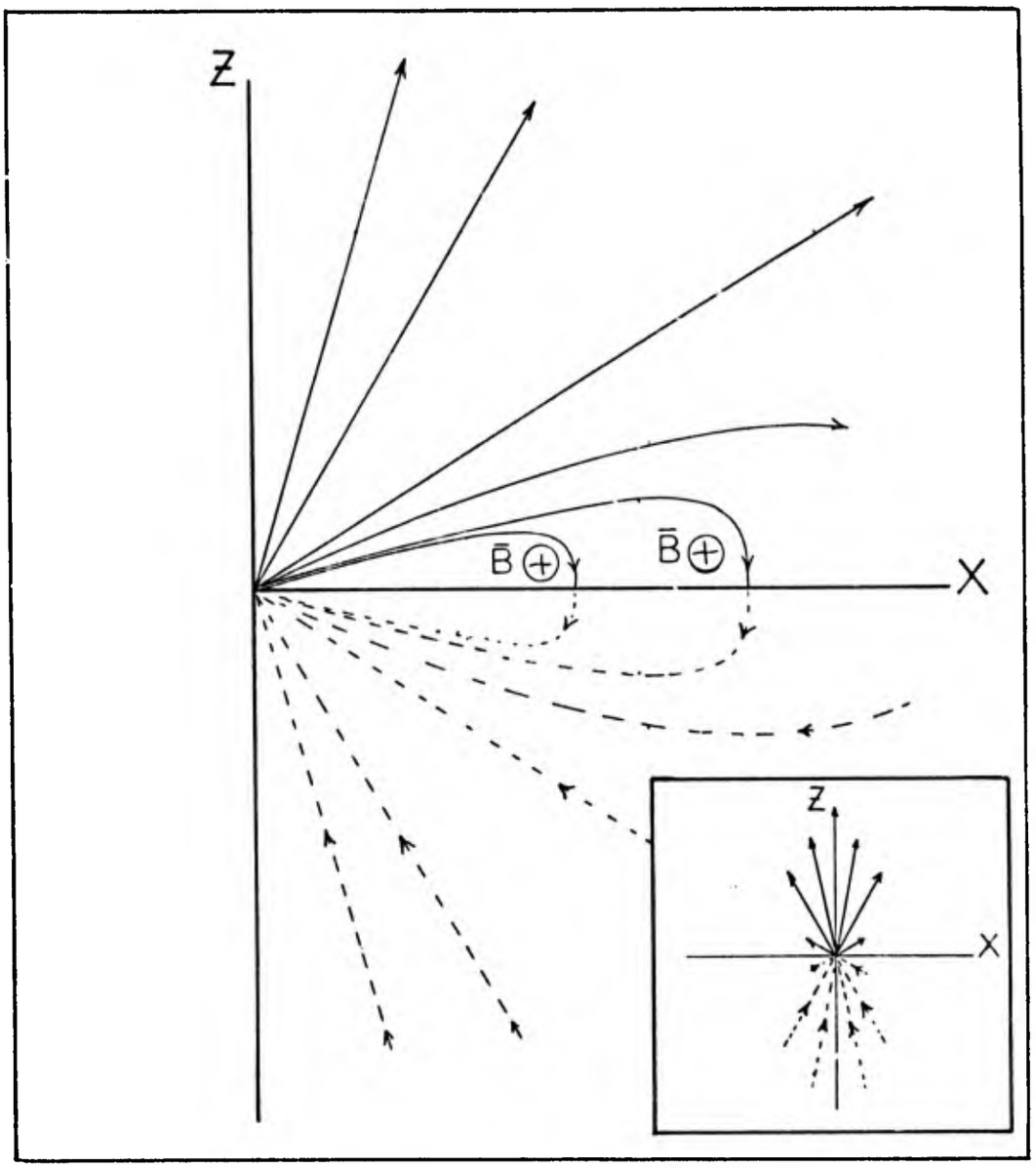

Fig. 27. Surface Burst with Image Currents. The burst is axially symmetric about Z. The lines shown are sections through surfaces of rotation. The currents intersect the X surface normally. The image currents shown dotted) must flow in the direction indicated. The inset depicts the current model, Eq (146).

extent toward the ground plane as shown in Fig. 27.[86] The current and image current form a large loop of current which creates a transverse magnetic field into the paper in Fig. 27. This time varying magnetic field creates a time varying electric field also in the transverse direction and the mechanism for a radiated signal is formed.

In line with our discussion of the path of the currents in this intermediate time, let us propose a current distribution

$$\bar{J} = 2 J_0 \frac{\cos\theta}{r^2} f(t) \hat{a}_r \tag{146}$$

which is shown in the inset to Fig. 27. The radial current is greatest along the vertical axis and zero along the horizontal axis. The image current given by this function does not contradict the behavior specified for image currents. We will find the $\bar{H}$ field that this current generates and then discuss the radiated field that it would generate.

For the saturated-field time regime, Maxwell's law $\nabla \times \bar{H} = \bar{J} + \partial \epsilon_0 \bar{E}/\partial t$ becomes Ampere's Law

$$\nabla \times \bar{H} = \bar{J} \tag{147}$$

inside of the current region since the electric field is constant in time. By carrying out the indicated curl operation we get the following vector differential equation:

$$\frac{1}{r^2 \sin\theta}\left[\hat{a}_r \frac{\partial}{\partial\theta}(r \sin\theta H_\phi) - r\hat{a}_\theta \frac{\partial}{\partial r}(r \sin\theta H_\phi)\right] = J(r,t)\hat{a}_r \quad (148)$$

where we have kept only the H_ϕ component of $\bar{H}$ by virtue of the behavior of an axially symmetric model. By equating the $\hat{a}_r$ components of this equation we get a differential equation which integrates easily:

$$\frac{\partial(\sin\theta H_\phi)}{\partial\theta} = \frac{2J_o \cos\theta \sin\theta f(t)}{r} \quad (149)$$

or

$$\sin\theta H_\phi = \frac{2J_o \sin^2\theta f(t)}{2r} \quad (150)$$

or

$$H_\phi = \frac{J_o \sin\theta f(t)}{r} \quad (151)$$

This magnetic field behaves logically for the environment we have described. The field is zero at $\theta = 0$, i.e., along the axis of symmetry and the field's magnitude is decreasing with radius. The singularity at $r = 0$ is removable in reality since the net current there is zero. After we look at the differential equation for the magnetic field external to the source region, we shall see that the specific current we chose is unable to provide fields that will match

the boundary conditions demanded by a radiated field. In order to get those radiated fields we must return to Maxwell's equations.

By using the two curl equations, we shall derive the wave equation which the electric fields outside the burst must obey.[87] Outside the source region there are no conduction currents

$$\nabla \times \bar{H} = \epsilon_0 \frac{\partial \bar{E}}{\partial t} \tag{152}$$

By taking the curl of this equation and then inserting the expression for $\nabla \times \bar{E}$ from Faraday's law we get

$$\nabla \times \nabla \times \bar{H} = \epsilon_0 \frac{\partial (\nabla \times \bar{E})}{\partial t} \tag{153}$$

and

$$\nabla(\nabla \cdot \bar{H}) - \nabla^2 \bar{H} = -\epsilon_0 \frac{\partial^2 \bar{B}}{\partial t^2} \tag{154}$$

or

$$\nabla^2 \bar{H} - \frac{1}{c^2} \frac{\partial^2 \bar{H}}{\partial t^2} = 0 \tag{155}$$

where we have used $\bar{H} = \mu_0^{-1} \bar{B}$; $\nabla \cdot \bar{B} = 0 = \mu_0^{-1} \nabla \cdot \bar{H}$ and $c^2 = \frac{1}{\epsilon_0 \mu_0}$. This is just the wave equation which has solutions of the form

$$\bar{H} = \bar{H}(x-ct) + \bar{H}(x+ct) \qquad (156)$$

These solutions are inward and outward propagating waves. If the form of the $\bar{H}$ field is separable into space and time functions, the space part of the wave equation becomes

$$\nabla^2\bar{H} + k^2\bar{H} = 0 \qquad \text{(Helmholz Equation)} \quad (157)$$

where k^2 is the separation constant.[89] If we carry out the indicated operation on the $\bar{H}$ field of Eq (151) we would find that it could be a solution for Eq (157) only if $\bar{J}$ was identically zero. That is, the radiated $\bar{H}$ field cannot meet the specified boundary condition therefore the boundary conditions are invalid.

To get a correct solution for this period of the surface burst, we would have to use the full set of Maxwell's equations and conservation of charge.

Ionic Conduction Phase. The last phase of the surface burst, the ionic conduction phase, begins more than a microsecond after the burst.[90] Low frequency, less intense signals are the main features of this phase since ionic conduction is slower than electron conduction. The current pattern is similar to that of the electronic phase and the radiated field is somewhat the same. Because of this similarity we shall not pursue the description further.

Summary of the Surface Burst

The asymmetry of the surface burst means that the first

approximation to the radiating mechanism is a dipole radiator. The real mechanism could be represented by an expansion of the currents as an infinite series of multipole radiators but the radiation of higher multiplicity than dipole are less important than the dipole contribution.

Assuming that the earth is a perfect conductor does not affect the radiated fields to a great extent since the earth is a fair conductor. There would be no penetration of the electric field into the earth if the earth were a perfect conductor, but because it is not, the fields do penetrate the surface. We shall consider electric fields in the earth in Chapter VI.

HIGH ALTITUDE BURST

The second mechanism for producing asymmetric current flow is the interaction of electrons with a magnetic field. The asymmetric current from this cause is the major source of the EMP from a high altitude burst.

Electron-Magnetic Field EMP Mechanism

Any magnetic field will cause an electron to turn in an amount proportional to the electron's velocity perpendicular to the field. This does cause cyclotron radiation which is a minor effect in this case. The primary EMP source mechanism however is due to the coherent turning of many high energy electrons and the coherent flow of conduction current in the electric field they form. After a high altitude

nuclear burst, this coherent motion may be present due to the geomagnetic field.

The geomagnetic field has a value which varies in direction and intensity over the earth. For our purpose we shall consider a region in the upper atmosphere on the magnetic equator with an assigned field strength of 0.5×10^{-4} webers/meter^2 (0.5 gauss, cgs).[91] The Compton and photoelectrons interact with this field at all altitudes but in the dense lower atmosphere the range of the electron is so short that the effect on the EMP is secondary to that of other mechanisms. In addition the ranges of the photoelectrons are so short that they are absorbed in the region ionized by the gamma pulse and cannot radiate.[92] In the upper atmosphere, however, electrons do have long enough ranges and lifetimes to interact significantly with the geomagnetic field.

The photon radiation from a high altitude burst interacts to produce electrons in one or two regions depending upon the height of the burst. If the burst is above $\sim$110 kilometers there are two regions of interaction: $\sim$ 100-110 km where the X-rays interact and $\sim$ 20-40 km where the gamma rays interact. If the height of burst is between $\sim$ 20-100 km, only one region of interaction around 20-40 km exists. The X-rays are not a significant EMP source within this region for the same reasons this mechanism is not significant in the dense lower atmosphere.

In order to investigate the reason why a thin layer of the atmosphere is the interaction region rather than a diffuse, broad region we must consider the absorbtion cross section as a function of air density. The photon absorbtion function $g(y)$ is

$$g(y) = A e^{-\int_{y_B}^{y} \mu(y)\,dy} \tag{158}$$

where we assume a plane wave incident in order to avoid the geometric ($1/4\pi r^2$) attenuation; μ is the total cross section; y_B is the burst height, and A is a proportionality constant.[93] The distance (y, y_B) are measured with y positive in the direction of increasing air density (or downward) and can be measured from any intermediate level, y_o ,-for this discussion we chose y_o to be the interaction altitude.

Now $\mu(y)$ can be represented by different exponential functions, each valid over a specific altitude range:[94]

$$\mu(y) = \mu N(y) \tag{159a}$$

$$= \mu N_o e^{y/H} \tag{159b}$$

$$= \mu e^{y/H} \tag{159c}$$

where μ is the microscopic cross section; $N(y)$ is the particle density at y ; N_o is the particle density at y_o , H is the scale height at y_o , and μ is the macroscopic cross section at y_o .

The attenuation function is then

$$g(y) = A\, e^{-\mu_a H \int_{y_B}^{y} e^{y/H}\, d(y/H)} \tag{160a}$$

$$= A\, e^{-\mu_a H \left[e^{y/H} \right]_{y_B}^{y}} \tag{160b}$$

$$= A\, e^{-\mu_a H \left[e^{y/H} - e^{y_B/H} \right]} \tag{160c}$$

but in our coordinate system and for the plane wave approximation y_B is large and negative therefore the factor $e^{y_B/H} \to 0$

$$g(y) = A\, e^{-\mu_a H e^{y/H}} = A / e^{+\mu_a H e^{y/H}} \tag{161}$$

Now the exponent in $g(y)$ is small when $y < 0$ compared to its size when $y > 0$. In fact $g(y) \to 0$ very rapidly because of the rapid growth of the term in the denominator of Eq (161) or, restating this, most of the photons interact in a shallow region.[95]

The behavior of the attenuation function means that the density of electrons dislodged by the photon flux will rise exponentially in a particular region (but the electron density will abruptly drop to zero further down because the attenuation removes all the photons). These regions of high electron production are thin relative to the distance to an observer on earth.

Gyromagnetic Motion. The electrons dislodged by the photon flux experience a force due to the geomagnetic field,

$$\bar{F} = e(\bar{v} \times \bar{B}) \tag{48a}$$

where we have ignored any electric fields (See Fig. 28). Since the force is normal to the magnetic field and the velocity, the electron motion in a homogeneous magnetic field $\bar{B}$ is circular with a constant velocity (if the small cyclotron radiation losses are disregarded). By equating the centrifugal force, $mv_\perp/r_g$ to the field force we can find the radius of the circle

$$\frac{m v_\perp^2}{r_g} = e v_\perp B \tag{162a}$$

$$r_g = \frac{m v_\perp}{e B} \tag{162b}$$

where $v_\perp$ is the velocity perpendicular to the magnetic field and r_g is the radius of the circle. From the relation $\omega = v/r$ we can find the radian frequency of this rotation:

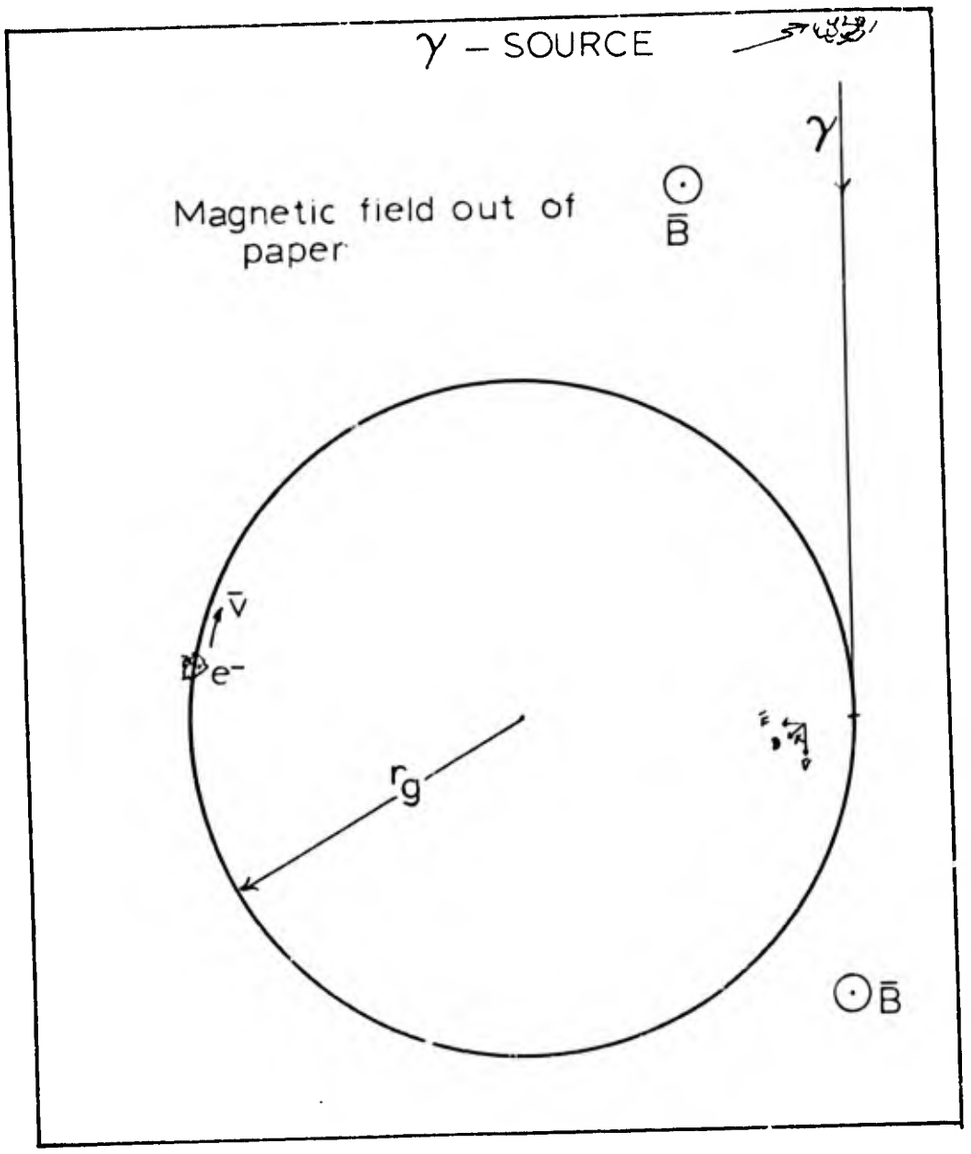

Fig. 28. Electron Motion in Magnetic Field. In a homogeneous constant magnetic field B the energetic electron from a photon-electron interaction moves on a circle of radius $r_g = v_\perp m\gamma/eB$ The electron will radiate a frequency equal to its gyromagnetic frequency, $\omega = eB/m\gamma$.[96]

$$\omega = \frac{e B}{m} \tag{163}$$

These are called the gyromagnetic radius and gyromagnetic frequency respectively.

These equations must be corrected for the relativistic increase in the mass of the particle and the resultant equations are

$$r_g = \frac{v_1 m \gamma}{e B} \quad ; \quad \omega = \frac{e B}{m \gamma} \tag{164}$$

where $\gamma = \sqrt{1-\beta^2}$ and $\beta = v/c$.* For photoelectrons, from 3.8 KeV photons, β is 0.12 and for 0.7 MeV Compton electrons β is ~ 0.9. The relative sizes of these means that relativistic corrections may be ignored for photoelectrons but must be considered for Compton electrons.[98]

Electron Motion. Let us return to a more detailed look at the motion of the electrons. By supposition the gamma rays are produced by a nuclear burst high above the interaction layer. The photons interact in a flat interaction layer and produce electrons whose initial velocity is in the same direction as the photon momentum. Their subsequent motion is a combination of linear motion along a guiding axis (horizontal lines at 1, 2, 3 and 4 in Fig. 29) about

---

*Relativistic relations: T is particle energy in MeV; $m_o c^2 = 0.511$ MeV for electrons; $W = \frac{T}{m_o c^2} + 1$; $\beta^2 = 1 - 1/W^2$; $\gamma = \sqrt{1-\beta^2}$; $\gamma = W$.

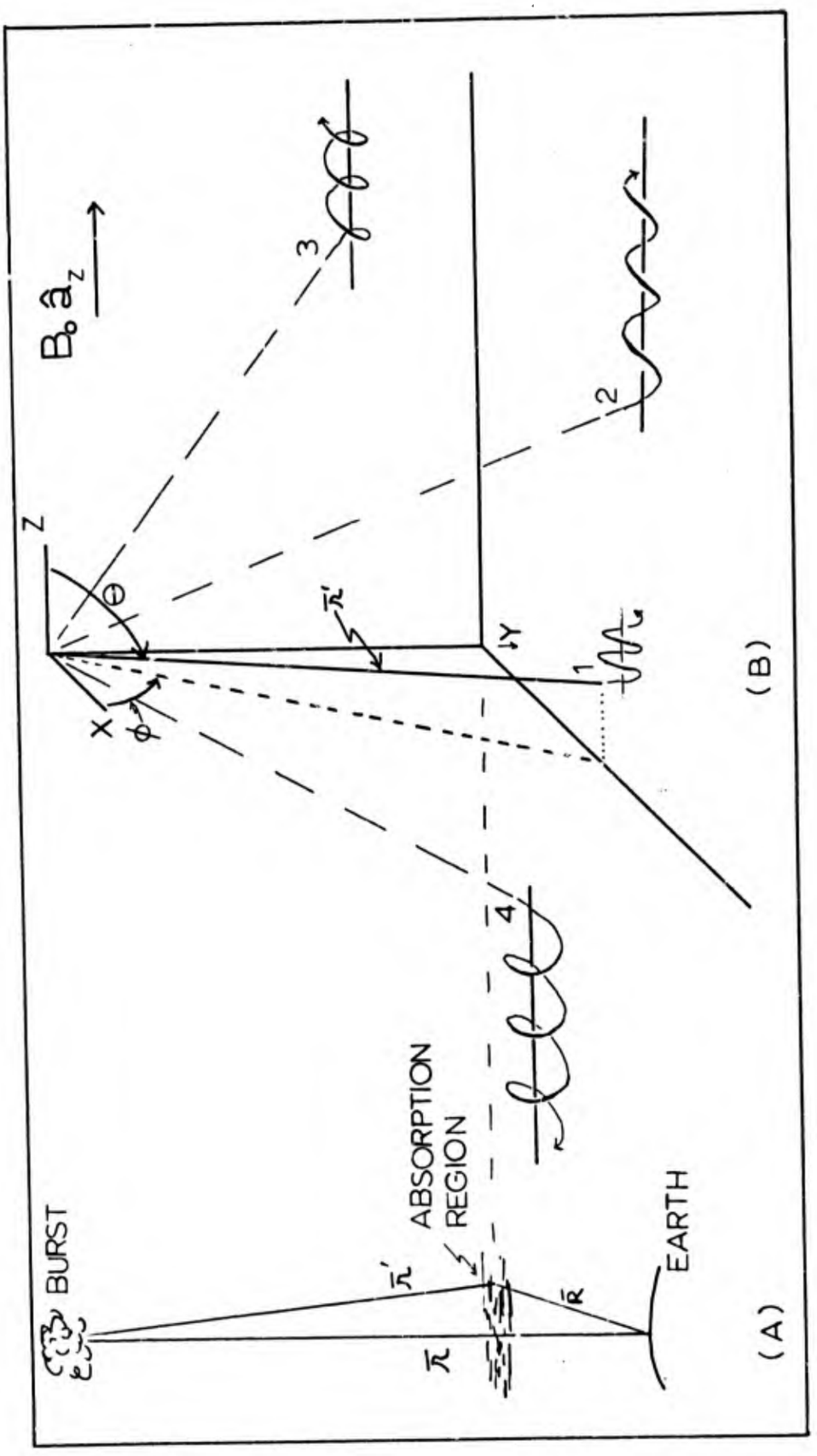

Fig. 29. A. The burst, absorption layer, and observer location are pictured here. Points 1-4 are in the absorption layer. At point 1 most of the electron motion is circular. Points 2, 3, and 4 illustrate that symmetric currents flow away from the x-y plane.

the same guiding axis.[99]

The linear motion is due to the component of the initial velocity parallel to the magnetic field. The only force affecting this motion is the electric attraction of the parent ion and any collisions with the atmosphere. The magnitude of this linear motion varies from zero when $\theta'' = \pi/2$ to $V_o \cos\theta''$ when ϕ'' is $\pi/2$. Because of this linear motion, the circular motion appears helical to an external observer.

The circular motion is all we shall consider in our example. The circling speed of the electron is $V_o \sin\theta''$ where θ'' is the angle between the magnetic field and the gamma momentum. Because $V_\perp = V_o \sin\theta''$ the gyromagnetic frequency will be affected through the relativistic corrections and the gyromagnetic radius will be altered through both the velocity and relativistic terms.

By considering the motion of the electrons as pictured in Fig. 30 we can see the distinctive features of the high altitude EMP generating mechanism. The figure depicts a gamma pulse five shakes (one shake = 10^{-8} second) wide ($\sim$15 meters) generating electrons which immediately start turning. In the time for these electrons to complete one orbit, tens of meters, the gamma pulse has traveled a distance the order of hundreds of meters.[100] The electrons in this column have a horizontal velocity component which varies with a gyromagnetic frequency ω ($\sim 10^6$ radians/second)

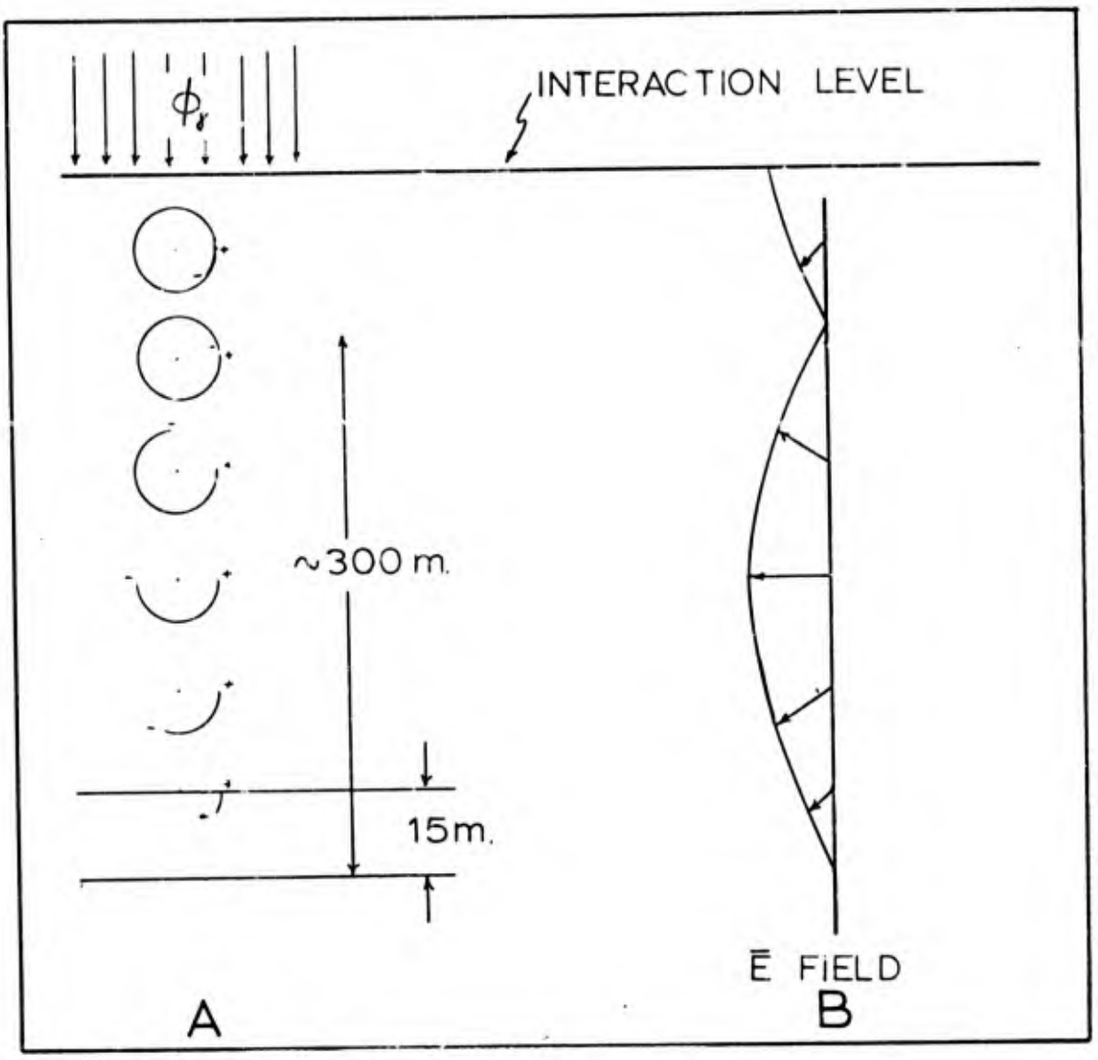

Fig. 30. Electron Motion in High Altitude Burst. A. A series of electrons produced by the leading edge of the gamma pulse are shown in their relative positions during their first orbit. B. The electric field vector between the electron and parent ion is shown in Fig. B.

and whose spacial variation has nodes about three hundred meters apart.

Now because the generating mechanism was a photon pulse moving with the speed of light, any downward radiation generated by the topmost electron will be almost in phase with the electrons below it so they contribute to the amplitude of the signal, i.e., there will be constructive interference for a downward moving wave. An upward moving wave would at some time in its travels encounter an out of phase electron and undergo destructive interference.

Since the electrons are assumed to work together we shall replace the entire interaction region by a delta function current sheet oscillating in the x-z plane. The geometry of the integration we shall perform is indicated in Fig. 31 where we have moved the origin to an interaction height. A current density, $\bar{J}$, which might be used to find a vector potential is

$$\bar{J}(r,t) = J_o \hat{a}_x \delta(y') \sin\theta'' \cos\omega t' \qquad (165)$$

where θ'' is the angle between the photon momentum and magnetic field and where ω is given by Eq (160) or (161). Because the expression for the vector potential would be too complicated to integrate if the correct expression for $\sin\theta''$ was inserted, we shall use

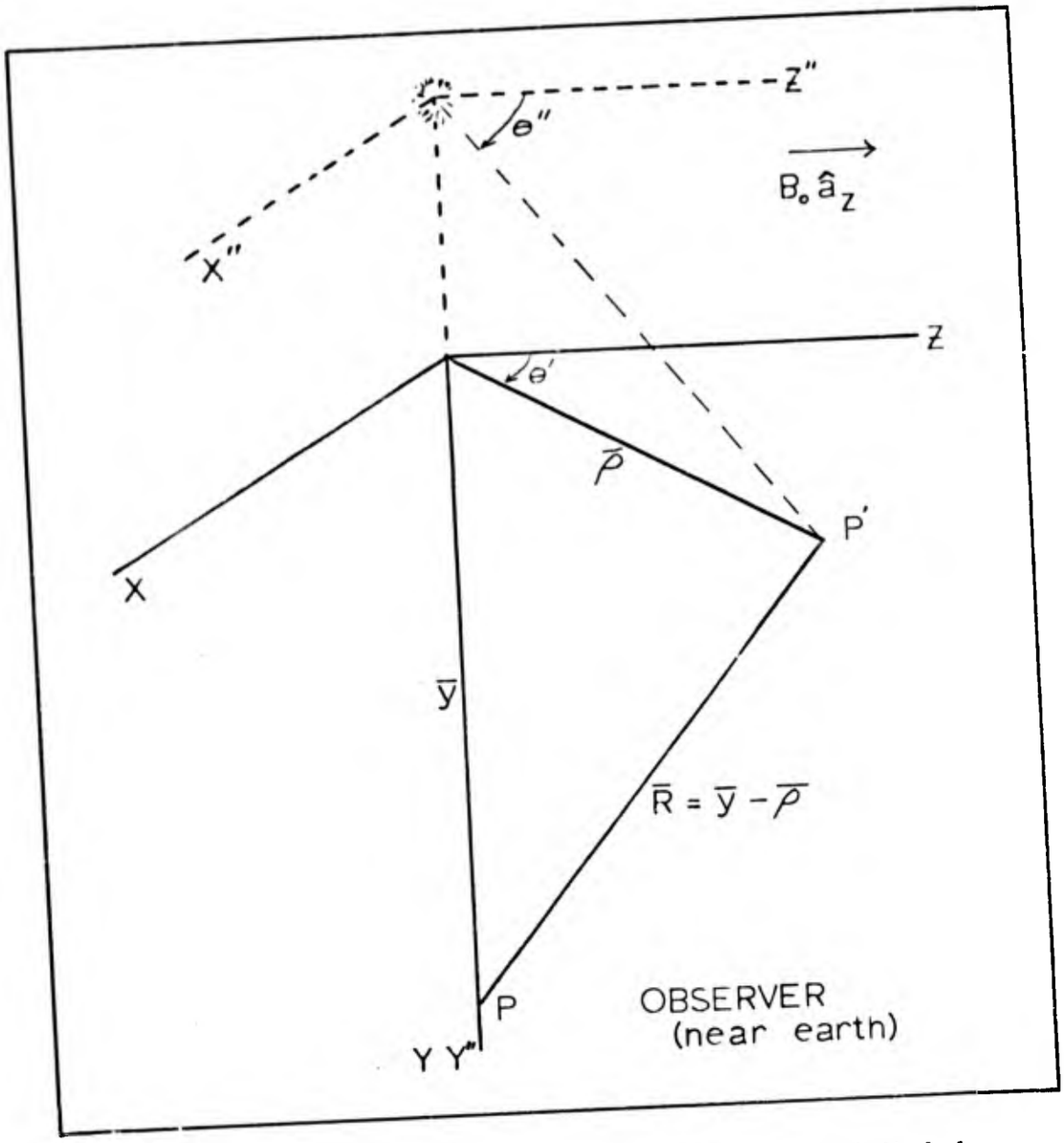

Fig. 31. Geometry for Electron-Magnetic Field Model. The photons from the burst interact in the X-Z plane forming an oscillating sheet of current density J $\hat{a}_x$.

$$\bar{J}(\bar{r},t) = J_o(\hat{a}_\rho \sin\theta' + \hat{a}_\theta \cos\theta')\delta(y')\sin\theta'\cos\omega t' \qquad (166)$$

where the factor $\sin\theta'$ has been inserted in place of $\sin\theta''$. This replacement assumes that the burst height is close to the interaction plane.

By replacing the time variation with the real part of $e^{j\omega t}$ we can write the current function in phasor notation:

$$\bar{J}(\bar{r},t) = J_o(\hat{a}_\rho \sin\theta' + \hat{a}_\theta \cos\theta')\delta(y')\sin\theta' e^{j\omega t} \qquad (167)$$

(For a discussion of phasor notation, see Plonsey and Collin[101] page 311.)

The vector potential $\bar{A}(\bar{r},t)$ [102] for a sinusoidal time varying potential is

$$\bar{A}(\bar{r},t) = \bar{A}(\bar{r})T(t) = \frac{1}{4\pi\mu_o}\int_{V'}\frac{\bar{J}(\bar{r}')e^{-jkR}}{R}\,dV'e^{j\omega t} \qquad (168)$$

where $k = \omega/c$ is the propagation constant (meter^{-1})

$\bar{r}'$ vector to source point (meter)

$\bar{r}$ vector to field point (meter)

V' source volume (meter^3)

$\bar{R} = \bar{r} - \bar{r}'$ vector from source point to field point (meter)

It is re-emphasized that the primes indicate the source dimensions, the variables of integration. Since the time and space variables are separable we shall drop $e^{j\omega t}$ until

the final expressions are formed.

Using cylindrical coordinates for the volume integral the vector potential becomes

$$\bar{A}(\bar{r}) = \frac{1}{4\pi\mu_o^{-1}} \int_0^{2\pi}\int_0^{\infty}\int_{y=0} dy'd\rho'd\theta'\rho' \; J_o(\hat{a}_\rho \sin\theta' + \hat{a}_\theta \cos\theta')$$

$$\times \delta(y')\sin\theta' \; \frac{e^{-jk\sqrt{\rho'^2+y^2}}}{\sqrt{\rho'^2+y^2}} \qquad (169)$$

which after integrating over y' and replacing ρ' with u' where $u'^2 = \rho'^2 + y^2$ and $2u'du' = 2\rho'd\rho'$ becomes

$$\bar{A}(y) = \frac{J_o}{4\pi\mu_o^{-1}} \int_0^{2\pi}\int_y^{\infty} du'd\theta'(\hat{a}_\rho \sin\theta' + \hat{a}_\theta\cos\theta')\frac{u'}{u'} \qquad (170)$$
$$\times e^{-jku'}\sin\theta'$$

or

$$\bar{A}(y) = \frac{J_o}{4\pi\mu_o^{-1}} \int_0^{2\pi}(\hat{a}_\rho \sin\theta' + \hat{a}_\theta\cos\theta')\sin\theta' d\theta' \int_y^{\infty} e^{-jku'} du' \qquad (171)$$

Integrating this we have

$$\bar{A}(y) = \frac{J_o}{4\pi\mu_o^{-1}} \left[\hat{a}_\rho\left(\frac{\theta'}{2} - \frac{\sin 2\theta'}{4}\right) + \hat{a}_\theta\left(\frac{\sin^2\theta'}{2}\right)\right]\Bigg|_0^{2\pi}$$
$$\times \left[\frac{e^{-jku'}}{-jk}\right]\Bigg|_y^{\infty} \qquad (172)$$

Inserting the limits of integration is straightforward except for $u' \rightarrow \infty$.

In order to evaluate the limit as $u' \rightarrow \infty$ we must consider the nature of the propagation constant k .[103] The propagation constant is, in general, complex:

$$k = k' - jk'' \tag{173}$$

where k' is the intrinsic phase constant and k'' is the intrinsic attenuation constant.[104] This means that $e^{-jku'}$ can be written as

$$e^{-jku'} = e^{-jk'u'} e^{-k''u'} \tag{174}$$

which is the product of a function bounded by ± 1 and a function that monotonically approaches zero as $u' \rightarrow \infty$. Therefore in the limit as $u' \rightarrow \infty$, $e^{-jku'}$ would in fact be zero. Other than for this explanation, the complex nature of the propagation constant will be ignored.

The complex vector potential is then

$$\bar{A}(y) = \frac{J_o}{4\pi/\mu_o^{-1}} \left[\hat{a}_\rho \pi\right] \cdot \left[\frac{e^{-jky}}{jk}\right] \tag{175}$$

The complex magnetic field $\bar{H}'$ is found by taking the curl of $\bar{A}$:

$$\bar{H}' = \mu_o^{-1} \bar{B} = \mu_o^{-1} \nabla \times \bar{A} \tag{176a}$$

$$= \frac{\mu_o^{-1}}{\rho} \begin{vmatrix} \hat{a}_\rho & \rho\hat{a}_\theta & \hat{a}_y \\ \frac{\partial}{\partial\rho} & \frac{\partial}{\partial\theta} & \frac{\partial}{\partial y} \\ A_\rho & \rho A_\theta & A_y \end{vmatrix} \tag{176b}$$

$$= \frac{\mu_o^{-1}}{\rho}(-\rho\,\hat{a}_\theta)(-\frac{\partial A_\rho}{\partial y}) \tag{176c}$$

$$= -\hat{a}_\theta \frac{J_o}{4} e^{-jky} \tag{176d}$$

Restoring the time variation and taking the real part of the resultant expression gives us the magnetic field:

$$\bar{H} = \mathrm{Re}\ \hat{a}_\theta \frac{J_o}{4} e^{-jky} e^{j\omega t} \tag{178}$$

$$= \hat{a}_\theta \frac{J_o}{4} \cos(\omega t - ky) \tag{179}$$

The electric field can be found from the expression $E_\rho = Z H_\theta$ where Z is the intrinsic impedance of the medium (120π for free space):[105]

$$\bar{E} = \hat{a}_\rho 30\pi J_o \cos(\omega t - ky) \tag{180}$$

We have assumed in the above that the electrons stay in phase with the propagated signal. In fact their velocity is less than that of light and therefore the phase differences should be considered in a careful analysis. The electrons were assumed to have circular motion and no motion along the guiding center which is patently false but the error should not be serious for our purposes.

We shall return to this equation in order to discuss its validity and compare it to results obtained by Karzas and Latter after we discuss the magnitude of the current, and the times and frequencies plausible from this mechanism.

Current Density. In order to estimate the current density to use in the model we have proposed, we must discuss the equivalence theorem from electromagnetic theory. The equivalence theorem asserts that if the fields at a boundary are replaced by suitable current sheets, an observer within the bounded region would not see any change in the fields around him.[106] Since in most cases the fields at a boundary are unknown, the procedure often used is to guess a plausible current. This is the procedure followed below.

The magnitude of the current density on the boundary surface is found from the magnitude of the fields at that point. We will use the saturated electric field in the interaction layer to find the equivalent current. That current is given by

$$\bar{J} = \frac{\bar{E}_{sat}}{Z_o} \tag{181}$$

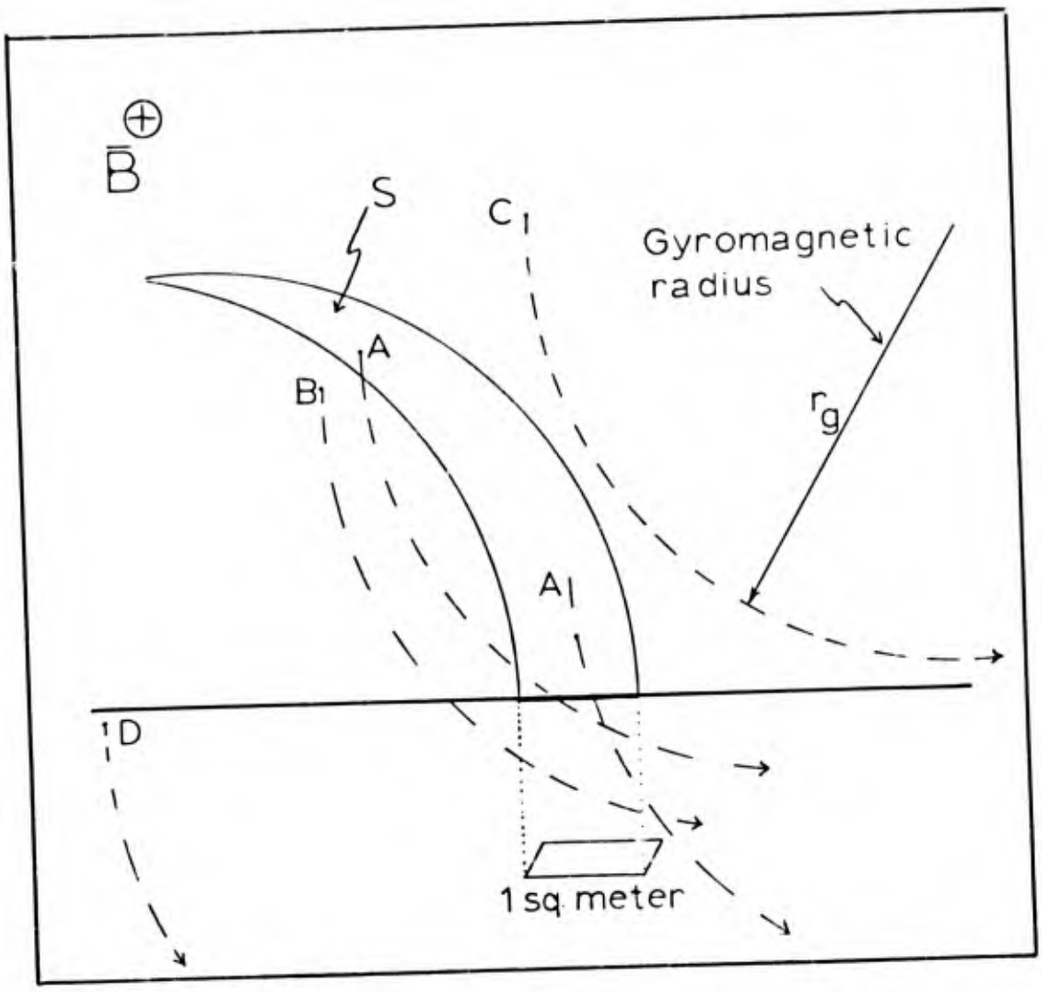

Fig. 32. Compton Current in Magnetic Field. Only electrons (A) starting from within S will pass through the square meter shown. Electrons outside of S will not pass through this surface; Electron B misses the chosen surface; C turns altogether too soon; and D is part of another loop system.

where Z_o is again the impedance of free space (c.f., Ohms law, $I = E/R$).[107] We see immediately that our development gives the magnitude of the radiated electric field as $E_{SAT}/4$.

In order to estimate the saturated electric field we can use an approach similar to that used in the symmetric burst. However here we must alter the depth of the region behind the surface which contributes to current through the surface (the MFR_e in the planar case). The turning of the electron will reduce the length of the region behind the surface as shown in Fig. 32. The effective range is ~ 7 meters for a gyromagnetic radius of 10 meters. However because the electron makes multiple passes through this region we multiply the current production by (eiectron range/$2\pi r_g$).

The saturated field is then

$$E_{SAT} = \frac{n(ER_e)(\alpha + \nu_a)\ 32.5}{T_e(10^6)\ \mu_e} \qquad (182)$$

where n = the number of passes through a region

ER_e = the effective production length for current

α = the gamma production time constant

ν_a = the attachment rate ($\nu_a \ll \alpha$ at 25 km)

$T(10^6)/325$ = secondary electron production per primary electron

μ_c = the mobility ($=\mu_{e(s.l.)}e^{Z/H}$ - where H is the scale height and Z is the vertical altitude.

The saturated field found by evaluating Eq (182) is

$$E_{SAT} = \frac{(1.5)(7)(10^8)(32.5)}{(0.7 \times 10^6)(1.0 \times e^{25/8})} \qquad (183a)$$

$$= 2.5 \times 10^3 \quad \text{(volts/meter)} \qquad (183b)$$

Finally we have the magnitude of the radiated signal predicted by this model from Eq (194): 2500/4 = 620 volts/meter. By using the relativistic correction shown in Karzas and Latter's development - $(1 - \beta)^{-1}$ - the field strength is increased ten fold to 6200 volts/meter.

Discussion of this result will follow in the next section.

Frequency and Duration. The high altitude gamma EMP may have the frequencies in it that are in the oscillating source currents. Since the expression for the radian frequency, $\omega = eB/m\gamma$, contains the velocity in it there will be a spectrum of frequencies in the high altitude EMP. A variety of frequencies are shown in Table 4 for a variety of electron energies.

The duration of the electromagnetic pulse from this mechanism in a high altitude burst depends on the lifetime of the rotating synchronous movement of the electrons. Using distance = velocity x time we have a means of determining the lifetime of the pulse and it is tabulated in Table 5.

Table 4

Gyromagnetic Frequency vs. Electron Energy

Electron Energy	Radian Frequency (rad/sec)	Photon Energy* Required	Gyromagnetic Radians (m)	γ
3.8 KeV	9.0×10^6	3.8 KeV	4.3	1.007
0.4 MeV	5.0×10^6	1.0 MeV	8.0	1.78
0.7 MeV	4.0×10^6	1.5 MeV	10.	2.37
1.5 MeV	2.3×10^6	2.9 MeV	17.	3.94
2.5 MeV	1.5×10^6	4.0 MeV	25.	5.89

*Photon energy from Fig. 15.

Table 5

Electromagnetic Pulse Duration vs. Electron Energy

Electron Energy	Electron Velocity ($\beta = v/c$)	Mean Free Range at ( ) Kilometers** (meters)	Lifetime at ( ) Kilometers (seconds)
1.0 KeV	0.06	25 (100)	1.4×10^{-6}
3.8 KeV	0.12	360 (100)	$10. \times 10^{-6}$
10. KeV	0.20	2500 (100)	$42. \times 10^{-6}$
0.7 MeV	0.90	40 (20)	1.5×10^{-7}
0.7 MeV	0.90	204 (30)	7.5×10^{-7}
2.5 MeV	0.97	40 (20)	1.4×10^{-7}
2.5 MeV	0.97	204 (30)	6.9×10^{-7}

** Ranges found using Eqs (133a) and (133b)

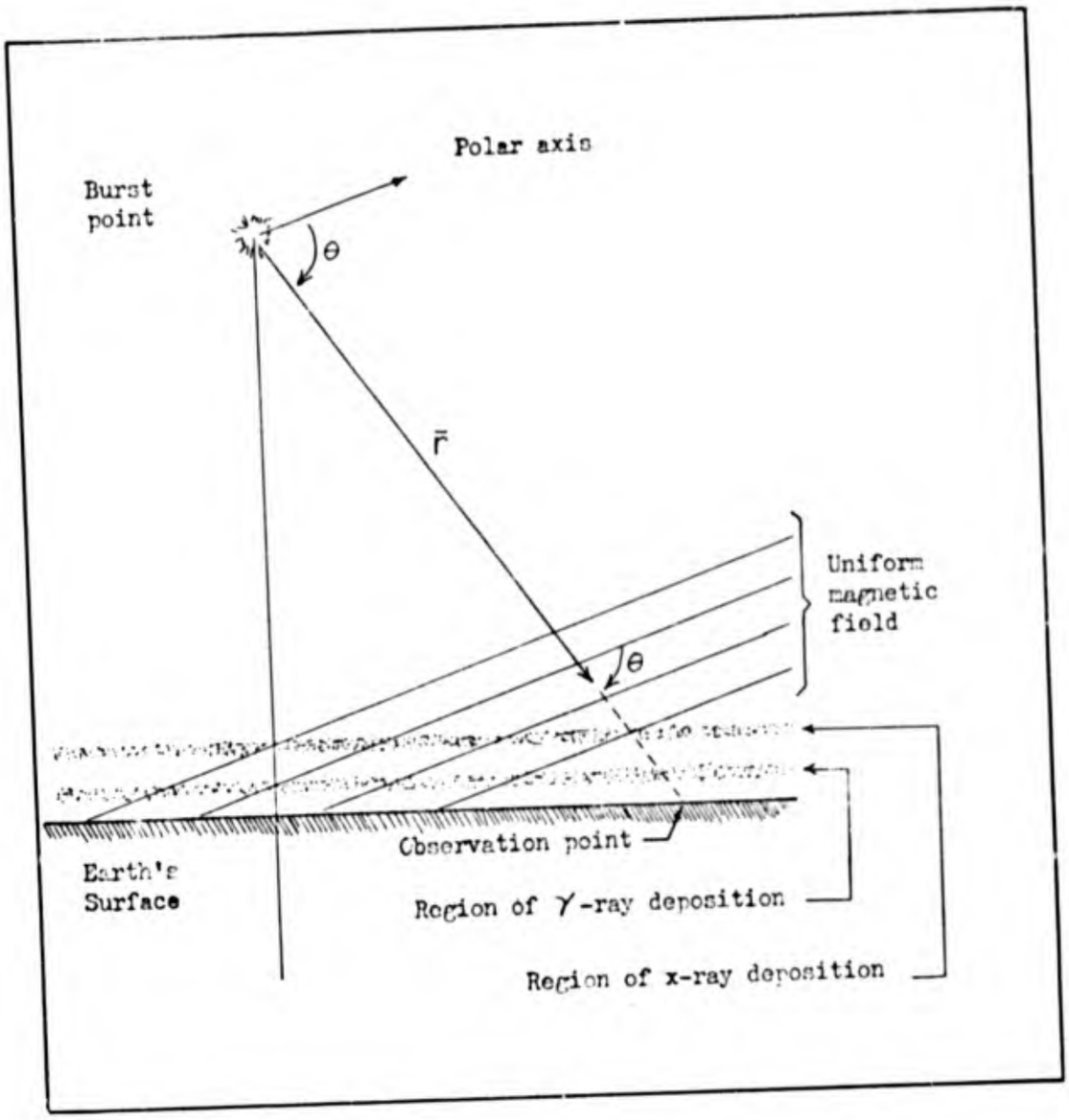

Fig. 33. Geometry of Karzas and Latter's Calculations. The curved surfaces of the earth, interaction layers, and magnetic fields were all assumed flat for their calculations. This is acceptable because most of the field at the observation point is due to the interactions between burst and observer. (Adapted from Ref 111).

Discussion. Karzas and Latter[108] obtain a result which we present for the non-relativistic case (photoelectrons) and without time retardation:

$$\bar{E} = E_o\left\{\sin\Theta\cos\Theta\left[\cos(\omega t - kz) - 1\right]\hat{a}_\Theta + \sin\Theta\sin(\omega t - kz)\,\hat{a}_\phi\right\} \quad , t < MFR_e/V_o \tag{184}$$

$$\bar{E} = 0 \quad , t > MFR_e/V_o \tag{185}$$

where the angle Θ is depicted in Fig. 33. For $\Theta = \pi/2$ which is the case for the model used in this thesis, their equation reduces to

$$\bar{E} = E_o \sin(\omega t - kz)\,\hat{a}_\phi \tag{186}$$

The result arrived at in our model is consistent with their result since sine and cosine differ only by a phase factor and both show the field direction trasverse to the line from burst to observer. Both models show the pulse lasting the lifetime of the orbiting electrons.[109] The minus one in the term $\left[\cos(\omega t - kz) - 1\right]$ is due to considering the motion along the guiding center parallel to the magnetic field. The factor E_o was found basically from J_c/σ and from procedures related to the saturated field calculations of Chapter IV. Their expression for E_o is

$$E_o \approx \frac{\eta m \omega \nu_c (MFR_e)(32.5)}{e T_e (10^6)(1-\beta)} \qquad (187)$$

where η is 1 for Compton electrons and $4/5\ v/c$ for photoelectrons (~ 0.1); m is electron mass (kg); ω gyromagnetic frequency (sec^{-1}); $\nu_c = 10^{12}\ \rho/\rho_o$ electron collision frequency (sec^{-1}); MFR_e is the electron range (m); $T_e(10^6)/32.5$ is the ion pair production figure; and $(1-\beta)$ is a relativistic correction.[110] For the X-ray interaction around 100 km Karzas and Latter found an electric field of 10 volts/meter and for the gamma interaction around 20-40 km they found 6×10^4 volts/meter which is at least one order of magnitude greater than predicted by our model. Apparently we must conclude that our simplified model is of limited validity.

SYMMETRIC BURST IN A MAGNETIC FIELD

The final mechanism for generating an EMP deals with the freezing (see paragraph below) of a magnetic field within an expanding ball of highly ionized gasses. To avoid other mechanisms we assume that the burst is symmetric except for the presence of a uniform magnetic field.

Hydrodynamic Exclusion of the Earth's Field

W. J. Karzas and R. Latter[112] describe the electromagnetic pulse generated by exclusion of the earth's magnetic field from the isothermal blast region, Fig. 34:

> "Surrounding a nuclear explosion is an intensely ionized region in which the air conductivity is sufficiently high to freeze in the magnetic field. As a result, when the blast wave causes the air to expand, the magnetic field is carried along. At the same time the magnetic field which is external to the ionized region is unable to penetrate the ionized region and is pushed outward."[113]

Hydrodynamic Formulation of the Problem. By following Karzas and Latter's method, but filling in some mathematical steps, we shall find a differential equation suitable for describing this generating mechanism. However the time dependence of the isothermal sphere's geometry and the conductivity are too complicated for analytical solution of this differential equation so we shall proceed to use a simplified model which satisfactorily describes the mechanism.

The total electric field in a region containing a moving conducting medium where the motion involves no separation of charge, i.e., not a plasma, is

$$\bar{E}_T = \bar{E} + \bar{v} \times \bar{B} \tag{188}$$

and Ohm's law, $\bar{J} = \sigma \bar{E}$ assumes the form

$$\bar{J} = \sigma(\bar{E} + \bar{v} \times \bar{B}) \tag{189}$$

Maxwell's equation, $\frac{\partial \bar{B}}{\partial t} = \nabla \times \bar{E}$ becomes

$$\frac{\partial \bar{B}}{\partial t} = -\nabla \times \left(\frac{\bar{J}}{\sigma} - \bar{v} \times \bar{B}\right) \tag{190}$$

Because the displacement current, $\partial \bar{D}/\partial t$, is small in the realm where hydrodynamic approximations are valid Ampere's

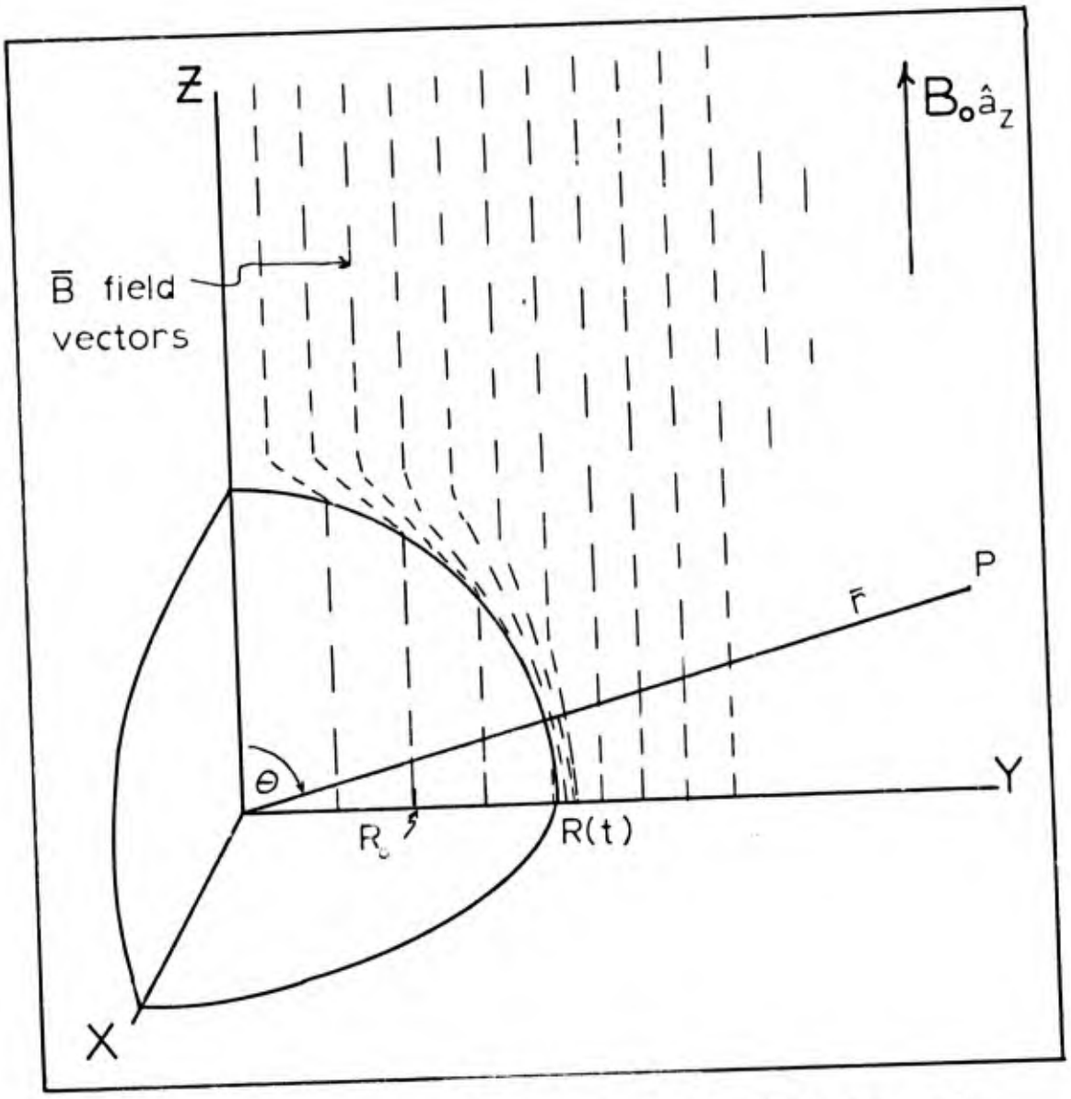

Fig. 34. Hydrodynamic Exclusion of Earth's Magnetic Field. The $\bar{B}_o$ field within the sphere of radius R(t) is expanded by the growth of the sphere and the $\bar{B}_o$ lines outside the sphere are compressed.

equation holds:

$$\bar{J} = \frac{\nabla \times \bar{B}}{\mu_o} \tag{191}$$

Therefore the equation governing the behavior of the magnetic field in this case is

$$\frac{\partial \bar{B}}{\partial t} = \nabla \times (\bar{v} \times \bar{B} - \frac{\nabla \times \bar{B}}{\mu_o \sigma}) \tag{192}$$

Isothermal Sphere Model. In order to simplify the solution of Eq (192) the expanding isothermal region is modeled by an expanding sphere which excludes the external magnetic field as it grows in radius. The approximation is fairly good as long as the relaxation time, τ, of the magnetic field is quite long, that is

$$\frac{\tau}{R(t)} \frac{dR(t)}{dt} \approx \sigma \mu_o R(t) \frac{dR(t)}{dt} >> 1 \tag{193}$$

Relaxation time (diffusion time in Jackson, Ref 114) is a measure of the time needed for the initial magnetic field to decay away; in this case $\tau \equiv \sigma \mu_o R(t)^2$ where $R(t)$, here the isothermal sphere's radius, is a "length characteristic of the spacial variation of $\bar{B}$".[115]

The isothermal sphere is nearly at rest, i.e., $v = 0$, at $t = 0$. Therefore Eq (192) reduces to

$$\frac{\partial \bar{B}}{\partial t} = \frac{\nabla^2 \bar{B}}{\mu_o \sigma} \tag{194}$$

and, if $\sigma \to \infty$ inside the isothermal sphere

$$\frac{\partial \bar{B}}{\partial t} = 0 \tag{195}$$

or the magnetic field is frozen.

The problem has been reduced to one of an expanding sphere with the original field frozen in. In the region of interest outside the sphere, $\sigma \cong 0$ and the displacement current is assumed to be zero, $\frac{\partial \bar{D}}{\partial t} = 0$, therefore

$$\nabla \times \bar{B} = 0 \tag{196}$$

and $\nabla \cdot \bar{B} = 0$ (from Maxwell's equation). Thus we can find the solution outside the sphere through the use of a magnetic potential Φ_m.[114] We want the solution of

$$\nabla^2 \Phi_m = 0 \tag{197}$$

which is

$$\Phi_m = \sum_{\ell=0}^{\infty} \left(A_\ell r^\ell + \frac{B_\ell}{r^{\ell+1}} \right) P_\ell(\cos\theta) \qquad \ell = 0,1,2,\cdots \tag{198}$$

where A_ℓ and B_ℓ are constants to be found by matching the boundary conditions and the $P_\ell(\cos\theta)$ are Legendre polynomials.

The magnetic field is the negative gradient of the potential or

$$\bar{B} = -\nabla \Phi_m \tag{199a}$$

$$= -\frac{\partial}{\partial r}\Phi_m \hat{a}_r - \frac{1}{r}\frac{\partial}{\partial \theta}\Phi_m \hat{a}_\theta \tag{199b}$$

$$= -\sum_{\ell=0}^{\infty}\left(A_\ell \ell r^{\ell-1} - \frac{B'_\ell(\ell+1)}{r^{\ell+2}}\right) P_\ell(\cos\theta)\hat{a}_r -$$

$$\sum_{\ell=0}^{\infty}\left(A_\ell r^{\ell-1} + \frac{B'_\ell}{r^{\ell+2}}\right)\frac{dP_\ell(\cos\theta)}{d\theta}\hat{a}_\theta \tag{199c}$$

The first boundary condition is the value of $\bar{B}$ at infinity:

$$\bar{B}(\infty) = B_\infty \hat{a} = B_\infty(\cos\theta\,\hat{a}_r - \sin\theta\,\hat{a}_\theta) \tag{200}$$

The presence of $\cos\theta$ in this boundary condition implies $\ell = 1$ since $P_1(\cos\theta) = \cos\theta$. By retaining only $\ell = 1$ and equating components from Eqs (200) and (199c) we get

$$\hat{a}_r: \quad B_\infty \cos\theta = -\left(A_1 - \frac{B'_1(2)}{r^3}\right) P_1(\cos\theta)\Big|_{r\to\infty}$$

$$\hat{a}_\theta: \quad -B_\infty \sin\theta = -\left(A_1 + \frac{B'_1}{r^3}\right)\frac{dP_1(\cos\theta)}{d\theta}\Big|_{r\to\infty} \tag{201}$$

Equation (201) becomes

$$B_\infty \cos\theta = -A_1 \cos\theta \tag{202a}$$

or

$$A_1 = -B_\infty \tag{202b}$$

To find the value for B_1' we must match the boundary at the surface of the isothermal sphere. Inside the isothermal sphere the frozen field is carried outward with the expansion of the sphere so the internal field[116] is

$$\bar{B} = B_\infty \hat{a}_z \frac{\pi R(0)^2}{\pi R(t)^2} \qquad r < R(t) \tag{203}$$

Again equating components as in Eq (201) gives

$$\hat{a}_r: \quad B_\infty \frac{R(0)^2}{R(t)^2}\cos\theta = -\left(-B_\infty - \frac{B_1'(2)}{r^3}\right)\cos\theta \Big|_{r=R(t)} \tag{204a}$$

or

$$B_1' = B_\infty\left(\frac{R(0)^2}{R(t)^2} - 1\right)\frac{R(t)^3}{2} \tag{204b}$$

The magnetic field for $r > R(t)$ is therefore

$$\bar{B} = -\left[-B_\infty - B_\infty\left(\frac{R(0)^2}{R(t)^2} - 1\right)\frac{R(t)^3 2}{2\ r^3}\right]\cos\theta\ \hat{a}_r - \tag{205a}$$

$$-\left[-B_\infty + B_\infty\left(\frac{R(0)^2}{R(t)^2} - 1\right)\frac{R(t)^3}{2r^3}\right](-\sin\theta)\,\hat{a}_\theta \tag{205b}$$

$$\bar{B} = B_o \hat{a}_z - B_o \left(1 - \frac{R(o)^2}{R(t)^2}\right) \frac{R(t)^3}{r^3} \left(\cos\theta\, \hat{a}_r + \frac{\sin\theta}{2}\, \hat{a}_\theta\right) \qquad (205c)$$

In order to get a numerical value for the magnetic field we follow the work of Karzas and Latter.

"Numerical results on the radiation and hydrodynamic flow for a sea level nuclear explosion give

$$R(t) = \left[5 + 120\left(\frac{t}{Y^{1/3}}\right)^{1/3}\right] Y^{1/3} \qquad (206)$$

for $0 < t/Y^{1/3} \leq 0.05$, where t is in seconds and Y in kilotons. For $0.05 \leq t/Y^{1/3}$

$$R(t) = R_{max} \simeq 50\, Y^{1/3} \qquad (207)$$

Equation (205) holds until Eq (206) breaks down, after which the second and third terms of Eq (205) decay to zero. The time constant for this decay is, approximately,"

$$\mu_o \sigma_o R_{max}^2 \qquad (208)$$

"where σ_o is the conductivity of the isothermal sphere when $R(t) = R_{max}$ A rough estimate of σ_o is"

$$\sigma_o = 1.11 \times 10^4 \quad \text{(amp/volt-meter)} \qquad (209)$$

"Consequently, $\mu_o \sigma_o R_{max}^2$ is of the order of a few times $Y^{2/3}$ seconds. Since this relaxation time is so long, other phenomena, such as fireball rise, and radiative and convective cooling, will determine the actual time for the

magnetic field to relax."[117]

Example 5. Some figures for a 200 Kt explosion are given in Table 6.

Table 6

Hydrodynamic Exclusion Parameters Due to a 200 KT Burst.*

$R(t) = 29.2 + 380\ t^{1/3}$	Radius to 10 PSI overpressure - 1600 m**
$R(0) = 29.2$ meters	$\bar{B}$ at 1600 m, $\theta = \pi/2$
$R_{max} = 290$ meters	$\sim 1.003\ B_o \hat{a}_z$
$t_{max} = 0.3$ sec	
τ (decay time) $\sim$ 1200 sec	

*Numbers computed from appropriate equations; **Ref 118.

From the values in Table 6, we see that the time to maximum sphere radius is relatively long. This means that any radiated signal would have a low frequency. That the actual time for the magnetic field to relax would not be τ is indicated by the large value found here: $\tau = 1200$ sec. At a radius equivalent to 10 PSI blast overpressure we see that the change in magnetic field is only $\sim 0.003\ B_o$ Which is very small.

Summary of Hydrodynamic Field Expulsion. The signal generated by this mechanism may not be of primary interest to atomic defense. However it has been suggested that the signal from this mechanism could be detected even for underground bursts. While true, it has been pointed out that a

simple gaussian loop which would cancel the earth's magnetic field near the burst would be sufficient to eliminate this signal.

Summary

The mechanisms for the production of a radiated EMP vary. We have studied three methods: the formation of asymmetric currents because of differences in the density of the surroundings; the formation of asymmetric currents because the electrons were given transverse velocity by the geomagnetic field; and finally, the third, minor, mechanism was the "tweak" of the geomagnetic field by the expanding isothermal sphere. Although the basics of each mechanism are relatively simple the analysis of actual situations is difficult because the mechanisms are present in combination with one another.

Simply stated, the models which approximate the three mechanisms are a dipole radiator for the surface burst; a radiating current sheet for the high altitude burst; and an expanding magnetic field for the hydrodynamic exclusion of the geomagnetic field.

The electric fields strengths found were on the order of 10^4 volts/meter in the first two models. This implies that the EMP should be of concern for atomic defense. The fact that all models formed radiated signals may be important for detecting nuclear explosions.

VI. Propagation of the Electromagnetic Pulse

The electromagnetic pulse must be studied as a propagating signal both for detection purposes and to assess its potential for damage. We study propagation of the EMP separate from its generation because the EMP generation is often studied using specialized coordinate systems and assumptions that do not consider the environment beyond what is significant to the explosion. Examples of these environmental factors include the ionosphere's natural electron density; the earth's curvature; and the earth's finite conductivity.

We will study three situations: a pulse propagating through an ionized layer (such as the ionosphere); a pulse propagating through the neutral region below the ionosphere; and, finally, a pulse propagating into the ground.

Propagation Through an Ionized Region

The propagation of the EMP through ionized regions is studied in order to understand several possible situations. For example, the EMP from a low altitude burst might be detectable by a satellite but indistinguishable from lightning static (spherics) if the EMP's characteristics are altered by its passage through the ionized region of the upper atmosphere (the ionosphere). In another situation, a weak case signal from a distant nuclear test might reach the ionosphere but go undetected on the ground because the ionosphere might

absorb the signal. Another situation requiring the study of EMP transmission through an ionized layer occurs when the EMP produced at high altitudes ($\sim$ 100 km) by X-rays must travel through the ionized layer around 20-40 km which the burst's gamma rays would create. In this situation the X-ray signal might be completely absorbed.

The remainder of this section considers EMP propagation as it might affect nuclear burst detection by a satellite. Because the other examples mentioned would be affected similarly we shall not consider them.

Two factors that affect the propagation of signals in an ionized region are the frequencies in the signal and the electron density along the propagation path. These are important because an electron density is characterized by a minimum frequency below which all signals are attenuated (or absorbed if the region is deep enough). We will find this minimum frequency by studying the propagation of a plane wave through an ionized region. The plane wave is described by the following equation

$$E = E_0 \cos(\omega t - kz) \tag{210}$$

or

$$E = \text{Real}\left[E_0 e^{-j(\omega t - kz)}\right] \tag{211}$$

where we have expressed the wave nature as a complex quantity and where ω is the radian frequency of the signal and k is

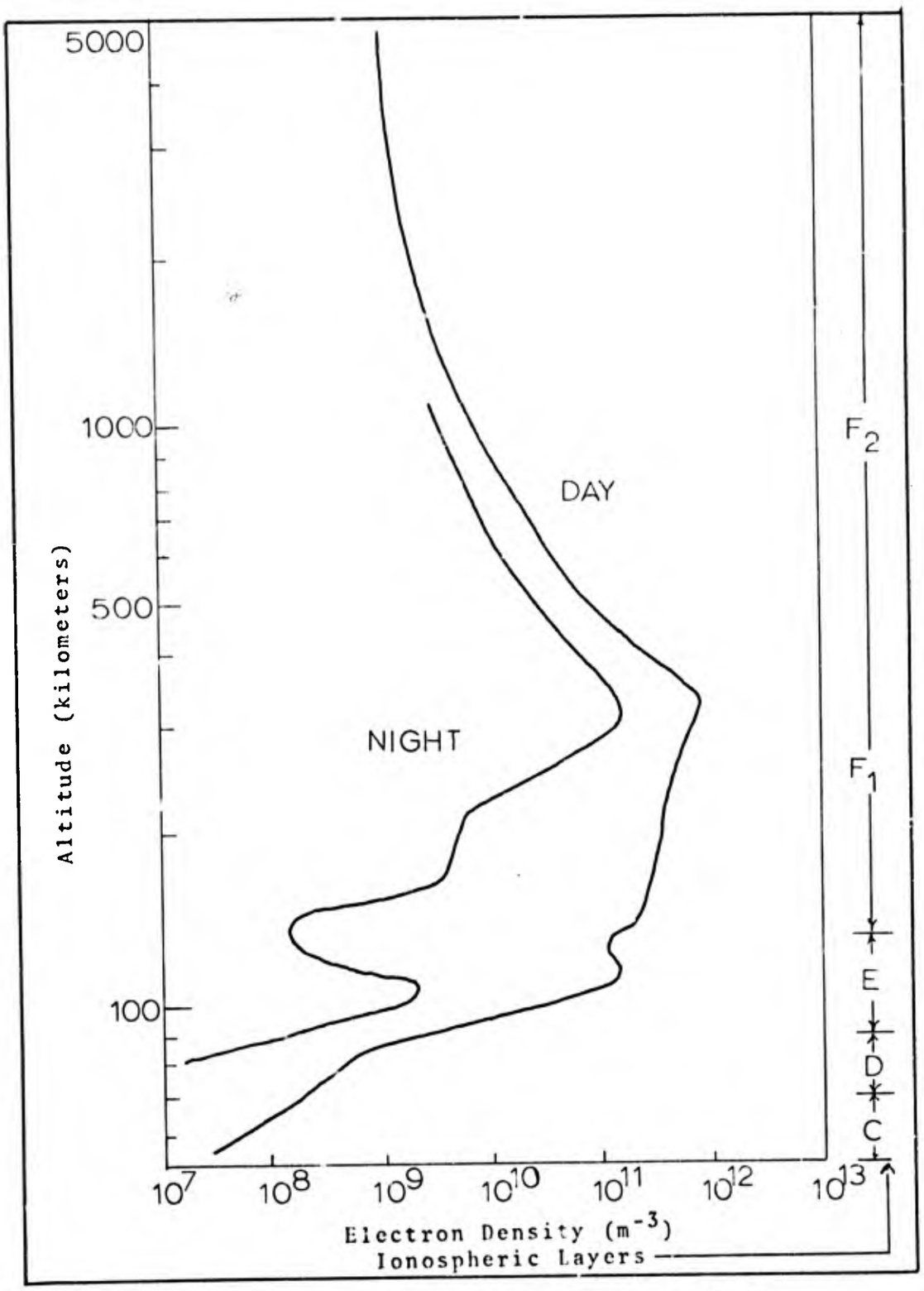

Fig. 35. Electron Density Profile (typical).[121]

the propagation constant. The propagation constant is

$$k = \omega\sqrt{\mu_o \epsilon} \tag{212}$$

where μ_o is the permeability of free space and ϵ is the permittivity of the region containing free electrons.[119] This permittivity is given by

$$\epsilon = \epsilon_o\left(1 - \frac{N e^2}{\omega^2 \epsilon_o m_o}\right) \tag{213}$$

where N , e , and m_o are the electron's number-density, charge, and mass respectively. If $Ne^2 > \omega^2 \epsilon_o m_o$ the propagation constant is imaginary and, in Eq (211), e^{jkz} becomes $e^{-k''z}$ where k'' is real. This means that the wave is now being attenuated exponentially:

$$E = E_o e^{-k''z} \cos \omega t \tag{214}$$

Typical values for the critical frequency (where $Ne^2 = \omega^2 \epsilon_o m_o$) range from 3 to 8 Mhz depending on season, time of day, and sunspot activity.[120] A typical natural electron density profile (Fig. 35) peaks around 100 km and again at higher altitudes.[121] The critical frequency for the 100 km peak in Fig. 35 is 4 Mhz.

In Fig. 36 we present a pulse shape recorded 44.6 km from a nuclear burst.[122] By looking at the frequency spectrum of this pulse,[123] Fig. 37 we see that most of the signal is unlikely to penetrate the ionosphere. However, Karzas and

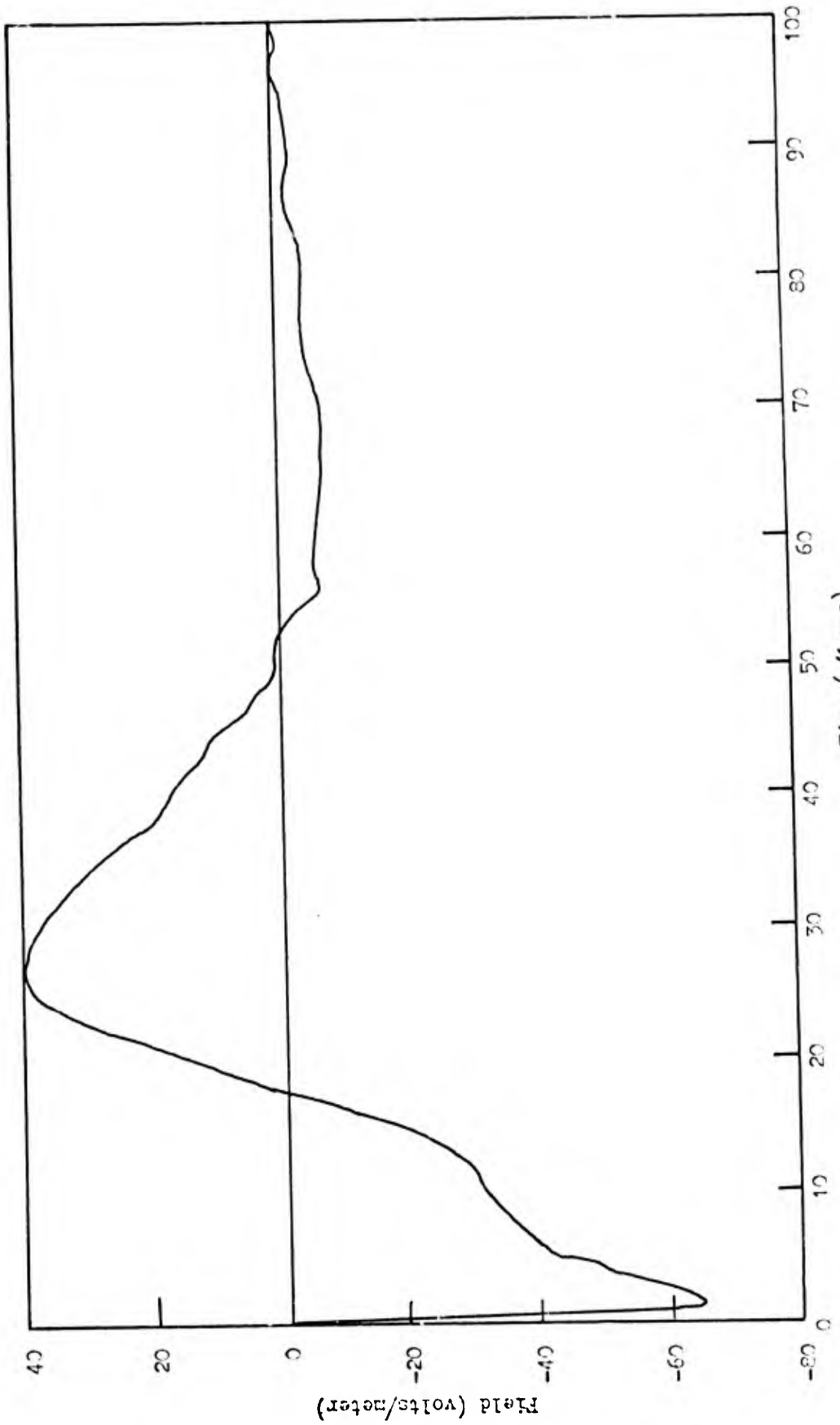

Figure 36. Observed Pulse at 44.6 Km.

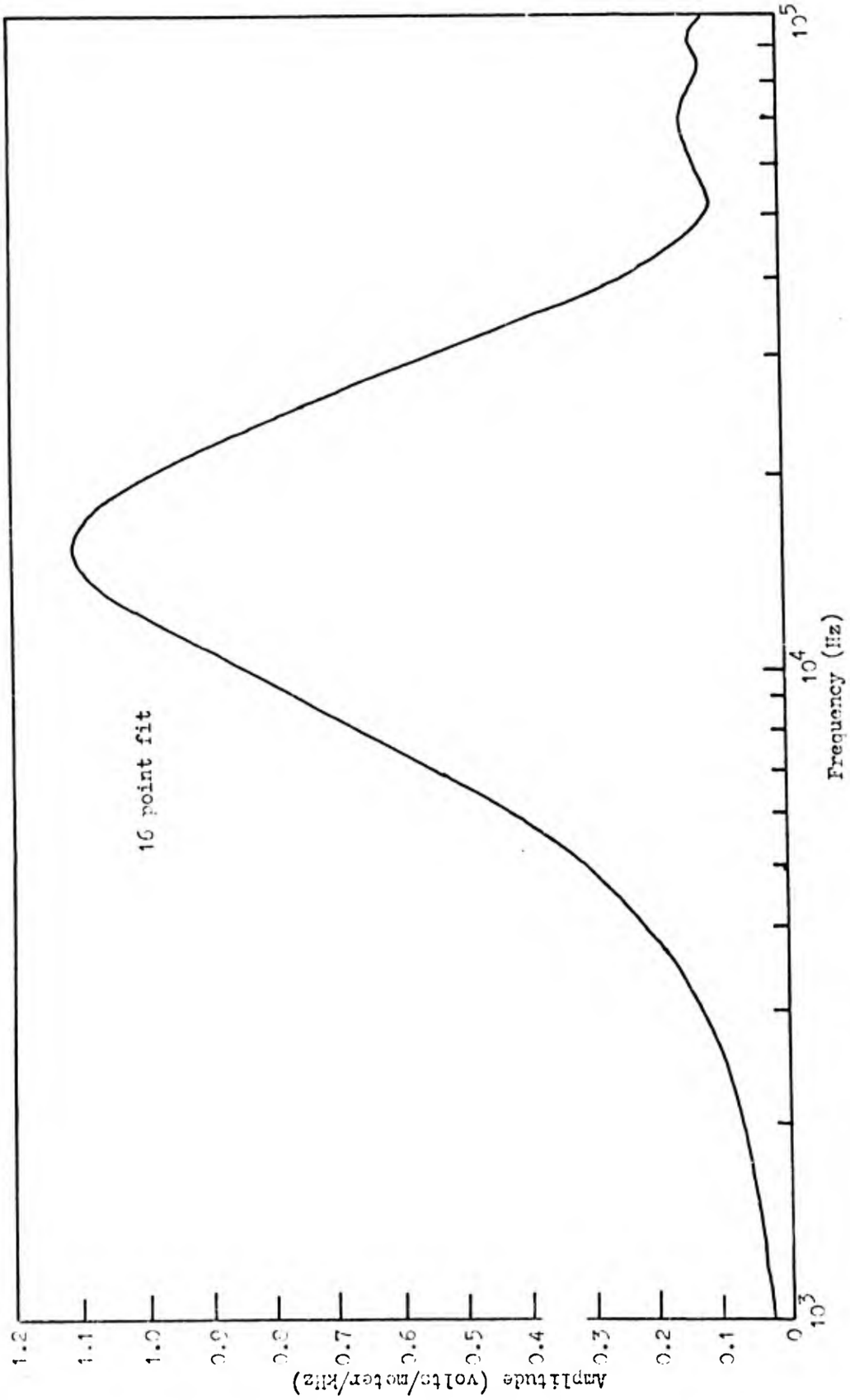

Figure 37. Spectrum of Observed Pulse.

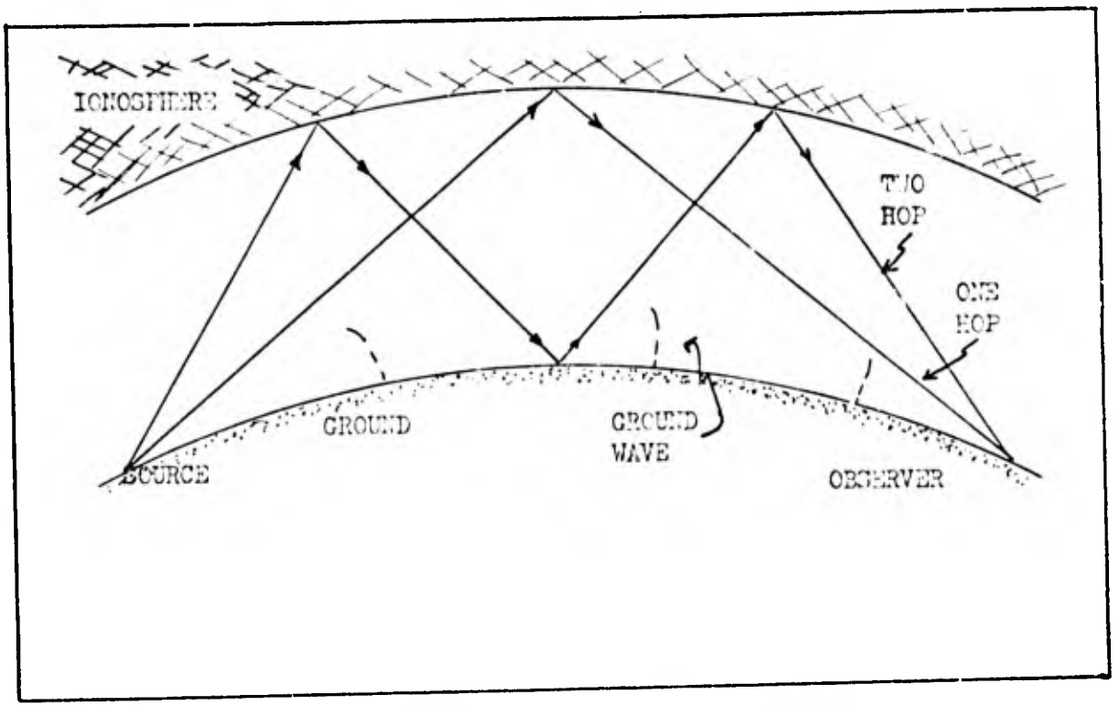

Figure 38. Ground and Reflected Electromagnetic Waves.

Latter state that the EMP does have a large enough high frequency component that a detectable and identifiable signal would penetrate the ionosphere.[124] The spectrum in Fig. 37 supports this since the 10^5 Hz signal is relatively large. Karzas and Latter also state that spherics would be largely attenuated by the ionized layers because of their low frequencies,[125] and therefore they would be of minor concern to the detection problem.

The pulse from a nuclear burst far in space would be affected by comparable attenuation below a comparable critical frequency. The electron density following a high altitude burst ($\gtrsim$ 100 km) may be so large that nearly all the electromagnetic radiation propagating into the ionized region would be attenuated (black-out effect).

Ground and Reflected Wave Propagation

The second type of propagation we shall consider is the propagation of a wave within the region between the ionosphere and the earth's surface. An electromagnetic pulse in this region will propagate as ground and reflected (or sky) waves. A ground wave is an unreflected wave in contrast to the sky waves which reflect off the ionospheric layers of the atmosphere[126] (See Fig. 38). The signal received at a distant station is a combination of these ground and sky waves and must be analyzed by unfolding the signals which arrived via various reflection paths if any indication of the original signal's shape is to be found. Since the

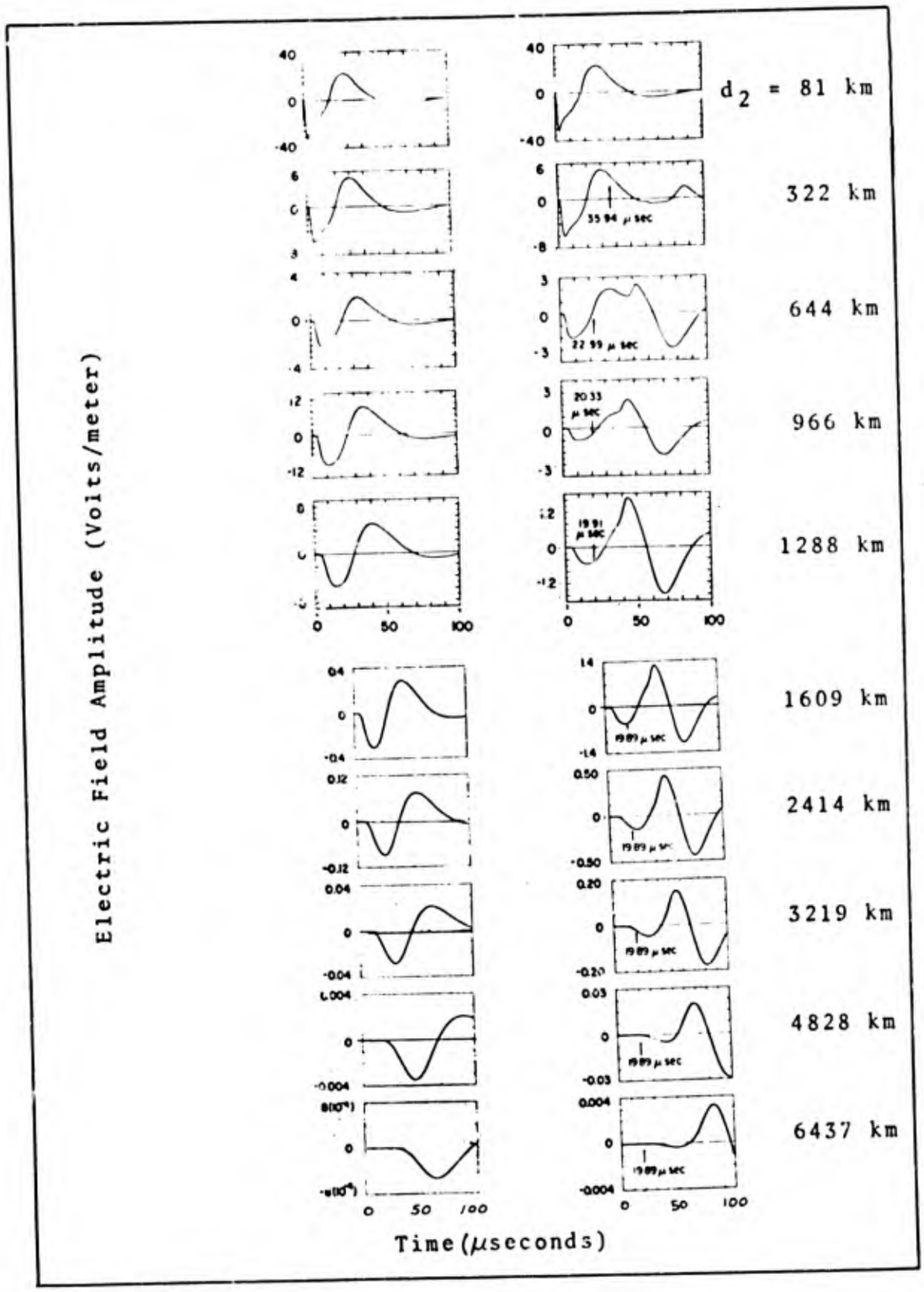

Fig. 39. Theoretical Propagation of Observed Waveform. The observed waveform (Fig. 36) was theoretically propagated as a groundwave (left column) and as sky waves. The sum of the groundwave and a first reflected wave are shown in the right hand column.

electronic signature of a nuclear burst is distinctive, the study of pulse propagation may be important to test ban treaty policing. After the 1958 high-altitude nuclear weapons tests there was a report of radios damaged at a range of 2500 miles;[127] damage which might have been due to ground and reflected waves adding.

In order to show the effect of propagation on a wave shape we present the series of graphs in Fig. 39. These graphs show the pulse shape measured at 44.6 km as it would look if measured at the distances indicated. The graphs were drawn by mathematically propagating the signal around the earth as a ground wave and as reflected waves and summing the results.[128]

The pulse in Fig. 39 is realistic but may not be expressed as a simple function so we present a smooth function which may prove useful to the reader. Wait (Ref 129) gives a representation of the exponential source function as $\alpha e^{-\alpha t}$ which he alters to get a more realistic waveform for a lightning stroke current dipole radiator:

$$S(t) = \alpha \left[e^{-\alpha t} - e^{-\alpha_i t} \right] \qquad \alpha_i > \alpha \qquad (215)$$

This equation, for lightning, has a peak around 10-20 x 10^{-6} seconds. The form for this pulse is shown in Fig. 40. The dominant mode (the first wave which "fits" the waveguide formed by the earth and the ionosphere) of the propagated pulse is shown in Fig. 41 as it would look after traveling

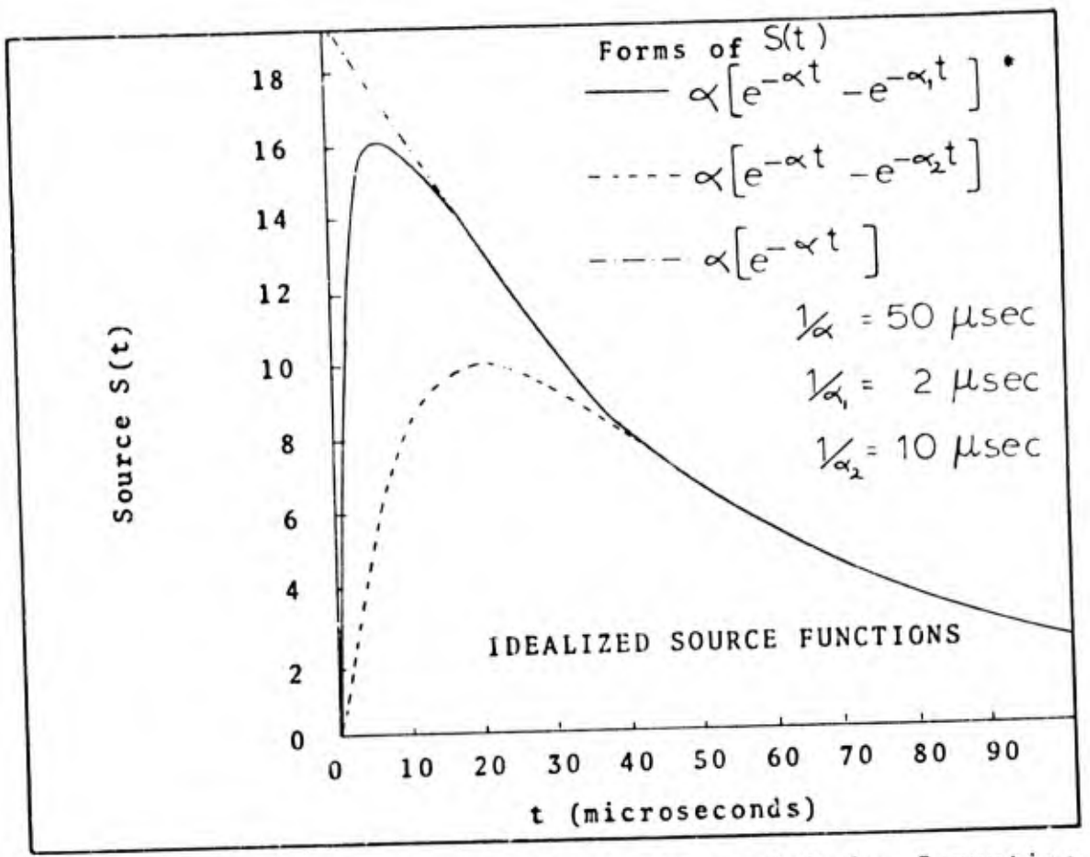

Fig. 40. Idealized Source Functions Useful for Computing Transient Responses. (*Used in Fig. 41).

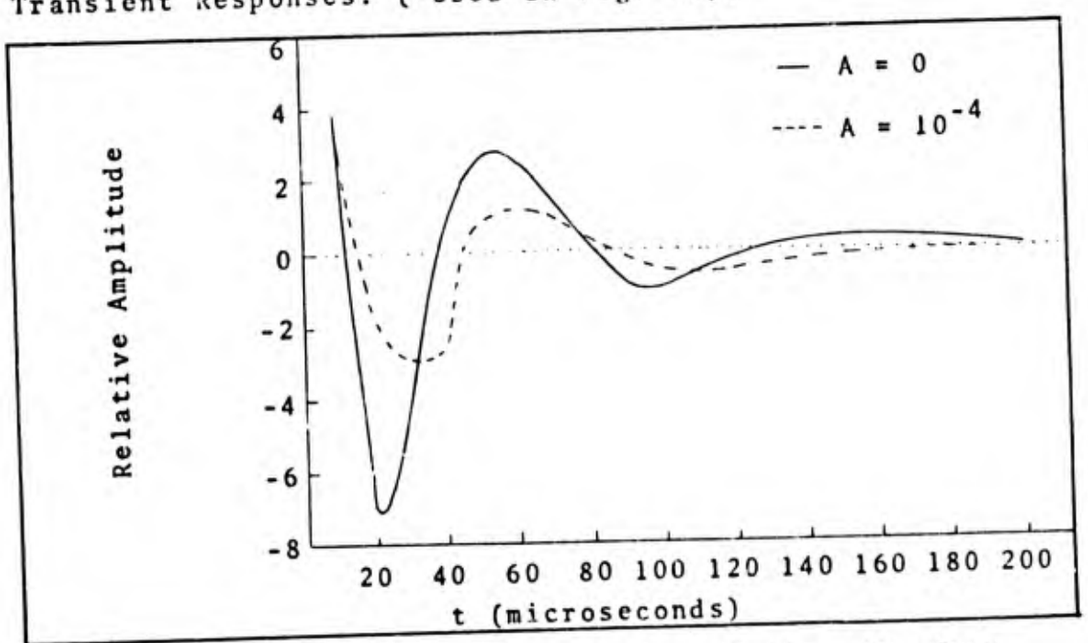

Fig. 41. Shape of the 2-μsec pulse of Fig. 40 after traveling 3000 km. The solid and dotted curves are for propagation over earth with infinite and finite conductivities respectively.

3000 km. It is to be noted that the wave is oscillatory at this distance and that the curve shown for finite conductivity has lower and more rounded peaks than the curve for a perfect conductor.

Propagation of the EMP into the Ground

The last signal propagation we shall consider is that of the EMP's penetration into the ground. This is an important problem since many power and communication links are underground. Previous studies of the effects of lightning on underground systems could provide a specific and detailed foundation for studying EMP effects (For example, see Ref 131). We shall not be as detailed in this paper as the cited reference is. If we suppose that the earth's conductivity is good we can treat the penetration of the electric field into earth as a skin effect problem.[132] The skin depth, δ, is a measure of the distance an electric signal will penetrate into a conductor before suffering an e-fold decrease in intensity. It is given by

$$\delta = \sqrt{\frac{2}{\omega \sigma \mu}} \qquad (216)$$

where σ is the conductivity in mhos/meter; ω is the radian frequency in radians/second; and μ is the permeability of the medium. Representative values of σ for sea water and earth are 4.5 and 10^{-2} mhos/meter respectively.[134] If we suppose a 10^4 volt/meter pulse with a frequency of 10^4 Hz,

we find that the electric field 50 meters into the earth (the skin depth) is reduced by e^{-1} but is still 4.4×10^3 volts/meter.

Summary

The ionized layers can attenuate the EMP significantly if the electron density is high enough. After a high altitude nuclear burst the electron density can be very high and will attenuate most signals incident upon it. The signal propagated through the atmosphere is altered significantly by waves reflecting off the ionosphere. The EMP will penetrate into the earth a distance which can be approximated using the skin depth, Eq 216.

VII. The Reception of the Electromagnetic Pulse

In general we shall gather into this section examples of the ways in which the EMP will interact with a system. Again we beg off on analytical or truly accurate solutions because of the effort involved in their development and solution. We remain focused on simple or approximate models intended to illustrate not precisely analyze.

There are two ways an EMP can interact with a system. Both involve inducing a difference in potential which in turn causes a current to flow. This current may represent a false signal in an electronic subsystem or, in extreme cases, it may even destroy the conductor or components it flows through. First the electric field will induce voltages, i.e.,

$$V = -\int_{\ell} \bar{E} \cdot d\bar{\ell} \tag{217}$$

Secondly the changing magnetic field will induce voltages, i.e.,

$$V = -\frac{\partial \Psi}{\partial t} \tag{218}$$

We will examine the voltage induced by the EMP in three cases: (1) the voltage between two points; (2) the voltage induced in a loop; and (3) the voltage on a short antenna. Following this we will consider the attenuation of the

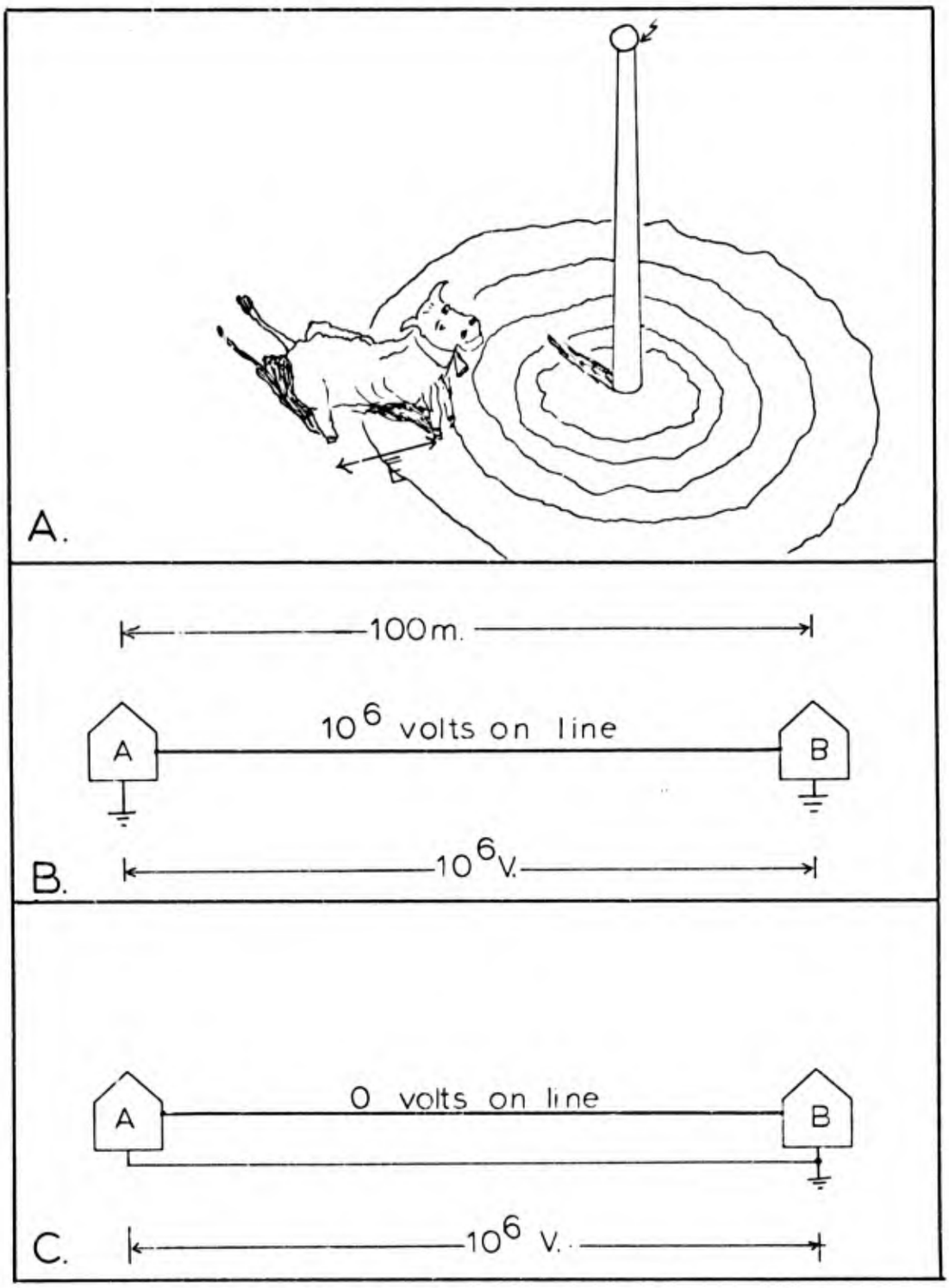

Fig. 42. Electric Field between Two Points. In A the cow has an electric field between her front and hind legs.[136] In B, A and B are individually grounded and feel a large impressed voltage. In C there is only one ground and the field in the vicinity has no effect.

impressed signal by shielding with a good conductor and with a good conductor having a hole in it.

The Voltage Between Two Points

An electric field between two points produces a voltage which is commonly accepted as a current source. We shall remind the reader of the similarity here to the lightning pulse and then extend the analysis to a model EMP field.

In Fig. 42a we see the effect of a lightning stroke near a cow. A large potential forms across the ground near a lightning stroke; about 30,000 volts/meter for $\sim$ two meters.[135] This potential between the front and rear of the cow effectively drives a current through the cow.

In the case of the EMP, which we assume to be a plane wave incident normal to the earth's surface, we find the open circuit voltage between A and B of Fig. 42b to be

$$V = \int_0^{\ell} \bar{E} \cdot d\ell = E\ell \qquad (219)$$

If the EMP amplitude is 10^4 volts/meter and ℓ is 100 meters the voltage between the points is 10^6 volts.

Now if we look at the grounded system shown in Fig. 42 we see that the two grounding points have 10^6 volts between them and if the wire joining the two pieces of equipment has a conductivity of 5.8×10^7 mhos/meter and is 2 mm x 2 mm in cross section the current flow is

$$I = V/R \tag{220a}$$

$$= V\sigma A/\ell \tag{220b}$$

$$= 10^6(58\times10^7)(4\times10^{-6})/100 \tag{220c}$$

$$= 2.3\times10^6 \quad \text{(amperes)} \tag{220d}$$

(where A is the area of the conductor in m^2).[137] Such a current may damage the equipment.

Of course the solution to this particular problem is to build equipment with a ground at one point only, as in Fig. 42c.[138]. This is analogous to having the cow stand on one foot during lightning storms.

This example oversimplifies the solution to the problem because the ground cable as shown in Fig. 42c has a finite conductivity and will therefore develop a potential along it which may couple to the active wire. Partial solutions are to use a three wire system in which the two signal carrying wires are inside a grounded sheath (the third wire).

Voltages Induced by Time Varying Magnetic Fields

The second means of coupling the EMP to a circuit is by the effect of a time varying magnetic field upon a loop

within the circuit. We shall in this section derive a simplified formula for the induced voltage and then apply this voltage to a time varying pulse of the form given for a lightning stroke in the last chapter. Values will be assigned to the amplitude of the EMP field in order to work examples which illustrate the magnitude of the induced voltages.

Faraday's law, the third Maxwell equation, is basic to the study of voltages due to time varying magnetic fields:

$$V = -\frac{\partial \Psi}{\partial t} = \frac{d \int_S \bar{B} \cdot d\bar{S}}{dt} \tag{221}$$

We shall concern ourselves only with loops which have fixed boundaries so we can rewrite the equation as

$$V = -\int_S \frac{\partial \bar{B}}{\partial t} \cdot d\bar{S} \tag{222}$$

and if we further concern ourselves with a plane surface and magnetic fields which are not a function of position on the surface S, we can say that

$$V = -\frac{\partial \bar{B}}{\partial t} \cdot \bar{S} \tag{223}$$

If $\bar{B} = \bar{B}_0 f(t)$, where

$$f(t) = \alpha (e^{-\alpha t} - e^{-\alpha_1 t}) \quad , \alpha_1 > \alpha \tag{ }$$

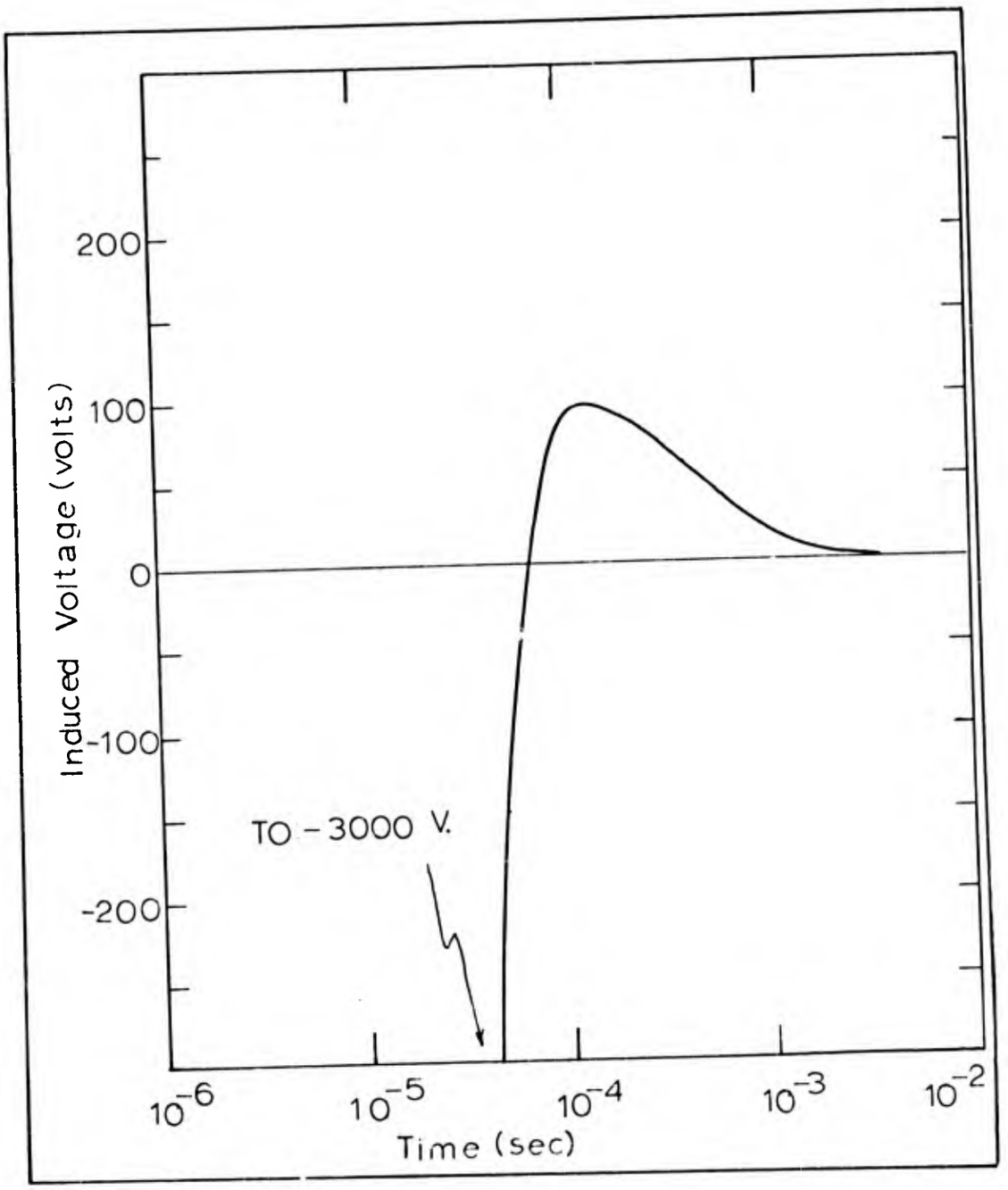

Fig. 43. Voltage Induced in a Circuit by a Lightning Stroke Model.

as in the lightning stroke of Fig. 40, then

$$V = -\bar{S}\cdot\bar{B}_0 \propto \frac{\partial}{\partial t}\left(e^{-\alpha t} - e^{-\alpha_1 t}\right) \tag{225a}$$

$$= -\bar{S}\cdot\bar{B}_0 \propto \left(-\alpha e^{-\alpha t} + \alpha_i e^{-\alpha_1 t}\right) \tag{225b}$$

$$= \frac{\bar{S}\cdot\bar{H}_0}{\mu_0^{-1}} \propto^2 \left(e^{-\alpha t} - \frac{\alpha_i}{\alpha} e^{-\alpha_1 t}\right) \tag{225c}$$

The voltage V is negative for the early parts of the pulse since $\alpha < \alpha$ and positive later in the pulse. If we insert values into this equation we have

$$V = S\,\frac{10^4}{120\pi}(4\pi \times 10^{-7})(2\times 10^4)^2(e^{-\alpha t} - 25e^{-\alpha_1 t}) \tag{227a}$$

$$= S(1.3\times 10^4)(e^{\alpha t} - 25e^{-\alpha_i t}) \tag{227b}$$

where α = 2 x 10^4 sec^{-1} and α_1 = 5 x 10^5 sec^{-1}). For a loop 0.1 x 0.1 meters (S = 1 x 10^{-2} m^2, about the size of a hand) the field varies between a negative 3000 volts to a positive 90 volts (See Fig. 43).

Let us return to the example of the two pieces of equipment separated by 100 meters (Fig. 42c). Suppose they are joined by ordinary household electric cord (two wires,

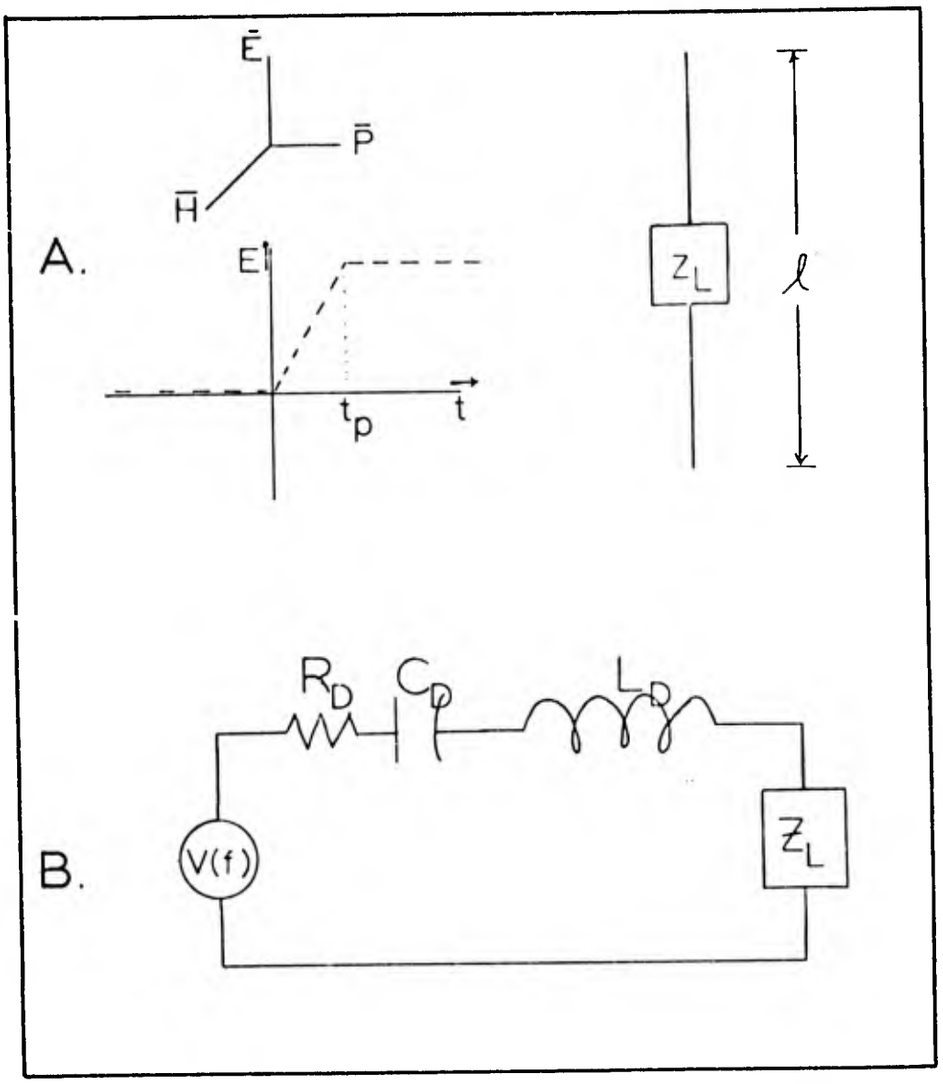

Fig. 44. Short Antenna in an Electric Field.[141]

untwisted, separated by $\sim$ 1 mm of insulation). The area between the wires is 0.1 m^2 and therefore the voltages induced will be -30,000 volts to +900 volts. The most effective partial solution to this problem is to use tightly twisted wires ($\sim$ 18 turns/foot)[139] to reduce the net loop size.

EMP Received on a Short Antenna

The EMP received on a short antenna, which will be described next, is an additional example of an electric field inducing a voltage on a circuit. We use this example as a vehicle to introduce the ideas of equivalent circuits and mathematical transformations, specifically the Fourier transform from the time to frequency domain. The Fourier and other transforms are used to relate fields incident upon a boundary to fields transmitted through the boundary and so are very important for advanced study of EMP transmission.

Following the work of D. S. Wilson let us consider the system depicted in Fig. 44a where we have a dipole antenna with a load in the center.[140] By using a wire that is short compared to any wavelength in the EMP we can make some approximations about the effects of the pulsed field. Because this short wire could be some part of a complete circuit, e.g., the leads on a carbon resistor where the resistor is the load, we see that this is a practical model. The equivalent circuit for the short antenna is shown in Fig. 44b as a voltage generator $V(f)$ in series with the

resistance $R_D(f)$, capacitance $C_D(f)$, and inductance $L_D(f)$ of the dipole and a load Z_L. The dipole parameters are all functions of the frequency, f. The load Z_L has internal capacitance C_L, resistance R_L, and inductance L_L.

The voltage impressed is

$$V = \int_{-\frac{\ell}{2}}^{\frac{\ell}{2}} E(t)d\ell = E(t)\ell \qquad (228)$$

since the antenna is so short the field is essentially constant over the length of the antenna.

We shall find the natural resonant frequency for the antenna system and the frequency spectrum of the driving signal in order to illustrate some of the techniques useful in EMP analysis. The resonant frequency of a circuit is the frequency at which the impedance becomes purely resistive. The impedance is

$$Z = \sqrt{R^2 + (\omega L - 1/\omega C)^2} \qquad (229)$$

which is purely resistive when $\omega L = 1/\omega C$ or

$$\omega = \frac{1}{\sqrt{LC}} \qquad (230)$$

The resonant frequency in the model circuit is

$$f = \frac{\omega}{2\pi} = \frac{1}{2\pi}\left[\frac{1}{(C_c + C_L)(L_c + L_L)}\right]^{1/2} \qquad (231)$$

The time dependence of the driving pulse we have assigned is

$$E = \begin{cases} 0 & , t < 0 \\ \dfrac{E_o t}{t_p} & , t \in (0, t_p) \\ E_o & , t > t_p \end{cases} \tag{232}$$

In order to find the frequency description of this function we must use a Fourier transformation[142] on it or

$$V = E(f)\ell = \ell \int_{-\infty}^{\infty} E(t) e^{-j\omega t} dt \tag{233}$$

$$\frac{V}{\ell} = \int_0^{t_p} \frac{E_o t}{t_p} e^{-j\omega t} dt + \int_{t_p}^{\infty} E_o e^{-j\omega t} dt \tag{234a}$$

$$= \frac{E_o}{t_p}\left[\frac{t e^{-j\omega t}}{-j\omega} \Bigg|_0^{t_p} - \frac{1}{-j\omega} \int_0^{t_p} e^{-j\omega t} dt \right] + \frac{E_o}{-\omega t} e^{-j\omega t} \Bigg|_{t_p}^{\infty} \tag{234b}$$

$$= \frac{E_o}{t_p}\left[\frac{-t_p e^{-j\omega t_p}}{j\omega} + \frac{1}{(j\omega)(-j\omega)} e^{-j\omega t} \Bigg|_0^{t_p} \right] + \frac{E_o}{j\omega} e^{-j\omega t_p} \tag{234c}$$

$$V = \frac{E_o \ell}{t_p (j\omega)^2}\left[1 - e^{-j\omega t_p}\right] \tag{235}$$

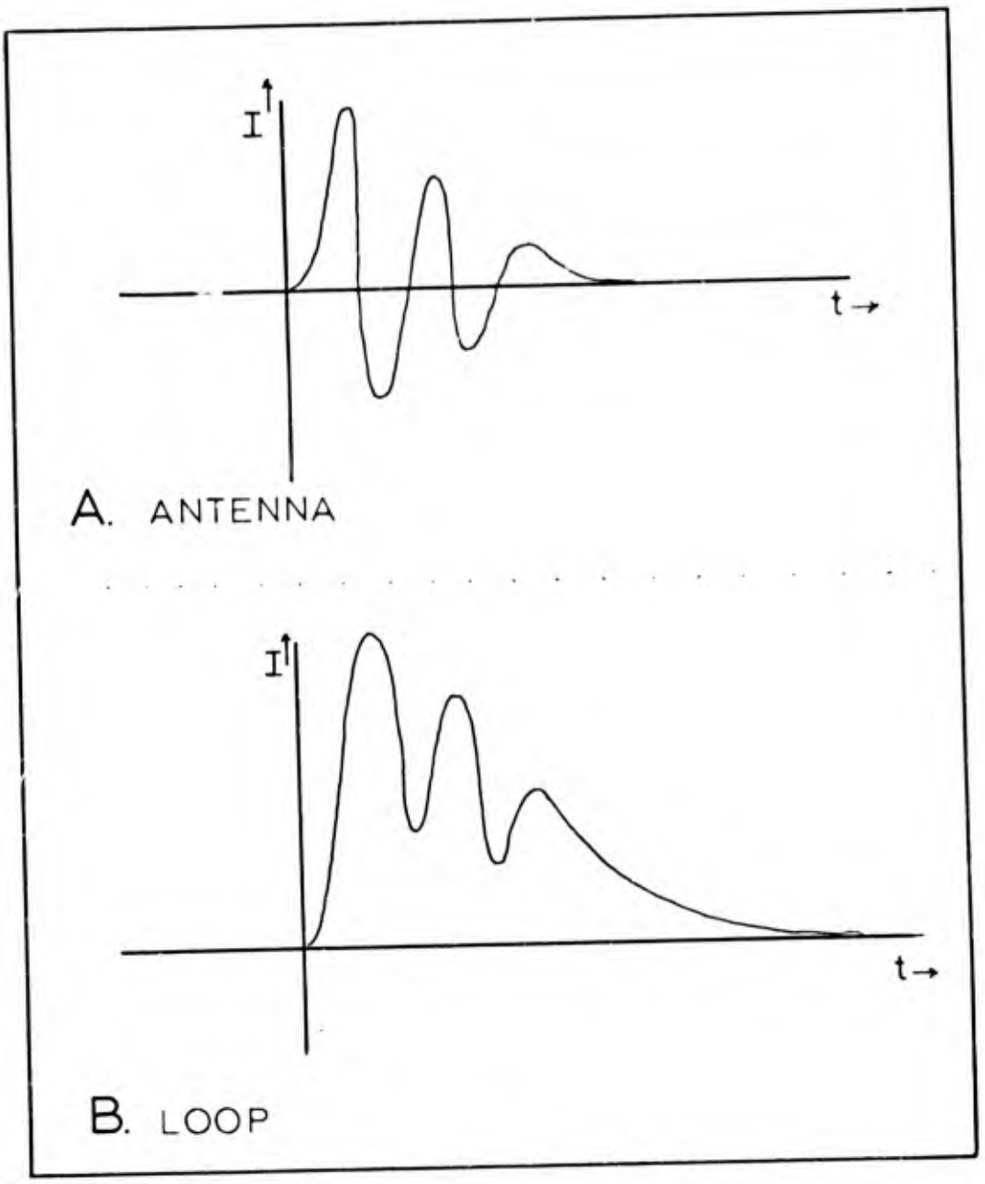

Fig. 45. Current Induced in Antenna and Loop by Pulse.[144]

This voltage as a function of frequency is due to the EMP coupling into the circuit in question. If the circuit is sensitive to any particular frequency we now have the signal's strength and can determine the protection necessary. Since this circuit is resonant it will support sustained oscillations at the resonant frequency (ringing) which damp out with the time constant[143]

$$\alpha = \frac{R_o + R_L}{2(L_o + L_L)} \quad (\sec^{-1}) \tag{236}$$

An example of this behavior is shown in Fig. 45a. Figure 45b is the current response to a magnetic loop antenna. It is to be noted that both circuits oscillate at their resonant frequencies and that there is a net current flow from the magnetic loop but not from the electric dipole. Naturally this spurious noise could cause difficulties.

Using $E\ell$ to approximate the voltage across the dipole is valid only if $\ell < \lambda$ for all λ in the spectrum. This would be the case if the circuits under consideration are short, the circuits within a radio cabinet, for example. If however the behavior of a long antenna were under study more careful consideration of the phase of the signals, angle of incidence, and other factors of the overall process would be in order.

Shielding Considerations

The methods by which an electromagnetic field induces currents in a wire, magnetic coupling in a loop and electric field potential differences, are straightforward in a very simple circuit. In large pieces of equipment, however, there are many complexities present. For example, the various circuits scatter any incident fields and the scattered fields may be weaker or stronger than the original wave. The mutual inductance between wires can couple energy received on one wire onto another wire which may or may not have been directly affected by the original signal. The literature often uses the generic term Radio Frequency Interference (RFI) for such phenomena.

In order to protect the various circuits from RFI a shield is usually put around the equipment. A good shield for radio frequencies would be of thick continuous aluminum or copper in order to be a good reflector and to contain any currents which were induced.[145] This however is impractical because water lines, input power, antenna couplers, ventilation holes and access doors all provide entry for unwanted signals. These various unwanted signals interact with circuit components where they may be rejected doing no harm, or they may cause inappropriate actions within the circuit such as changing the state of a flip-flop circuit, or they may be strong enough to burn out a circuit.

The effectiveness of a shield against RFI is measured in decibels (db). This unit expresses the ratio between

two amounts of power:[146]

$$S = 10 \log \frac{P_1}{P_2} \tag{237}$$

Since electrical power is proportional to the electric vector amplitude squared we have

$$S = 10 \log \frac{E_1^2}{E_2^2} = 20 \log \frac{E_1}{E_2} \tag{238}$$

where E_1 is the incident field intensity and E_2 is the exiting field intensity.

We shall look at three factors applicable to attenuation through shields: the reflection of signals from the shield; the transmission of signals through shields, and the effects of apertures.

Reflection of Electromagnetic Waves. The reflection of an electromagnetic wave from a conducting surface is a function of the wave's polarization, angle of incidence, and the reflector's properties. For a linearly polarized wave incident normal to a plane surface the reflection coefficient is

$$R = \frac{Z_2 - Z_1}{Z_2 + Z_1} \tag{239}$$

where Z_1 and Z_2 are the wave impedances of the two mediums. Since there may be material properties and thickness for

which $Z_1 = Z_2$, there are possible frequencies for which the material is transparent to the electromagnetic signal (e.g., optical coatings). However for frequencies of interest in the EMP this does not occur. In order to compute the reflectivity of aluminum to waves from free space we use the relationship

$$R = \frac{Z_{Al} - Z_o}{Z_{Al} + Z_o} \qquad (240)$$

where Z_o is the impedance of free space (377 ohms) and Z_{Al} is the impedance of aluminum but Z_{Al} is very small--therefore $R \simeq 1$. Because Eq (240) is inadequate to find the attenuation by reflection from a shield, we present without derivation an equation from C. B. Pearlston:

$$R = 108.2 + 10 \log \frac{G \times 10^6}{\mu_r f} \qquad (241)$$

where G is the conductivity relative to copper ($\sigma_{Cu} = 5.8 \times 10^7$), μ_r is the relative permeability ($\mu_r = \mu/\mu_o \sim 1$), and f is the frequency in Hz.[147] For example let us find the attenuation a signal would undergo by reflection from an aluminum sheet. The conductivity of aluminum is 3.54×10^7 mho/meter, $\mu_r \sim 1$, and we choose the frequency to be 1 Mhz. Equation (241) is then

$$R = 108.2 + 10 \log \frac{\frac{3.54 \times 10^7}{5.8 \times 10^7} \times 10^6}{(1)(10^6)} = 106.1 \qquad (242)$$

The signal penetrating into the aluminum will be reduced by 106.1 db. from its initial intensity.

Transmission of Signals through Shields. If a shield is thick enough to have structural rigidity, then higher frequency signals will usually be attenuated by that thickness to a point where the transmitted signal is negligible.[148] The measure of the rate of attenuation of the field strength is given by the skin depth which is the distance for an e-fold decrease in intensity. Skin depth is given by

$$\delta = \sqrt{\frac{2}{\mu \sigma \omega}} \tag{216}$$

which for aluminum is 2.7×10^{-3}, 2.7×10^{-4}, and 8.5×10^{-5} meters for signals of 1 Khz, 100 Khz, and 1 Mhz respectively. Note that the depth of penetration is large for lower frequencies (2.7 mm at 1 Khz). Pearlston gives the following expression for the attenuation through a shield

$$A = 1.33 \times 10^{2}\, t \sqrt{f G \mu_r} \tag{243}$$

where t is the shield thickness in meters.[149]

The total attenuation by reflection and attenuation is given by

$$S = A + R \tag{244}$$

Apertures. Any aperture in a shield can allow signals to leak into the shielded area where they can interact in

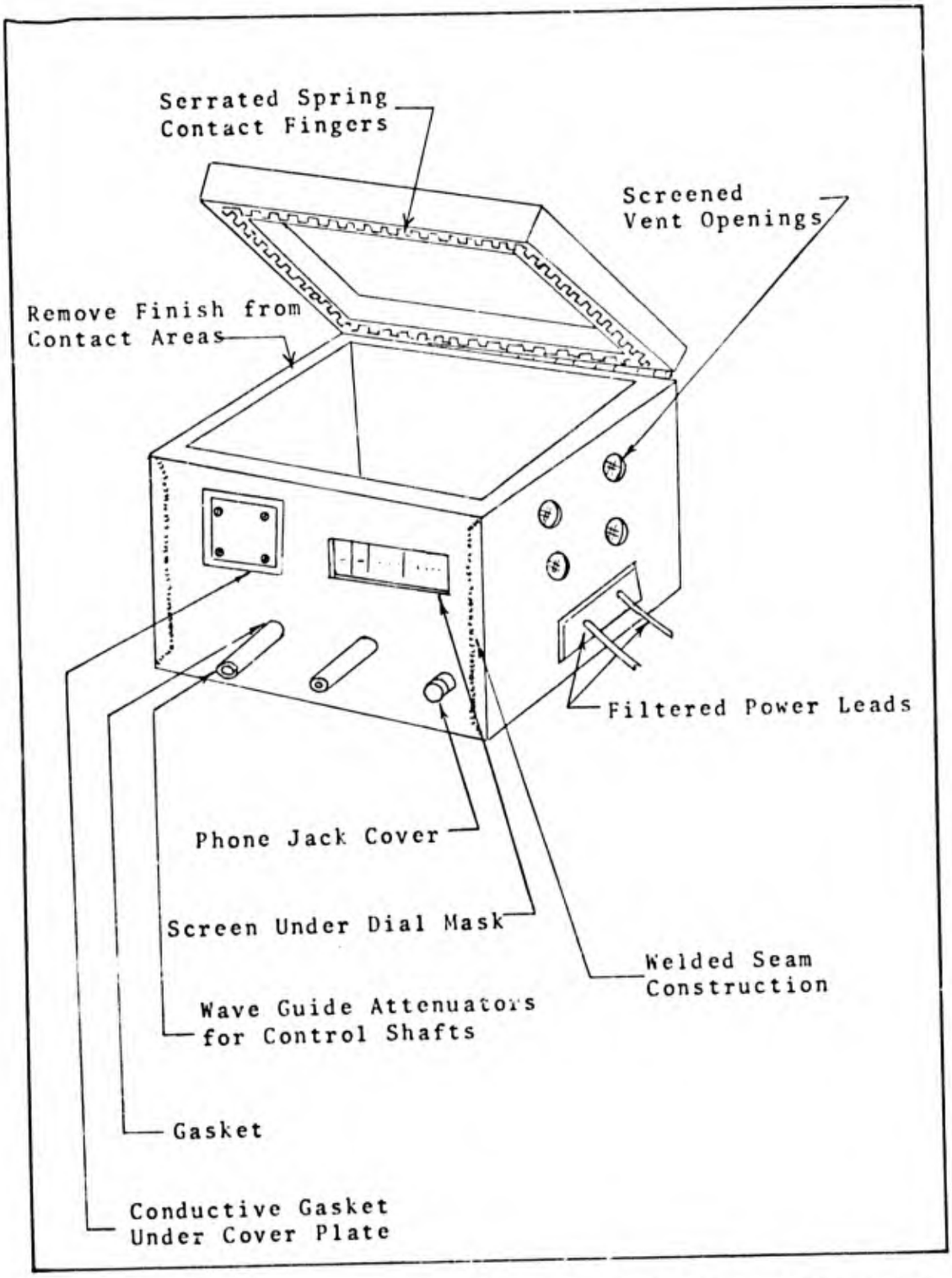

Fig. 46. Features of an Effective Shielded Equipment Case.[151]

ways previously described. The study of aperture transmission is quite complex even for very simple shapes but there are some systematic approaches available. The first approach is to model the aperture by a radiator of the same shape and size, for example, a half wave length slot may be modeled by a half wave antenna. Another approach is to replace the electric field across the aperture by the equivalent magnetic current sheet and then find that current's radiation pattern. Another possible approach when the aperture opens into a cavity is to treat the system as the aperture driving a resonant cavity.

We shall make a few generalized statements in lieu of an analytical attack:[150]

Any holes into the protected area must be kept small in comparison to the operating wavelength.

For a given distance from a single hole the leakage intensity is proportional to the cube of the hole dimensions, e.g., doubling the diameter of a round hole will cube the intensity of the leakage field.

Wave guide attenuators are useful for large holes, since they pass frequencies above a cutoff frequency and attenuate all frequencies below that frequency.

In Fig. 46 we see the features of an effectively shielded equipment case.

Summary

The two basic mechanisms for coupling the EMP to a physical system are most clearly stated by the equations

$$V = \int E \cdot d\ell \quad ; \quad V = -\frac{\partial \psi}{\partial t}$$

The EMP is attenuated by shielding which must be thick and continuous to be completely effective. Since shielding must always have entry and egress holes, engineers must design shields and circuits keeping the EMP in mind.

Final Comment

This thesis provides a basic description of the EMP from source to coupling with circuits. Improvements in future work might include finding a simple, self-consistent surface-burst current distribution that will match the boundaries conditions imposed by the radiated field equations. Another improvement would be the addition of a simple aperture leakage calculation to illustrate the physics of the problem. For this last problem it is suggest that Ref 152 be found.

References

CHAPTER I

1. EMP Protection for Emergency Operating Centers TR-61A. Washington D.C.: Department of Defense/Office of Civil Defense, 1971. Page 3.

2. Rexrode, L. O. "Noiseproof a Digital Electronic Control System." Control Engineering, 15:66-71 (Nov 1968). Page 66.

3. Collins, A. Frederick. The Radio Amateur's Handbook, 12th Ed. Thomas Y. Crowell Co., New York, 1970. Page 262.

4. Lamont, Lansing. Day of Trinity. New York: Atheneum, 1965. Page 231.

5. Lamont, page 247.

6. Gilinsky, V. "The Kompaneets Model for Radio Emission from a Nuclear Model." Rand Corporation Report Memorandum, RM-4134:1-20 (August 1964). Page 4 (Also published as EMP Theoretical Note 36, DASA 1882-2).

CHAPTER II

7. Elliott, Robert S. Electromagnetics. New York: McGraw Hill Book Co., 1966. Page 112.

8. Jordan, E. C. and K. G. Balmain. Electromagnetic Waves and Radiating Systems. Englewood Cliffs, N. J.: Prentice-Hall, Inc., 1968. Page 33.

9. Elliott, page 222.

10. Elliott, page 259.

11. Elliott, page 258.

12. Jordan and Balmain, page 102.

13. Elliott, page 264.

14. Elliott, page 341.

15. Jordan and Balmain, page 105.

16. Elliott, pages 225-230.

CHAPTER III

17. Bridgman, Charles J. (Private Communication).

18. Baran, Michael. Introduction to EMP. 1968. (Unpublished notes, Air Force Institute of Technology, Physics Department, Wright-Patterson Air Force Base, Ohio.) (Adapted from figure on page 89.)

19. LeLevier, R. E. "The Compton Current and the Energy Deposition Rate from Gamma Quanta--A Monte Carlo Calculation." Rand Corporation Report Memorandum, RM 4151 PR: 1-43 (June 1964). Page 20. (Also published as EMP Theoretical Note 37).

20. LeLevier, R. E. page 39.

21. Karzas, W. J. and R. Latter. "Detection of the Electromagnetic Radiation from Nuclear Explosions in Space." Rand Corporation Report Memorandum, RM-4306: 1-40 (October 1964). Page 24. (Also published in Physical Review, Vol 137, No. 5B. pages 1369-1378, March 8, 1965, and as EMP Theoretical Note 40).

22. Lederer, Michael C. et. al. Table of Isotopes. (Sixth Edition). New York: John Wiley and Sons, Inc., 1967. Page 158.

23. Karzas and Latter, RM-4306, page 20.

24. Schaefer, R. R. and C. A. Stevens, Neutron Induced Electrical Sources, AFWL Technical Report AFWL-TR-69-8. Kirtland Air Force Base, New Mexico: Air Force Weapons Laboratory, May 1969. Page 5. (EMP Theoretical Note 61). The Authors are associated with Gulf General Atomic, Inc.

25. Schaefer and Stevens, page 29.

26. Stehn, John R., et al. Neutron Cross Sections Vol 1, Z = 1 to 20, BNL 325 Supplement 2 (Second Edition). Washington: Brookhaven National Laboratory, May 1964. Page 7-14-2.

27. Hale, Clovis R. Neutron-Induced Ionization Rate and Electron Current From a Point Source (Dissertation). Wright-Patterson AFB, Ohio: Air Force Institute of Technology (AU), May 1970. Page 6.

28. Schaefer, R. R. Charge Currents and Conductivity Arising from Inelastic and Fast Capture Collisions of Neutrons in the Air Surrounding a Nuclear Detonation, EMP Theoretical Note 15. Kirtland Air Force Base, New Mexico: Air Force Weapons Laboratory, February 1966. (Theoretical Notes 1-21 published in EMP-2, DASA 1882-1, May 1967). Page 3.

29. Schaefer, Theoretical Note 15, pages 2-4.

30. Hale, pages 16-28.

31. Evans, Robley D. The Atomic Nucleus. New York: McGraw Hill Book Co., 1955. (Figure adapted from page 713).

32. Kompaneets, A. S. Radio Emission From an Atomic Explosion. Soviet Physics JETP, 35 (8): 1076-1080 (June 1959) Page 1076.

33. LeLevier, page 2.

34. Evans, pages 695-701.

35. Lederer, page 567.

36. Davisson, C. M. and R. D. Evans. "Gamma-Ray Absorption Coefficients." Reviews of Modern Physics, 24: 79-107 (April 1952). Page 91.

37. Karzas and Latter, RM 4306, page 29.

38. Davisson and Evans, page 81.

39. Evans, page 691.

40. Davisson and Evans, page 106.

41. Schaefer, Theoretical Note 15, page 7.

42. Freyer, Gustav J. Lecture notes of Physics of the Upper Atmosphere, PH 5.75. Wright-Patterson Air Force Base, Ohio: Air Force Institute of Technology (AU), Spring 1970. Page 77.

43. Evans, Robley D. The Atomic Nucleus. McGraw Hill, New York, 1955. Page 611.

CHAPTER IV

44. Korn, G. A. and M. Korn. Mathematical Handbook for Scientists and Engineers (Second Edition). New York: McGraw Hill Book Co., 1968. Pages 874-879.

45. Elliott, pages 126-127.

46. Jackson, John D. Classical Electrodynamics. New York: John Wiley & Sons, Inc., 1962. Pages 2-3.

47. Gilinsky. RM-4134, page 7.

48. Electromagnetic Pulse (EMP) Fundamentals. Wright-Patterson Air Force Base, Ohio: Air Force Institute of Technology, November 1969. Page 7. (This is an unclassified handout prepared by the Physics Department.)

49. Electromagnetic Pulse (EMP) Fundamentals, page 7.

50. Price, William J. Nuclear Radiation Detection, (Second Edition). New York: McGraw Hill Book Co., Inc., 1964. Page 15.

51. Price, page 6.

52. Gilinsky, Victor. "The Development of a Radio Signal from a Nuclear Explosion in the Atmosphere." Rand Corporation Report Memorandum, RM 4988:1-20 (August 1966). Page 6. (Also published as EMP Theoretical Note 47).

53. Whitten, Robert C. and I. G. Poppoff, Physics of the Lower Ionosphere. Englewood Cliffs, N. J.: Prentice Hall, Inc., 1965. Pages 98-125.

54. Barron, page 95.

55. Whitten and Poppoff, pages 98-125.

56. Whitten R. C. and Poppoff, pages 98-125.

57. Whitten and Poppoff, page 127.

58. Whitten and Poppoff, page 127.

59. Barron, page 101.

60. Gilinsky, Victor. RM 4134. Page 9.

61. Gilinsky, Victor. RM 4134. Page 11.

62. Gilinsky, Victor. RM 4134. Page 11.

63. Gilinsky, Victor. RM 4134, Page 4.

64. Karzas, W. J. and R. Latter. "Satellite Based Detection of the Electromagnetic Signal from Low and Intermediate Altitude Nuclear Explosions." Rand Corporation Report Memorandum, RM-4542:1-22 (June 1965). Page 5. (Also published as EMP Theoretical Note 42).

65. Evans, page 689.

CHAPTER V

66. Valley, Shea L. (ed). Handbook of Geophysics and Space Environments. Bedford, Mass: Air Force Cambridge Research Laboratories, 1965. Page 17-24.

67. Karzas and Latter, RM 4542, page 12.

68. Goldrick, W. B. et. al. "A Modular System of Logic for the VELA A Satellite Program." IEEE Proceedings, Vol 53:1959-1969 (December, 1965). Page 1961.

69. Karzas and Latter, RM 4306, page 4.

70. Karzas and Latter, RM 4542, page 4.

71. Karzas and Latter, RM 4306, pages 1-39.

72. Karzas and Latter, RM-4306, page 7.

73. U. S. Standard Atmosphere, 1962. Washington, D.C.: United States Weather Bureau, December 1962. (Tables I and II starting page 33.)

74. Howerton, Robert J. Tabulated Neutron Cross Sections, Part 1, Vol 1, UCRS-5226 (Revised). Washington: Department of Commerce, October 1959.

75. Knight, R. L. "Numerical Solutions of Maxwell's Equations with Azimuthal Symmetry in Prolate Spheroidal Coordinates." Electromagnetic Pulse Theoretical Notes, EMP 2-3. Kirtland Air Force Base, New Mexico: Air Force Weapons Laboratory, June 1970. Pages 62-1, 62-44. Page 4.

76. Harrington, Roger F. Time-Harmonic Electromagnetic Fields. New York: McGraw Hill Book Co., 1961. Pages 103-106.

77. Harrington, pages 98-100.

78. Harrington, pages 110-113.

79. Harrington, page 111.

80. Harrington, page 105.

81. Plonsey, R. and R. E. Collin. Principles and Applications of Electromagnetic Fields. New York: McGraw-Hill Book Co., 1961. Pages 310-311.

82. Jackson, page 268.

83. Harrington, page 78.

84. Harrington, page 79.

85. Harrington, page 39.

86. Schaefer, R. R. "Prompt Gamma Effects in the Vicinity of a Ground-Air Interface." Electromagnetic Pulse Theoretical Notes, EMP 2-1, 1:1-21 (26 May 1965). Theoretical Note 10. Page 11.

87. Plonsey and Collin, page 304.

88. Plonsey and Collin, page 305.

89. Harrington, page 143.

90. Gilinsky, page 8.

91. Sollfrey, W. "An Analytically Solvable Model for the Electromagnetic Fields Produced by Nuclear Explosions." Rand Corporation Report Memorandum, RM-3744-PR: 1-23 (July 1963). Page 6. (Also published as EMP Theoretical Note 53).

92. Karzas and Latter, RM 4542, page 4.

93. Kompaneets, page 1076.

94. Whitten and Poppoff, page 135.

95. Karzas and Latter, RM 4306, page 21.

96. Rose, D. J. and M. Clark, Jr. Plasmas and Controlled Fusion. Cambridge, Mass: The M.I.T. Press, 1961. Page 72.

97. Evans, pages 890-892.

98. Karzas and Latter, RM 4306, page 9.

99. Rose and Clark, pages 198-200.

100. Karzas and Latter, RM 4306, pages 13-14.

101. Plonsey and Collin, page 311.

102. Jackson, page 269.

103. Soper, Gordon K. Private communication, January 1971.

104. Harrington, page 50.

105. Harrington, page 87.

106 Harrington, pages 106-110.

107. Harrington, page 106.

108. Karzas and Latter, RM 4306, page 23.

109. Karzas and Latter, RM 4542, page 7.

110. Karzas and Latter, RM 4306, page 22.

111. Karzas and Latter, RM 4306, page 39.

112. Karzas, W. J. and R. Latter. "The Electromagnetic Signal due to the Exclusion of the Earth's Magnetic Field by Nuclear Explosions." Rand Corporation Report Memorandum, RM-2890-PR:-1-16 (December 1961). Pages 1-16. (Also published in Journal of Geophysical Research, Vol 67, No. 12 (November 1962) pp 4635-4640 and as EMP Theoretical Note 28).

113. Karzas and Latter, RM-2890-PR, page 12.

114. Jackson, page 313.

115. Jackson, page 156.

116. Karzas and Latter, RM-2890-PR, page 13.

117. Karzas and Latter, RM-2890-PR, page 13-14.

118. Glasstone, Samuel. The Effects of Nuclear Weapons. Washington D.C.: U.S. AEC, April 1962. Page 135.

CHAPTER VI

119. Harrington, page 38.

120. Plonsey and Collin, page 475.

121. Jordan and Balmain, page 669.

122. Sollfrey, W. "Exact Solution for the Propagation of Electromagnetic Pulses over a Highly Conducting Spherical Earth." Rand Corporation Report Memorandum, RM-5792-PR: 1-46 (October 1968). Page 31.

123. Solfrey, page 33.

124. Karzas and Latter, RM-4542, page 2.

125. Karzas and Latter RM-4542, page 2.

126. Johler, J. Ralph. Electromagnetic Pulse Propagation in a Disturbed Terrestial Waveguide, U. S. Dept. of Commerce, ESSA Technical Report, IER-22 ITAS-22 Washinton: U. S. Dept. of Commerce, December 1966. (EMP Theoretical Note 55, page 14.)

127. "Radiation Burns out Radios." New York Times, Vol 108:27 (August 10, 1958).

128. Johler, J. Ralph. "Propagation of an Electromagnetic Pulse from a Nuclear Burst," IEEE Trans. Antennas and Propagation, Vol. AP-15, No. 2; 256-263 (March 1967). Page 261.

129. Wait, J. R. "Propagation of Electromagnetic Pulses in Terrestrial Waveguides." IEEE Trans. Antennas and Propagation, Vol. AP-13, No. 6: 904-918 (November 1965). Page 913.

130. Wait, page 914.

131. Wait, page 913.

132. Harrington, page 53.

133. Plonsey and Collin, page 356-357.

134. Plonsey and Collin, page 526.

135. Beck, Edward. Lightning Protection for Electric Systems. New York: McGraw Hill Book Co., 1954. Page 288.

136. Beck, page 283.

137. Plonsey and Collin, page 166.

138. Pearlston, Carl B. Jr. "Case and Cable Shielding, Bonding, and Grounding Considerations in Electromagnetic Interference." IRE Transactions on Radio Frequency Interference, RFI-4 No. 3:2-20 (October, 1962). Page 11.

139. Pearlston, page 10.

140. Wilson, D. S. "Coupling of EMP to Circuits Within Complex Equipment Racks." Instrumentation for Nuclear Weapon Effects Simulation Symposium, Vol. 1 Electromagnetic Pulse; Air Force Special Weapons Center Technical Report No. AFSWC-TR-70-5, Vol 1. Kirtland Air Force Base, New Mexico, March 1970. Page 67.

141. Wilson, page 78.

142. Korn and Korn, page 900.

143. Wilson, page 68.

144. Wilson, page 78.

145. Pearlston, page 2.

146. Reference Data for Radio Engineers (Fifth Edition). Indianapolis, Ind: Howard W. Sams & Co., Inc., 1968. Page 3-13.

147. Pearlston, page 2.

148. Pearlston, page 2.

149. Pearlston, page 1.

150. Pearlston, page 6.

151. Pearlston, page 8.

152. Kaden, Heinrich. "Wirbelstrome und Schirmung." Nachrichentechnik [Communications Journal]. Springer-Verlag, 1959. [Cited in DASA EMP (Electromagnetic Pulse) Handbook, page 9.8].

Gauss' Law

No Free Magnetic Poles

Faraday's Law

Ampere's Law (with displacement current)

Conversion Factors

1 KT = 10^{12} calories

= 2.6×10^{25} MeV

= 4.184×10^{12} Joule

1 Cal = 4.184 Joule

= 3.086 ft-lb

= 2.61×10^{-3} MeV

= 3.966×10^{-3} BTU'

1 eV = 1.6×10^{-19} Joule

= 11610°K

1 kb (Kilobar) = 10^{8} newtons/m^2 = 986.92 atmospheres

Appendix A

Useful Equations and Conversion Factors

I. $\nabla\cdot\bar{D} - \rho(r) = 0 \;:\; \oint_S \bar{E}\cdot\hat{n}\,ds = \int_V \frac{\rho(r)}{\epsilon}\,dV$

II. $\nabla\cdot\bar{B} = 0 \;:\; \oint_S \bar{B}\cdot\bar{ds} = 0$

III. $\nabla\times\bar{E} + \frac{\partial\bar{B}}{\partial t} = 0 \;:\; \oint_C \bar{E}\cdot\bar{dl} = -\frac{d}{dt}\int_S \bar{B}\cdot\bar{ds}$

IV. $\nabla\times\bar{H} - \frac{\partial\bar{D}}{\partial t} - \bar{J} = 0 \;:\; \oint_C \bar{H}\cdot\bar{dl} = \frac{d}{dt}\int_S \bar{D}\cdot\bar{ds} + \int_S \bar{J}\cdot\bar{ds}$

$\bar{F} = q(\bar{E} + \bar{v}\times\bar{B}) \;;\; \bar{A} = \frac{1}{4\pi\mu_0^{-1}}\int_V \frac{\bar{J}}{R}\,e^{-jkR}\,dv$

$\nabla\cdot\bar{J} + \frac{\partial\rho}{\partial t} = 0 \;;\; \int_S \bar{J}\cdot\bar{ds} = -\frac{d}{dt}\int_V \rho(r)\,dv$

$\bar{D} = \epsilon_0\bar{E} \;;\; \bar{H} = \mu_0^{-1}\bar{B} \;;\; \bar{J} = \sigma\bar{E} \;;\; \bar{B} = \nabla\times\bar{A}$

VECTORS : cartesian : $h_1, h_2, h_3 = 1, 1, 1$
cylindrical : $= 1, r, 1$
spherical : $= 1, r, r\sin\theta$

$$\nabla^2(\,) = \frac{1}{h_1h_2h_3}\left[\frac{\partial}{\partial x_1}\left(\frac{h_2h_3}{h_1}\frac{\partial}{\partial x_1}\right) + \frac{\partial}{\partial x_2}\left(\frac{h_3h_1}{h_2}\frac{\partial}{\partial x_2}\right) + \frac{\partial}{\partial x_3}\left(\frac{h_1h_2}{h_3}\frac{\partial}{\partial x_3}\right)\right](\,)$$

$$\nabla\times(\,) = \frac{1}{h_1h_2h_3}\begin{vmatrix} h_1\hat{a}_1 & h_2\hat{a}_2 & h_3\hat{a}_3 \\ \frac{\partial}{\partial x_1} & \frac{\partial}{\partial x_2} & \frac{\partial}{\partial x_3} \\ h_1(\,)_1 & h_2(\,)_2 & h_3(\,)_3 \end{vmatrix}$$

$$\nabla(\,) = \frac{\hat{a}_1}{h_1}\frac{\partial(\,)}{\partial x_1} + \frac{\hat{a}_2}{h_2}\frac{\partial(\,)}{\partial x_2} + \frac{\hat{a}_3}{h_3}\frac{\partial(\,)}{\partial x_3}$$

$$\nabla\cdot(\,) = \frac{1}{h_1h_2h_3}\left[\frac{\partial}{\partial x_1}\left(h_2h_3(\,)_1\right) + \frac{\partial}{\partial x_2}\left(h_3h_1(\,)_2\right) + \frac{\partial}{\partial x_3}\left(h_1h_2(\,)_3\right)\right]$$

$\nabla\cdot\nabla\times\bar{A} = 0 \;;\; \nabla\times\nabla\phi = 0 \;;\; \nabla\times\nabla\times\bar{A} = \nabla(\nabla\cdot\bar{A}) - \nabla^2\bar{A}$

CONSTANTS

$\mu_0 = 4\pi\times10^{-7} \qquad \epsilon_0 = \frac{1}{36\pi\times10^{-9}}$

Appendix B

Integration of Electron Density Equations

The differential equation for the electron density, Eq (107). can be integrated for any time dependence if the recombination term is neglected and if the electron source term is separable, i.e.,

$$S_e(r,t) = S_e(r)T(t)$$

Karzas and Latter do this in their treatment of air conductivity.[1] Baran also follows this method.[2] We shall integrate the differential equation for the electron density using four forms of the time dependence as pictured in Fig. 6. Following the integration we present a brief justification for neglecting the recombination term.

In this Appendix the notation 0 ( ) means the operation in the brackets was used to proceed from one step to the next, e.g., Eq A; 0 (x 2); Eq B means that Eq B was obtained by multiplying Eq A by 2.

From Eq (107) we have the basic differential equation (neglecting recombination)

$$\frac{dN_e}{dt} + \nu_a N_e = S_e(r)T(t) \tag{B1}$$

$0(x e^{\nu_a t} dt)$ This makes the LHS a perfect differential.

$$d(N_e e^{\nu_a t}) = S_e(r)T(t)e^{\nu_a t}\,dt \tag{B2}$$

0(Integrate--we will assign lower limits later.)

$$\int_{\text{Init.}}^{N_e e^{\gamma_a t}} d(N_e e^{\gamma_a t}) = S_e(r) \int_{T_{\text{initial}}}^{t} T(t) e^{\gamma_a t} dt \qquad \text{(B3)}$$

$t \epsilon (0, T_1)$

For the time interval from $t = 0$ to $t = T_1$ the time dependence is $T(t) = e^{\alpha t}$ therefore Eq (B3) becomes 0(Let $T(t) = e^{\alpha t}$ and apply limits)

$$N_e e^{\gamma_a t} \Big|_0^{N_e e^{\gamma_a t}} = S_e(r) \int_0^t e^{\alpha t} e^{\gamma_a t} dt \qquad \text{(B4)}$$

0 (integrate; insert limits)

$$N_e e^{\gamma_a t} = \frac{S_e(r)}{\alpha + \gamma_a} \left(e^{(\alpha + \gamma_a) t} - 1\right) \qquad \text{(B5)}$$

which becomes 0 ($\times e^{-\gamma_a t}$)

$$N_e = \frac{S_e(r)}{\alpha + \gamma_a} \left| e^{+\alpha t} - e^{-\gamma_a t} \right| \qquad \text{(B6)}$$

which is Eq (112c).

0($t > 0$; $e^{-\gamma_a t} \rightarrow 0$)

$$N_e = \frac{S_e(r)}{\alpha + \gamma_a} e^{\alpha t} \qquad \text{(B7)}$$

This is Eq (113a).

$t \in (T_1, T_2)$

In the next time interval, $t \in (T_1, T_2)$, the time dependence is $T(t) = e^{-\beta(t - T_1)}$ therefore Eq (B3) becomes

0(Replace $T(t)$; write limits)

$$\int_I^{N_e e^{\nu_a t}} d(N_e e^{\nu_a t}) = S(r) e^{\alpha T_1} \int_{T_1}^{t} e^{-\beta(t - T_1)} e^{\nu_a t} \, dt \qquad \text{(B8)}$$

where $I = S_e(r)(e^{(\nu_a + \alpha)T_1} - 1)/\nu_a + \alpha$

and where $S_e(r) e^{\alpha T_1}$ replaces $S_e(r)$ in order to match boundaries and the lower limit of the LHS is the value of $N_e e^{\nu_a T_1}$ from Eq (A5). 0(Integrate)

$$N_e e^{\nu_a t} - \frac{S_e(r)}{\alpha + \nu_a} \left| e^{-(\nu_a + \alpha)T_1} - 1 \right|$$

$$= \frac{S(r) e^{\alpha T_1} e^{\beta T_1}}{\nu_a - \beta} \left| e^{(\nu_a - \beta)t} - e^{-(\nu_a - \beta)T_1} \right| \qquad \text{(B9}$$

0(transpose; multiply all terms out)

$$N_e e^{\nu_a t} = \frac{S_e(r) e^{\alpha T_1} e^{\beta T_1} e^{-\beta t} e^{\nu_a t}}{\nu_a - \beta} -$$

$$\frac{S_e(r) e^{\alpha T_1} e^{-\beta T_1} e^{\nu_a T_1}}{\nu_a - \beta} + \frac{S_e(r) e^{(\alpha + \nu_a)T_1}}{\nu_a + \alpha} - \frac{S_e(r)}{\nu_a + \alpha} \qquad \text{(B10}$$

0(x $e^{-\nu_a t}$; factor $S_e(r) e^{\alpha T_1}$ out)

$$N_e = S_e(r)\, e^{\alpha T_1}\left[\frac{e^{-\beta(t-T_1)}}{\nu_a-\beta} - \frac{e^{-\nu_a(t-T_1)}}{\nu_a-\beta} + \right.$$

$$\left.\frac{e^{-\nu_a(t-T_1)}}{\alpha+\nu_a} - \frac{e^{-\alpha T_1}e^{-\nu_a t}}{\alpha+\nu_a}\right] \qquad \text{(B11)}$$

0(Drop last term as very small and decreasing; factor out $1/\nu_a-\beta$; clear fractions in last term.)

$$N_e = \frac{S_e(r)\, e^{\alpha T_1}}{\nu_a-\beta}\left[e^{-\beta(t-T_1)} - \left(\frac{\alpha+\beta}{\alpha+\nu_a}\right)e^{-\nu_a(t-T_1)}\right] \qquad \text{(B12)}$$

which is Eq (112b).

0(Let $t \gg T_1$; since $\nu_a \gg \beta$ the last term in bracket drops out leaving Eq 113b))

$t \in (T_2, T_3)$

For the third integration over the interval $t\epsilon(T_2, T_3)$ the source is constant or $T(t) = 1$ and Eq (B3) becomes

$$N_e e^{\nu_a t}\Big|_{N_e(T_2)e^{\nu_a T_2}}^{N_e e^{\nu_a t}} = S_e(r)\, e^{\alpha T_1}\, e^{-\beta(T_2-T_1)}\int_{T_2}^{t} e^{\nu_a t}\, dt \qquad \text{(B13)}$$

where $S_e(r)\, e^{\alpha T_1}\, e^{-\beta(T_2-T_1)}$ replaces $S_e(r)$

0(Integrate; apply limits)

$$N_e e^{\nu_a t} - N_e(T_2)e^{\nu_a T_2} = \frac{S_e(r)\, e^{\alpha T_1}\, e^{-\beta(T_2-T_1)}}{\nu_a}\left(e^{\nu_a t} - e^{\nu_a T_2}\right) \qquad \text{(B14)}$$

0(Integrate with limits from $t = T_3$ $t = t$

$$N_e = N_e(T_3)\, e^{-\nu_a (t - T_3)} \tag{B19}$$

which is Eq (112d). For $t \gg T_3$ we note that $N_e \to 0$ as we would expect with no source.

On the Validity of Dropping

Following Barron we find additional support for the validity of dropping $\propto N_+$ in comparison to ν_a by integrating the positive ion production from t = 0 to $t = T_1$ assuming no losses:

$$N_+ = \int_0^{T_1} S_e(r) e^{\propto t}\, dt \tag{B20}$$

$$= \frac{S_e(r)}{\propto} \left(e^{\propto T_1} - 1 \right) \tag{B21}$$

Inserting the source strength used to compute Fig. 21 gives

$$N_+ = \frac{3.4 \times 10^{25}}{10^8} \left(e^3 - 1 \right) \tag{B22}$$

$$\cong 7 \times 10^{18} \quad \frac{\text{positive ions}}{\text{meter}^3} \tag{B23}$$

which is below the approximate-validity-limit of 10^{19}.

For a discussion of the effect of neglecting recombination see reference one page

0(x $e^{-\nu_a t}$; transpose; factor out term)

$$N_e = \frac{S_e(r)e^{\alpha T_1}e^{-\beta(T_2 - T_1)}}{\nu_a}$$

$$\times\left[1 - e^{-\nu_a(t - T_2)} + \frac{\nu_a N_e(T_2)e^{-\nu_a(t - T_2)}}{S_e(r)e^{\alpha T_1}e^{-\beta(T_2 - T_1)}}\right] \qquad \text{(B15)}$$

The factor $N_e(T_2)$ could be replaced by the final value from Eq (B12) but this adds nothing to the analysis.

0(Let $t \gg T_2$ to get the steady state condition with a constant source.)

$$N_e = \frac{S}{\nu_a} = \frac{S_e(r)e^{\alpha T_1}e^{-\beta(T_2 - T_1)}}{\nu_a} \qquad \text{(B16)}$$

which is Eq (113c).

$t > T_3$

For times greater than T_3 there is no source, $T = 0$ and we return to Eq (107) in order to reformulate the differential equation:

$$\frac{dN_e}{dt} = -\nu_a N_e - \alpha_r N_+ N_- \qquad \text{(B17)}$$

Again we shall ignore recombination 0(x dt/N_e)

$$\frac{dN_e}{N_e} = -\nu_a\, dt \qquad \text{(B18)}$$

1. Karzas, W. J. and R. Latter. "Air Conductivity Produced by Nuclear Explosions," Rand Memorandum RM-3671-PR: 1-17 (May 1963) (Also published as EMP Theoretical Note 32).

2. Baran, Michael. Introduction to EMP. 1969. (Unpublished notes, Air Force Institute of Technology, Physics Department, Wright-Patterson Air Force Base, Ohio).

Vita

Otho V. Kinsley was [redacted]. He was graduated from high school in Tempe, Arizona in 1950, attended Arizona State College in Tempe from which he received the degree of Bachelor of Science and a commission in the U. S. Air Force in 1954. After attending navigation school, he received his navigator's wings in July 1955. For most of his early Air Force career he was a navigator with Military Airlift Command. In 1964 he was assigned to Air Force ROTC duty at Oregon State University. After a tour in Vietnam he attended the Air Force Institute of Technology where he received a Master of Science degree in Nuclear Engineering.

Permanent Mailing Address: [redacted]

This thesis was typed by Mrs. Jane Manemann.